NTIA Report 19-542

Received Signal Power Measurements On Select Air Traffic Control Radars In Colorado

Jeffery A. Wepman
Edward F. Drocella
April Lundy
Paul M. McKenna
Heather E. Ottke
Yeh Lo

report series

U.S. DEPARTMENT OF COMMERCE • National Telecommunications and Information Administration

NTIA Report 19-542

Received Signal Power Measurements On Select Air Traffic Control Radars In Colorado

Jeffery A. Wepman
Edward F. Drocella
April Lundy
Paul M. McKenna
Heather E. Ottke
Yeh Lo

U.S. DEPARTMENT OF COMMERCE

August 2019

DISCLAIMER

Certain commercial equipment and materials are referenced in this report to specify adequately the technical aspects of the reported results. In no case does such reference imply recommendation or endorsement by the National Telecommunications and Information Administration, nor does it imply that the material or equipment referenced is the best available for this purpose.

CONTENTS

FIGURES

TABLES

ACRONYMS/ABBREVIATIONS

AC	alternating current
AGL	above ground level
Ant	antenna
ASR-9	Airport Surveillance Radar, Model 9
BPF	bandpass filter
CARSR	Common Air Route Surveillance Radar
CW	continuous wave
dB	decibel(s)
dBi	decibel(s) referenced to isotropic
dBm	decibel(s) referenced to 1 milliwatt
Freq	frequency
GHz	gigahertz
GPS	Global Positioning System
IF	intermediate frequency
ITM	Irregular Terrain Model
ITS	Institute for Telecommunication Sciences
kHz	kilohertz
km	kilometer(s)
Lat	latitude
LNA	low-noise amplifier
Lon	longitude
LPF	low-pass filter
m	meter(s)
Max	maximum

Min	minimum
MHz	megahertz
NC	normally closed
NTIA	National Telecommunications and Information Administration
Num	number
OSM	Office of Spectrum Management
ppr	pulse repetition rate
pps	pulses per second
Prop	propagation
Pwr	power
Quart	quartile
RBW	resolution bandwidth
RF	radio frequency
RSMS-5G	Radio Spectrum Measurement System Fifth Generation
Rx	receiver
SPDT	single-pole, double-throw
Tx	transmitter
W	watt(s)

GLOSSARY

60 dB/ 3 dB Shape Factor: A measure of the steepness of the rolloff of a filter; given as the ratio of the 60-dB bandwidth divided by the 3-dB bandwidth of the filter.

Frequency Assignment: An NTIA-issued frequency authorization allowing an agency to operate an RF system on a specific frequency or frequencies at a particular location or within a defined area with specified technical parameters.

Irregular Terrain Model (ITM): A radio propagation model, developed by ITS, that predicts the median attenuation of a radio signal as a function of distance and the variability of the signal in time and in space, for frequencies between 20 MHz and 20 GHz.

Median Peak Over-The-Air System Noise Power: Median of the peak-detected RF power of the measurement system with the antenna connected to the RF input of the preselector and no intentionally emitted signals observable.

Noise Diode Calibration: A measurement procedure performed on an RF measurement system that provides the overall measurement system noise figure and preselector gain (if a preselector is present).

Noise Figure: A measure of the amount of noise a device or system produces above the thermal noise level; formally defined as the ratio of the input signal to noise ratio divided by the output signal to noise ratio of a device or system, expressed in decibels.

Over-The-Air System Noise Floor: The peak-detected power, measured by the measurement system with the antenna connected to the RF input of the preselector, as a function of frequency with no intentionally emitted signals observable.

Peak Detected Time Signature: The shape of the received signal power of the radar as the radar rotates and is captured with the spectrum analyzer sweep in zero-span mode.

Peak Detection: A spectrum analyzer detection mode where the value of each display point is the peak value of all digitized samples that were collected within the time duration used to generate the display point. For example, if the time duration used to generate an analyzer display point is 1 millisecond but 1,000 digitized samples were collected by the analyzer during that millisecond, then the peak-detected value for the display point is the highest-power of the 1,000 samples.

Potential Radar Signal: A signal identified by the automated data processing that appears to be a radar signal.

Preselector: A device used on the input of a radio receiver measurement system, after the receive antenna, that attenuates unwanted out-of-band signals, improves the sensitivity of the measurement system, and enables measurement system calibrations.

Propagation Mode: The classification of the type of radio propagation a signal experiences (line-of-sight, diffraction, tropospheric scatter) over a geographical path as predicted by ITM.

Quantitative Assessments of Spectrum Usage: Data from the frequency assignment for each RF system's individual transmitting and receiving stations used to develop an approximation of each RF system's actual use of the spectrum in terms of frequency, geography, and time.

Received Signal Power: The strength of a radio signal as measured at the receiver (RF input of the preselector in this measurement system), typically given in units of dBm in the receiver's resolution bandwidth (RBW).

Resolution Bandwidth (RBW): A measure of the width of the intermediate frequency (IF) filter (typically the 3 dB bandwidth) in a spectrum analyzer. It gives an indication of how closely spaced in frequency two continuous-wave (CW) signals can be and yet remain distinguishable.

Spectrum Analyzer Sweep: A set of signal power measurements collected and displayed on a spectrum analyzer at specified time intervals over a specified duration when the analyzer is in zero-span mode (or at specified frequency intervals over a specified frequency range when the analyzer is in its default mode). For example, a spectrum analyzer sweep might consist of 2,501 displayed points (each a separately measured power value) collected over the duration of 2.5 seconds. Each power value in the sweep represents the behavior of the analyzer's detector, in the analyzer's selected resolution bandwidth, for, in this example,

$$\frac{2500\ milliseconds}{(2501\ points - 1)} = 1\ millisecond\ of\ time.$$

Spectrum Usage Contour: The geographical region surrounding a transmitter outside of which the received signal power from the transmitter is predicted to be less than a pre-defined threshold relative to the thermal noise floor.

System Noise Floor: The peak-detected internal noise power, measured by the measurement system with a 50 Ω load on the RF input of the preselector, as a function of frequency.

Time-domain Measurements: Signal power measurements that are taken at specified intervals of time.

Valid Radar Signal: A potential radar signal that has all n data points (n = 10 and n = 8 for the ASR-9 and CARSR respectively) of its peak detected time signature above a threshold (6 dB above the median peak over-the-air system noise power level).

Zero-span Mode: A spectrum analyzer operating mode where the local oscillator is held at a constant frequency (the local oscillator sweeps in frequency in the spectrum analyzer default mode), causing the data output to be signal power as a function of time.

RECEIVED SIGNAL POWER MEASUREMENTS ON SELECT AIR TRAFFIC CONTROL RADARS IN COLORADO

Jeffery A. Wepman,[1] Edward F. Drocella,[2] April Lundy,[2] Paul M. McKenna,[1]
Heather E. Ottke,[1] and Yeh Lo[3]

Received signal power measurements were performed on the Common Air Route Surveillance Radar (CARSR) operating in the 1300–1370 MHz band in Parker, Colorado and on the Airport Surveillance Radar (ASR-9) operating in the 2700-2900 MHz band in Platteville, Colorado. The measurements were taken along five radials extending from each radar transmitter. Four or five fixed locations were chosen along each radial where predicted received signal power varied from relatively strong to weak levels. Multiple peak received power measurements were made at each location to provide statistically significant results. In another effort, these measurements will be used to validate spectrum usage contours and the methodology used to generate them as developed by the Office of Spectrum Management (OSM) of the National Telecommunications and Information Administration (NTIA).

Keywords: Received signal power measurements, peak received signal power, ASR-9, CARSR, radar measurements, spectrum usage contours

1. INTRODUCTION

The objective of this work was to conduct received signal power measurements on select air traffic control radars and provide measured data results that can be used (in a separate effort) to validate spectrum usage contours[4] and the Quantitative Assessments of Spectrum Usage methodology used to generate them, as developed by the Office of Spectrum Management (OSM) [1].To meet this objective, the Institute for Telecommunication Sciences (ITS) performed received signal power measurements on the Common Air Route Surveillance Radar (CARSR) operating in the 1300–1370 MHz band in Parker, Colorado and the Airport Surveillance Radar (ASR-9) operating in the 2700–2900 MHz band in Platteville, Colorado. Measurements were

[1] The authors are with the National Telecommunications and Information Administration (NTIA), Institute for Telecommunication Sciences (ITS), U.S. Dept. of Commerce, 325 Broadway St., Boulder, Colorado 80305.

[2] The authors are with the NTIA Office of Spectrum Management (OSM), U.S. Dept. of Commerce, 1401 Constitution Ave. NW, Washington, DC 20021.

[3] The author was formerly with the National Telecommunications and Information Administration (NTIA), Institute for Telecommunication Sciences (ITS), U.S. Dept. of Commerce, 325 Broadway St., Boulder, Colorado 80305.

[4] A spectrum usage contour represents the geographical region surrounding a transmitter outside of which the received signal power from the transmitter is predicted to be less than a pre-defined threshold relative to the thermal noise floor.

taken at a received antenna height roughly 3 m above ground level (AGL), using the ITS modified Chevrolet Express 3500 Extended Cargo Van (see Figure 1). A set of fixed-location measurements were taken along radials extending from each radar transmitter. Multiple measurements at each fixed location were made to provide statistically significant results.

Figure 1. ITS modified Chevrolet Express 3500 Extended Cargo Van.

2. MEASUREMENT SYSTEM

2.1 Measurement System Design

A block diagram of the measurement system used during the measurements is shown in Figure 2. The system consists of an antenna, a preselector, a spectrum analyzer, a GPS antenna and receiver, and a measurement controller. For these measurements, the measurement system was installed in the ITS modified Chevrolet Express 3500 Extended Cargo Van (Figure 1).

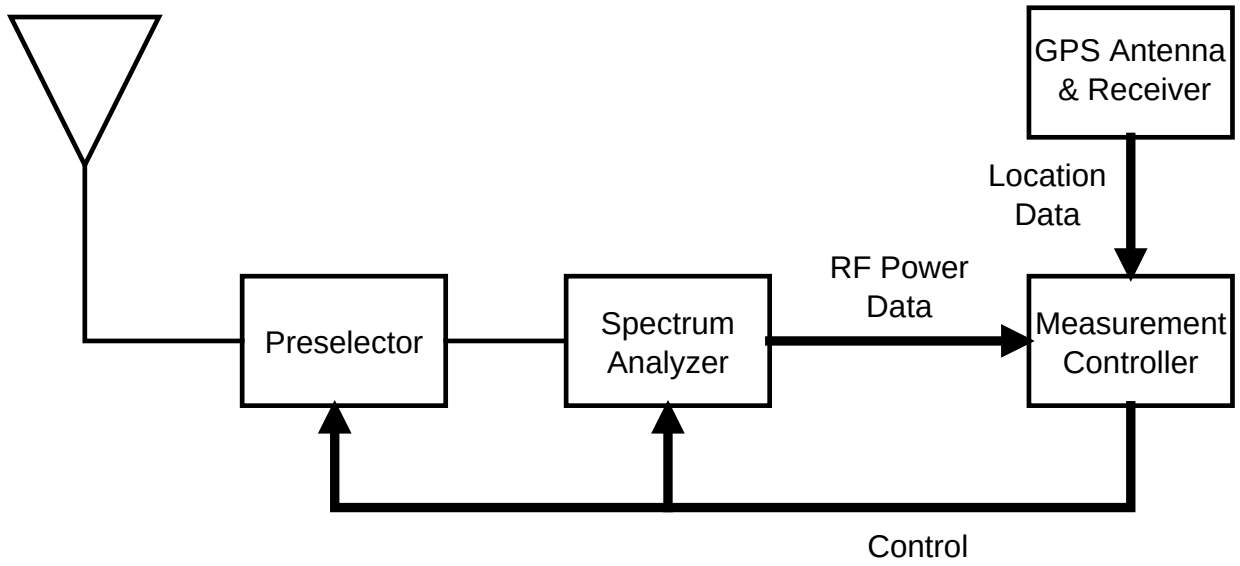

Figure 2. Block diagram of the measurement system.

Frequency assignment records list the polarizations of the antennas for both the ASR-9 and the CARSR as right and left-hand circular. The measurement system uses a slant-polarized, omnidirectional, biconical antenna (Watkins-Johnson WJ-48955). The slant-polarized antenna has the distinct advantage of being able to receive vertically, horizontally, and both left- and right-hand circularly-polarized signals with the same gain, albeit 3 dB lower than for slant-polarized signals. Hence, it is an appropriate antenna to use for these measurements.

Antenna gain and azimuthal pattern measurements were made with the slant-polarized omnidirectional antenna mounted on the measurement vehicle using the antenna turntable at the ITS Table Mountain Field Site and Radio Quiet Zone for 1601 frequencies from 1 to 3.9 GHz. (The photograph of the measurement vehicle shown in Figure 1 was taken during this antenna testing.) The antenna measurements were made by transmitting a vertically-polarized signal using a calibrated double-ridged guide horn antenna. An antenna gain and pattern measurement was made using another calibrated double-ridged guide horn antenna as the receive antenna mounted on the measurement vehicle. The measurement was then repeated using the slant-polarized omnidirectional antenna mounted on the measurement vehicle.

The gain as a function of azimuthal angle was then determined for the slant-polarized omnidirectional antenna. The median antenna gain (median of dBi values) over all azimuthal

angles at the center frequency of the ASR-9 measurements (2715 MHz) was -0.3 dBi while the median antenna gain (median of dBi values) over all azimuthal angles at the center frequency of the CARSR measurements (1320.59 MHz) was -4.1 dBi. Since the slant-polarized antenna will receive left or right-hand circularly-polarized signals with the same gain as a vertically-polarized signal, these gain values are valid for the circularly-polarized transmissions of the ASR-9 and CARSR radars.

A simplified block diagram of the preselector is shown in Figure 3. The preselector is custom-built by ITS and performs several crucial functions for the measurement system. It attenuates unwanted out-of-band signals via RF filtering, improves the sensitivity of the system with a low-noise amplifier, and enables measurement system calibrations via a built-in noise diode. Noise diode measurement system calibrations provide assurance that the measurement system is operating properly. They also provide measurements of the preselector gain and system noise figure. Preselector gain is particularly important to be able to determine absolute received power at the input to the preselector.

The preselector provides the capability to automatically switch between two filter paths under software control. Each filter path consists of a manually tunable bandpass filter with a 5% 3 dB bandwidth whose center frequency is set to the center frequency of the radar to be measured. One tunable bandpass filter covers the 1000–2000 MHz range with a 60 dB/3 dB shape factor of 3.2 while the other covers the 2000–4000 MHz range with a 60 dB/3 dB shape factor of 3.7. A low-noise amplifier can be invoked under software control after each of these filter paths to improve the sensitivity of the measurement system. This enables measurement of the low-level transmissions expected at distances far from the radar transmitter. The preselector also contains a noise diode that is utilized under software control to perform measurement system calibrations.

The spectrum analyzer (Agilent E4440A) is the core of the overall measurement system. It takes the RF signals received by the antenna and conditioned by the preselector, and provides peak power measurements of the received radar transmissions in a user-selected resolution bandwidth (RBW). Automated control of the preselector and spectrum analyzer is provided by the measurement controller. The measurement controller is also custom-built by ITS and consists of a custom-built computer, Ethernet switch, and power supply for the preselector.

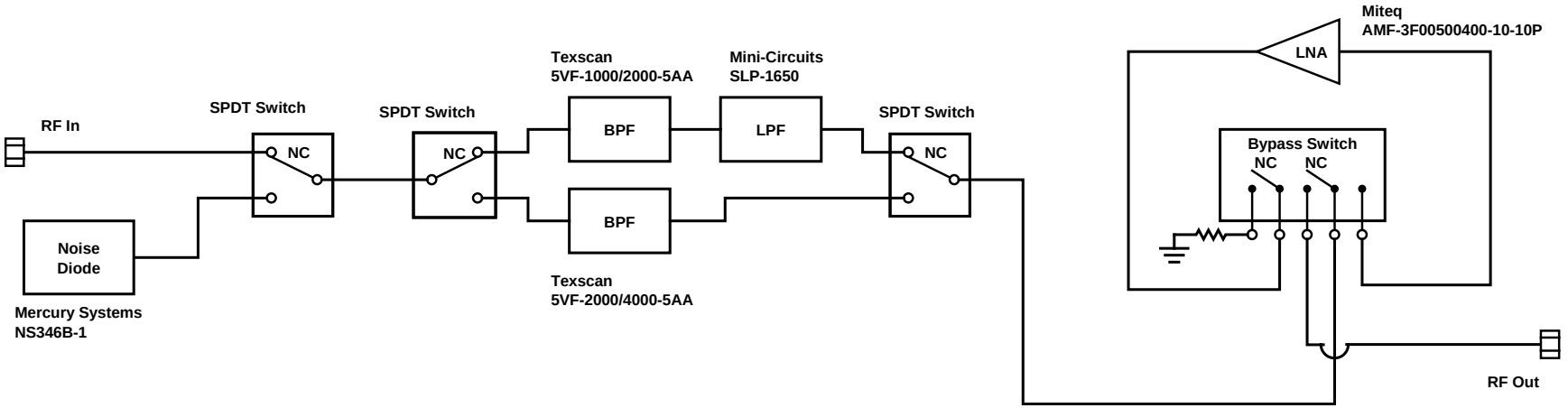

Figure 3. Simplified block diagram of the preselector (Ethernet control is not shown).

The spectrum analyzer, GPS antenna and receiver (GlobalSat Technology Corporation BU-353S4), and measurement controller combination collects the received signal RF peak power measurement data tagged with location information, formats the data, and saves the data to a local hard drive on the measurement controller.

2.2 Measurement System Noise Floor Characterization

To obtain an understanding of the received power levels that can be detected with the measurement system, a set of over-the-air noise measurements was performed to characterize the over-the-air system noise floor. These measurements were performed with the measurement system installed in the measurement vehicle with AC power supplied by the vehicle's internal generator. For these measurements, the vehicle was parked at the loading dock at the end of Wing 2 on the south side of Building 1 at the U.S. Department of Commerce Boulder Labs in Boulder, Colorado. The slant-polarized antenna was connected and the system was tuned to center frequencies near those of the ASR-9 and CARSR radar center frequencies but where no signals were detected. A frequency of 2740 MHz was used to represent the ASR-9 and 1300 MHz was used to represent the CARSR.

Figures 4 and 5 show the over-the-air system noise floor of the measurement system (referenced to the RF input of the preselector) at 2740 MHz (near in frequency to the ASR-9) both without and with the low-noise amplifier, respectively. Note that the RBW and detection were the same as used in the radar measurements, namely a 3 MHz RBW and peak detection. Comparison of these measurements with noise floor measurements taken with a 50 Ω load on the RF input to the preselector show negligible difference, indicating that any external noise is below the system noise floor. The median peak over-the-air system noise power (referenced to the RF input of the preselector) for the ASR-9 is -64.3 dBm without the low-noise amplifier and -93.9 dBm with the low-noise amplifier.

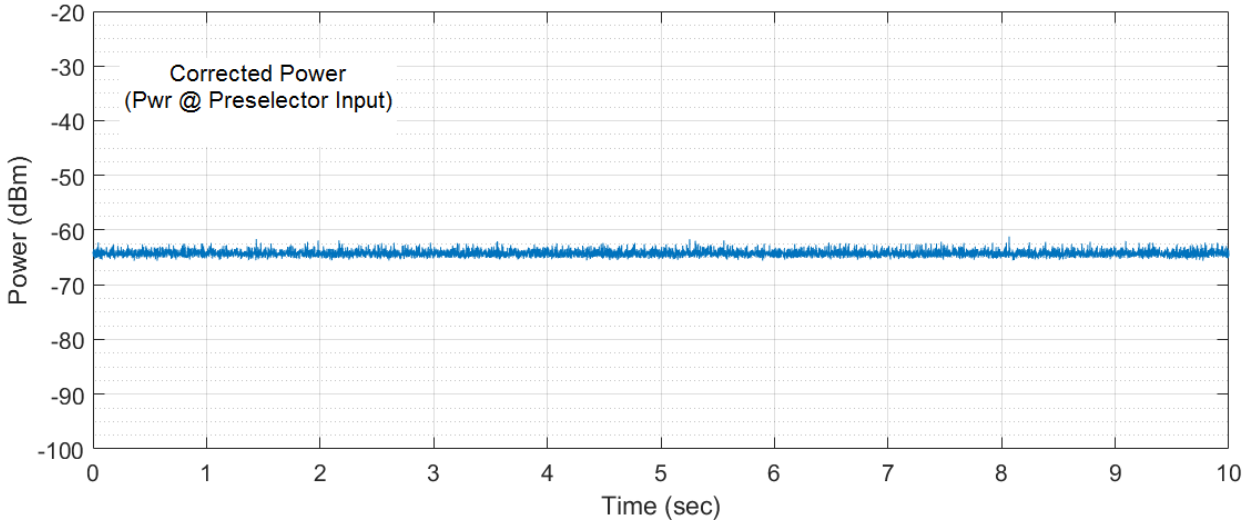

Figure 4. Over-the-air system noise floor of the measurement system at 2740 MHz in a 3 MHz RBW using peak detection without low-noise amplifier (AC power via internal generator).

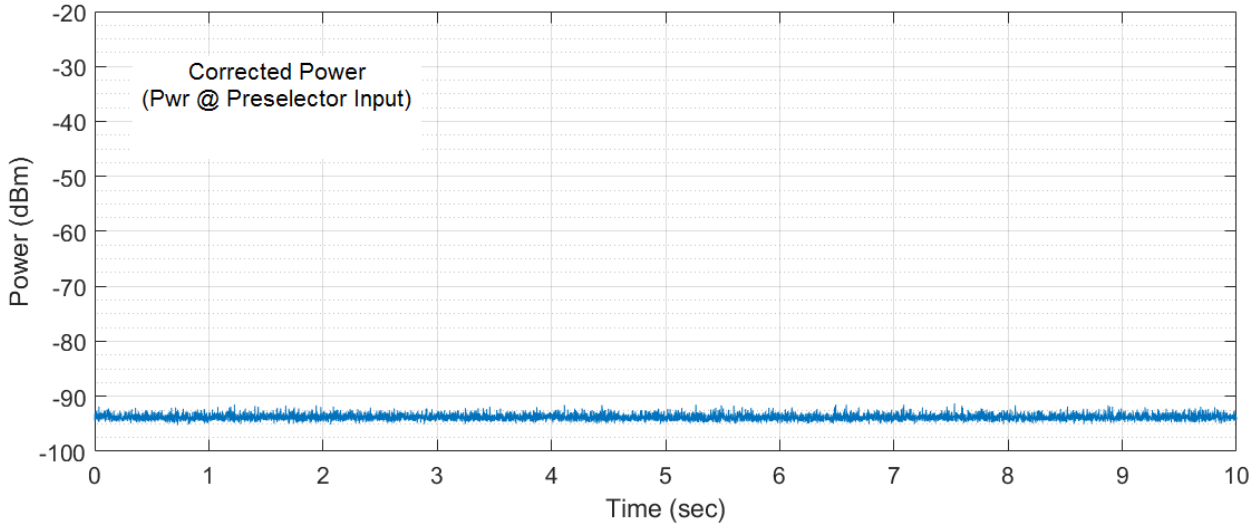

Figure 5. Over-the-air system noise floor of the measurement system at 2740 MHz in a 3 MHz RBW using peak detection with low-noise amplifier (AC power via internal generator).

Figure 6 shows the over-the-air system noise floor of the measurement system (referenced to the RF input of the preselector) at 1300 MHz (near in frequency to the CARSR) without the low-noise amplifier. Note that the RBW and detection were the same as used in the radar measurements, namely a 3 MHz RBW and peak detection. Comparison of this measurement with a noise floor measurement taken with a 50 Ω load on the RF input to the preselector shows negligible difference indicating that any external noise is also below the system noise floor. The median peak over-the-air system noise power (referenced to the RF input of the preselector) for the CARSR without the low-noise amplifier is -67.0 dBm.

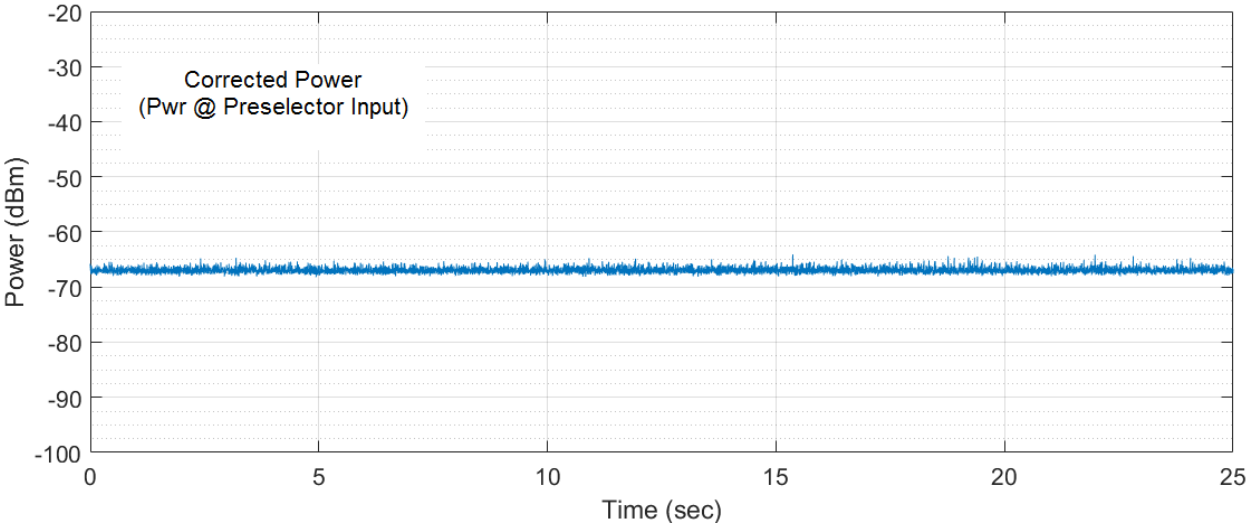

Figure 6. Over-the-air system noise floor of the measurement system at 1300 MHz in a 3 MHz RBW using peak detection without low-noise amplifier (AC power via internal generator).

Figure 7 shows the over-the-air system noise floor of the measurement system at 1300 MHz (near in frequency to the CARSR) with the low-noise amplifier. Note that the RBW and detection were the same as used in the radar measurements, namely a 3 MHz RBW and peak detection. The median peak over-the-air system noise power (referenced to the RF input of the preselector) for the CARSR with the low-noise amplifier is -95.6 dBm. Figure 8 shows this same measurement but with a 50 Ω load on the RF input to the preselector. Note the increased noise level of the over-the-air system noise floor in Figure 7 as compared to the system noise floor with a 50 Ω load on the RF input to the preselector as seen in Figure 8. This clearly shows that the increased noise is due to external noise being picked up by the antenna.

To investigate this further, other measurements were made of the over-the-air system noise floor but with AC power supplied to the measurement vehicle via shore power. An example of this measurement is shown in Figure 9. Note that some external noise is still present but not as much as that seen in Figure 7. The conclusion is that the vehicle's internal generator contributes a significant amount of external noise but there are other sources of external noise as well that are detected. Obviously, external noise from sources other than the vehicle's internal generator will be very time and location dependent. While the external noise from the generator and other external sources is undesirable, radar signals can still be easily discerned from this noise with proper processing as will be discussed later.

A summary of the median peak over-the-air system noise power for each preselector path (referenced to the RF input of the preselector) both with and without the low-noise amplifier is given in Table 1.

Table 1. Median peak over-the-air system noise power for each preselector path.

Preselector Path	**Median Peak Over-The-Air System Noise Power (dBm)**
ASR-9 without low-noise amplifier	-64.3 (3 MHz RBW)
ASR-9 with low-noise amplifier	-93.9 (3 MHz RBW)
CARSR without low-noise amplifier	-67.0 (3 MHz RBW)
CARSR with low-noise amplifier	-95.6 (3 MHz RBW)

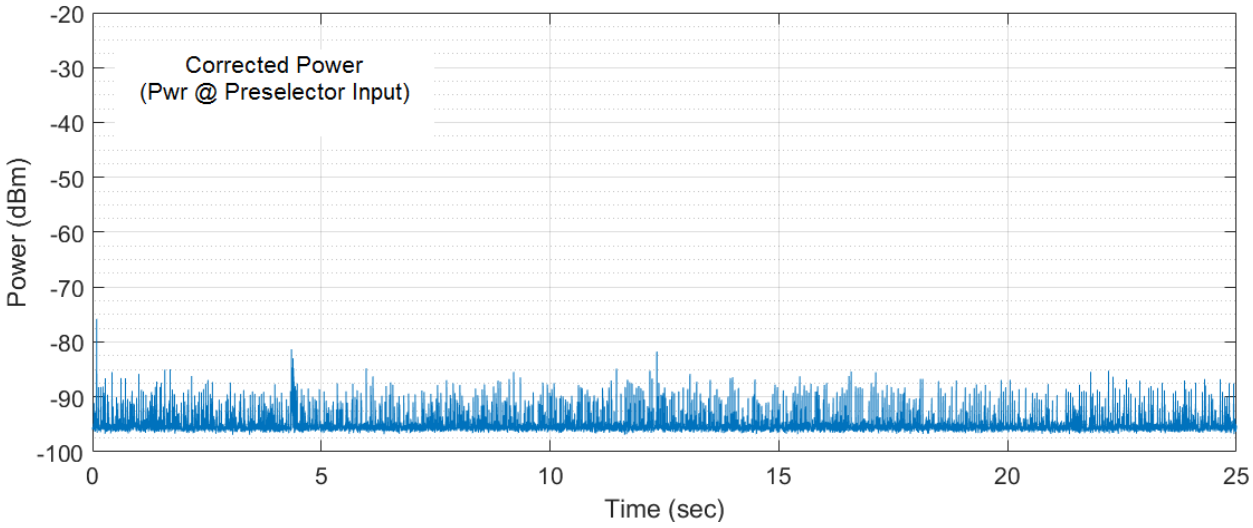

Figure 7. Over-the-air system noise floor of the measurement system at 1300 MHz in a 3 MHz RBW using peak detection with low-noise amplifier (AC power via internal generator).

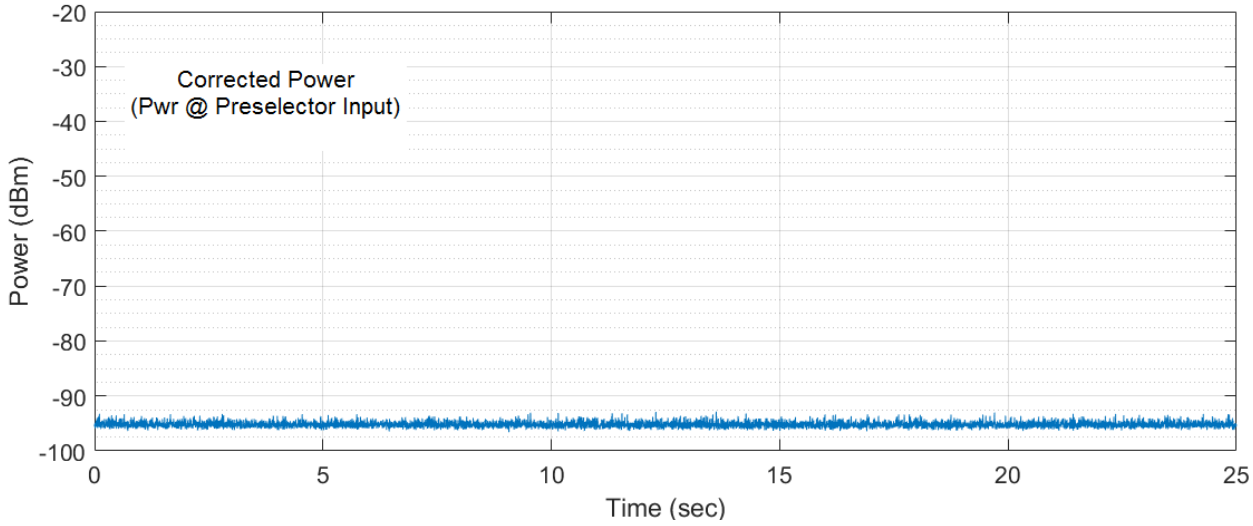

Figure 8. System noise floor of the measurement system with a 50 Ω load on the RF input to the preselector at 1300 MHz in a 3 MHz RBW using peak detection with low-noise amplifier (AC power via internal generator).

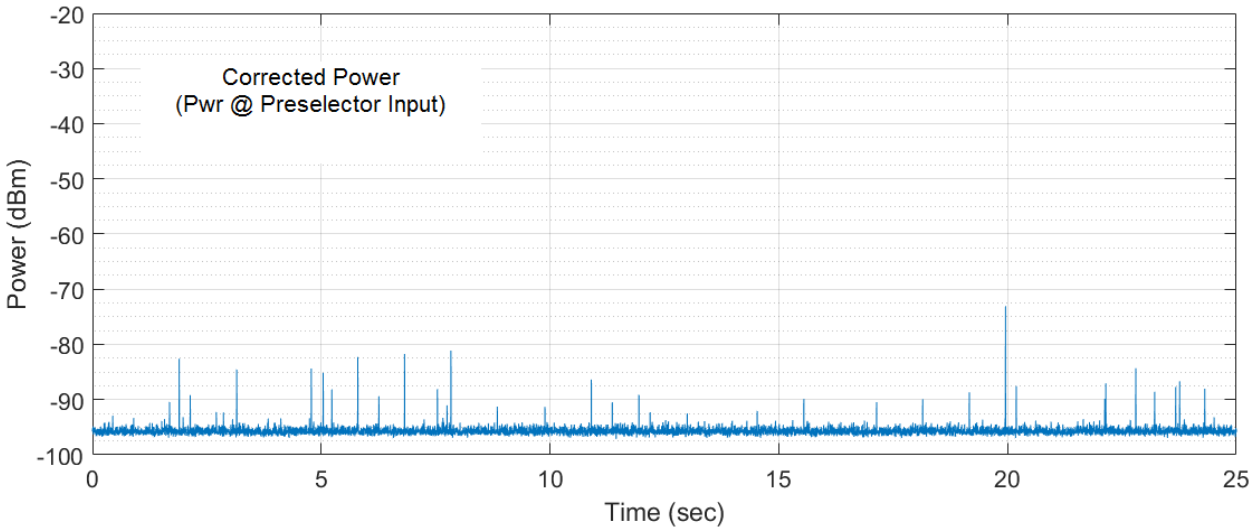

Figure 9. Example of over-the-air system noise floor of the measurement system at 1300 MHz in a 3 MHz RBW using peak detection with low-noise amplifier (AC power via shore power).

3. MEASUREMENT LOCATION SELECTION

Measurement sites were chosen roughly along radials emanating from the transmitter locations. Specific site locations along these radials were targeted with consideration of predicted received signal power at potential locations, predicted propagation modes at potential locations (such as line-of-sight, diffracted, etc.), the availability of suitable roads for access in the area, and the suitability of places to park the measurement vehicle to conduct measurements. The predictions of received signal power and propagation modes along the radials were determined using the Irregular Terrain Model (ITM) [2].

Five radials for each radar transmitter were chosen. Radials that would extend to the mountains west of the radar transmitters were avoided due to both more complicated radio propagation effects and limitations on practical measurement locations. An attempt was made to select four or five measurement locations along each radial for each transmitter where the predicted received signal power varied from a relatively strong to weak (but still detectable) level. An attempt was also made to select locations along the radials where as many different propagation modes as possible could be represented.

The measurements were taken at locations as close to the predicted measurement locations as possible given the practical constraints of roads, significant obstructions (such as large trees, power lines, buildings, etc.), and the ability to safely park the measurement vehicle. Figures 10 and 11 show the radials, the predicted spectrum usage contours, and the actual measurement locations for the ASR-9 in Platteville, Colorado and the CARSR in Parker, Colorado, respectively. Measurements were taken at a total of 21 measurement locations for the ASR-9. Measurements were taken at a total of 27 measurement locations for the CARSR.

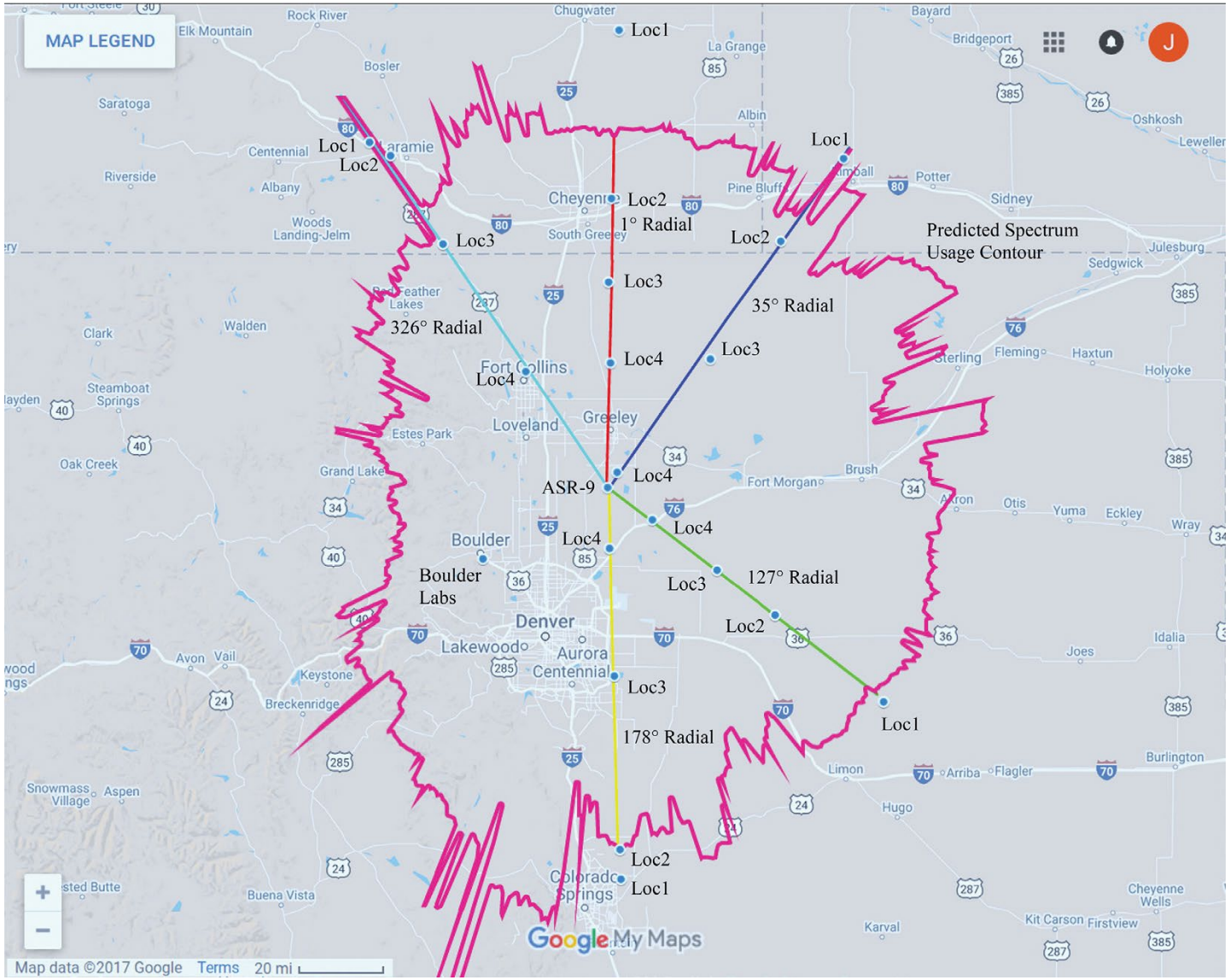

Figure 10. Spectrum usage contour, radials, and actual measurement locations for the ASR-9 in Platteville, Colorado.

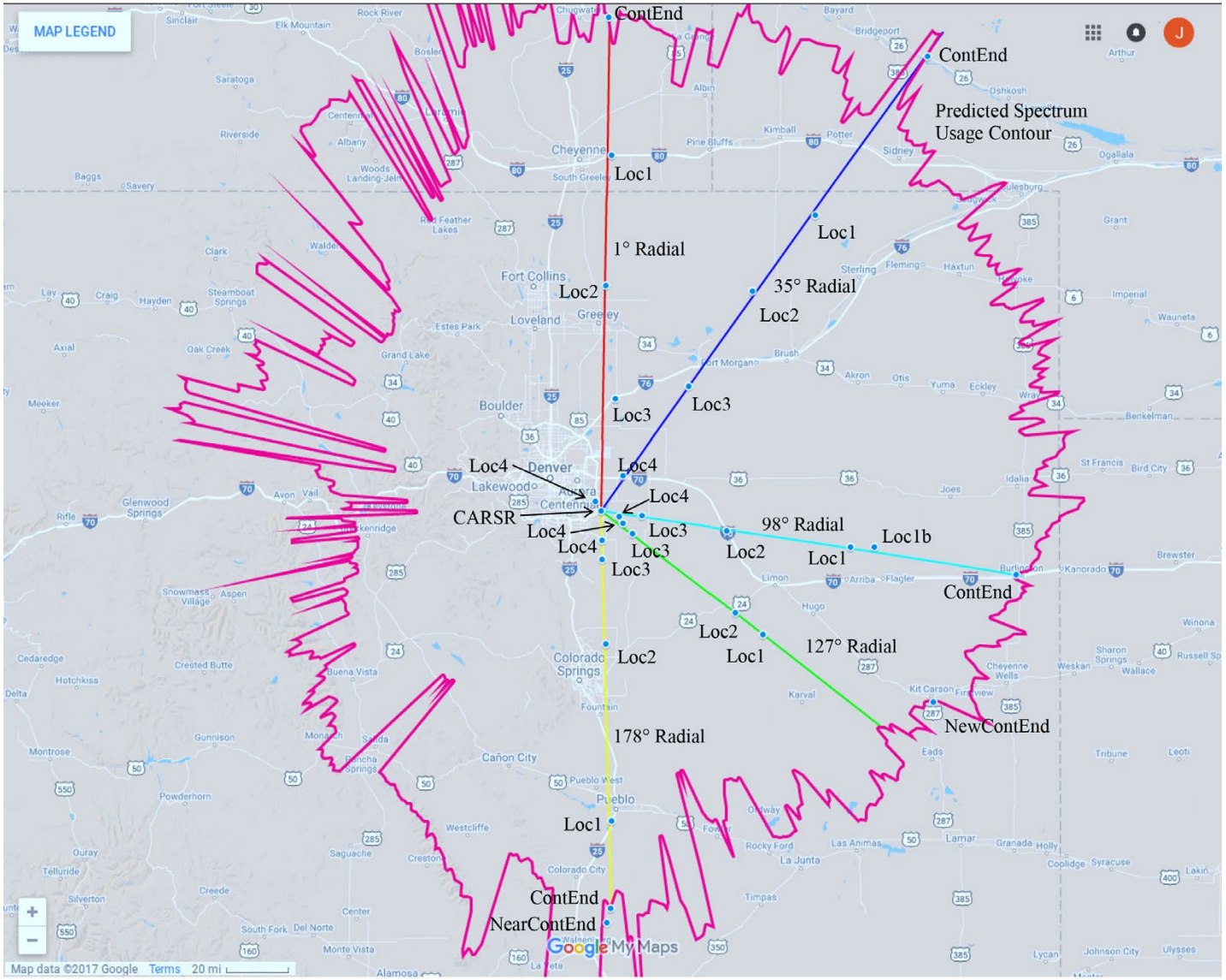

Figure 11. Spectrum usage contour, radials, and actual measurement locations for the CARSR in Parker, Colorado.

4. MEASUREMENT PROCEDURE

At each measurement location, the following general procedure was followed:

1) Set preselector path to use the appropriate tunable bandpass filter for the radar to be measured.

2) Determine if the low-noise amplifier is to be used or not based on the expected received signal power. No amplifier is used if the received signal power is expected to be greater than -40 dBm at the preselector input.

3) Perform a noise diode calibration with the current preselector settings. The noise diode calibration uses the traditional Y-factor method (where the calibration measurement is performed twice, once with the diode turned on and once with the diode turned off; the gain and noise figure are determined by *Y*, the difference between the measured power in decibels with the diode-on and the measured power in decibels with the diode-off). This calibration provides assurance that the measurement system is operating properly and provides measurements of the preselector gain and system noise figure. The preselector gain is subtracted from the received power measured at the RF input of the spectrum analyzer to provide calibrated power measurements referenced to the preselector input RF connector.

4) Start the radar measurement (details of the radar measurement are described in Section 5 below).

5) Observe the received signal power data being collected on the measurement controller computer display.

    a) The data are observed to ensure that the radar signal is detectible, to determine the appropriate spectrum analyzer attenuation to use,[5] to determine if the preselector low-noise amplifier should be used, and to determine if any measurement system overload conditions exist.

    b) Based on the results of this data observation, data collection is either allowed to continue to completion (signifying that the choice of using the amplifier or not was correct and the selection of spectrum analyzer attenuation was correct) or is terminated. If data collection is terminated, the preselector settings are changed. (The initial choice of using the amplifier or not is reversed and the spectrum analyzer attenuation is modified if needed.) Then the noise diode calibration is redone and the radar measurement is redone.

[5] Note that the default spectrum analyzer attenuation for the measurements was set to 10 dB. While this attenuation could be changed, it was not changed for the fixed location measurements discussed in this report. The option for increasing the attenuation exists to accommodate measuring very high signal levels when not using the amplifier. Decreasing the attenuation does not have a significant advantage for this measurement system since it will not significantly improve the system sensitivity and will slightly degrade the measurement accuracy. The reason that the system sensitivity is not significantly improved is that the low-noise amplifier gain in the preselector was high enough to overdrive the spectrum analyzer noise figure even with 10 dB of spectrum analyzer attenuation invoked.

5. RADAR MEASUREMENTS

The radar measurements were made using the swept-measurement mode of the Radio Spectrum Measurement System Fifth Generation (RSMS-5G) software. The spectrum analyzer was set up in the zero-span mode (providing time-domain measurements) using peak detection with a sweep time set slightly longer than two times the rotation period[6] of the radar to be measured. This ensures data capture of at least two rotations of the radar. Capturing at least two rotations of the radar allows for easier identification of the radar and permits the peak received power of the radar to be measured. The rotation period of the ASR-9 is roughly 4.6 seconds and a spectrum analyzer sweep time of 10 seconds was chosen. The rotation period of the CARSR is roughly 12 seconds and a spectrum analyzer sweep time of 25 seconds was chosen. The maximum number of points per sweep in the spectrum analyzer (8192) was used to provide the finest resolution of captured time domain data. Peak detection on the spectrum analyzer ensures that the maximum power of the received radar signal is not missed.

The RBW to use for the measurements was determined empirically by measurements of signals from both radars received at the U.S. Department of Commerce Boulder Labs in Boulder, Colorado. Measurements of peak received power from the radar transmissions were made at varying RBWs from 510 kHz to 8 MHz. Using this method, RBWs that are too narrow do not capture all of the power of the received radar emissions. RBWs that are too wide, while capturing all of the power of the received radar emissions, also include more noise (both internal measurement system noise and external noise) in the power measurement than is necessary. Additionally, in the case of the CARSR, bandwidths that are too wide include power from the nearby paired transmission of the radar thus providing inaccurate results. Using this method, a 3 MHz RBW was determined to be optimal for both the ASR-9 and the CARSR.

Fifty spectrum analyzer sweeps were taken at each location. The number of sweeps was chosen to be as large as practical to provide statistically significant results of peak received signal power. Measurement time at each location was limited due to the relatively large number of measurement locations, the significant time required to travel between the locations, measurement setup time, the need for occasional measurement system troubleshooting, and the need for calibration at each location. Since the data collection is asynchronous (i.e., the radar transmissions are not synchronized with the start of the sweeps in the spectrum analyzer) and the sweep time is long enough to always capture at least two main beam radar transmissions, the fifty sweeps provide the opportunity to capture at least 100 received radar signal power measurements per location.

Figure 12 shows an example captured sweep of a strong signal received from the ASR-9 transmitter at Location 3 along the 127° Radial. Note the two peaks that show the peak power of the ASR-9 as it rotates. The maximum of each peak provides the peak received power of the radar as measured at the RF input of the preselector. Note that the time between the peaks is the rotation period of the radar, approximately 4.6 seconds. Figure 13 shows a magnified view of the

[6] The ASR-9 and CARSR utilize mechanically rotated antennas that produce radiation beams that are narrow in azimuth but broad in elevation. They do not form pencil beams or perform any electronic beam steering or frequency hopping that would otherwise complicate the measurements.

first radar signal seen in Figure 12. This magnified view illustrates the "peak detected time signature" of the radar, which is simply the shape of the received signal power of the radar as the radar rotates and is captured with the spectrum analyzer sweep in zero-span mode. Figure 13 shows the shape of the radar's main beam, roughly 20 milliseconds wide at its 3 dB points. Each data point in the sweep is clearly seen in Figure 13. Each data point represents the peak received power over an interval of

$$\frac{Sweep\ Time\ (\text{sec})}{Number\ Data\ Points - 1} = \frac{10\ sec}{8191} \cong 1.22\ msec.$$

The period of the individual pulses of the ASR-9 is

$$\frac{1}{prr} = \frac{1}{1087\ pps} \cong 920\ \mu sec,$$

where *prr* is the pulse repetition rate and *pps* is the number of pulses per second. Since the period of the individual pulses of the ASR-9 is less than the time interval used to determine each data point, every data point in the sweep will show the peak received power of at least one individual radar pulse. This results in the relatively smooth, monotonically increasing and decreasing waveform seen in Figure 13 as the radar rotates.

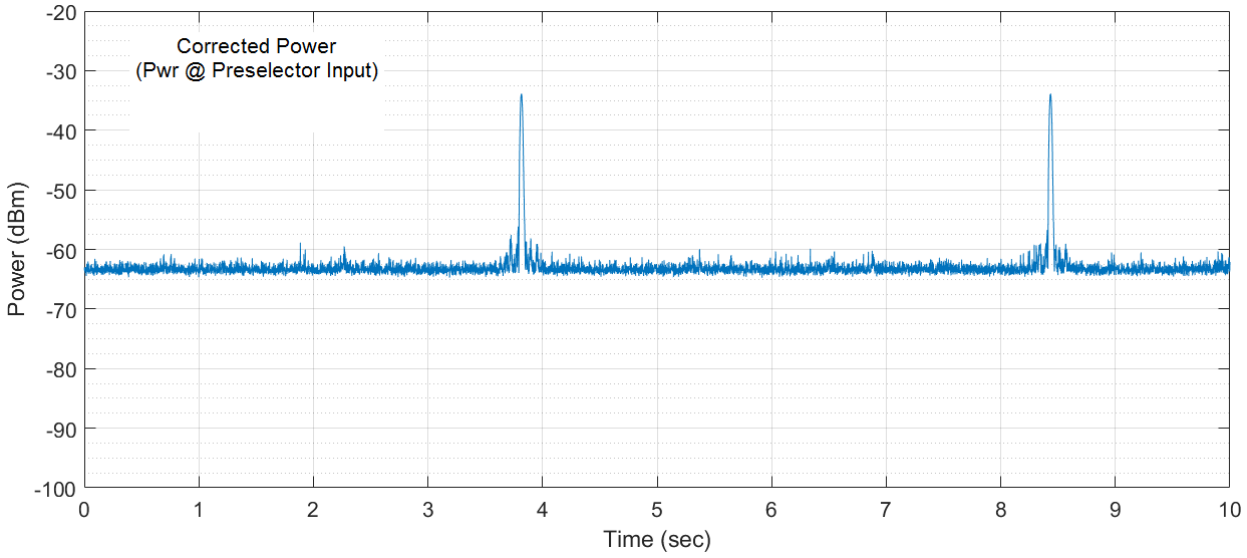

Figure 12. Example of a strong signal received at Location 3 along the 127° Radial for the ASR-9.

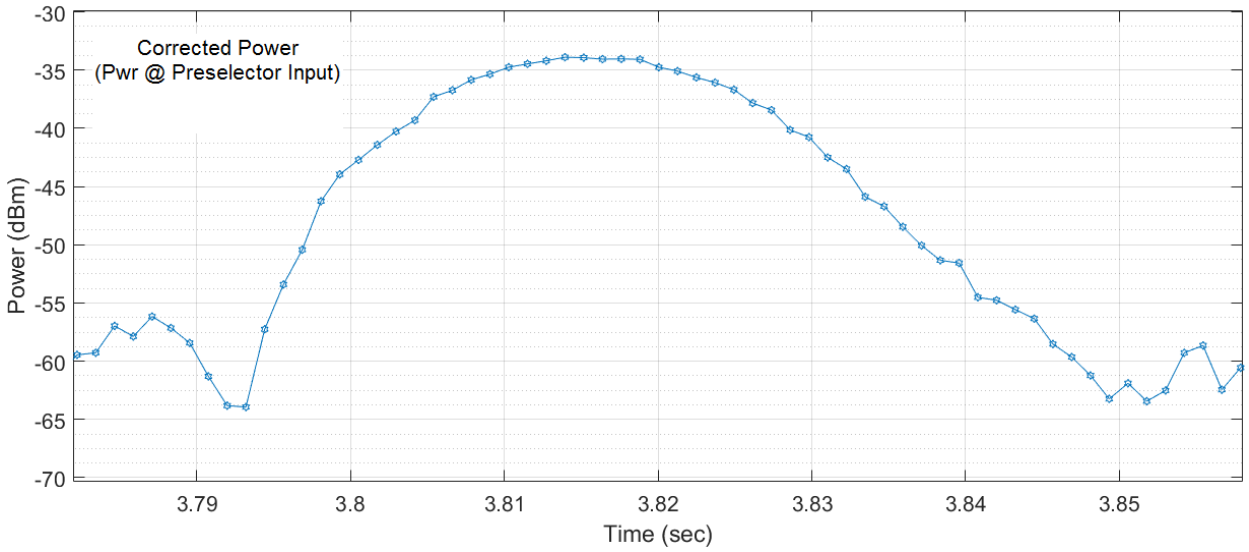

Figure 13. Magnified view of the signal received at Location 3 along the 127° Radial for the ASR-9.

Figure 14 shows an example captured sweep of a strong signal received from the CARSR transmitter at Location 4 along the 127° Radial. The three peaks show the peak power of the CARSR as it rotates. Again, the maximum of each peak provides the peak received power of the radar as measured at the RF input of the preselector. Note that the time between the peaks is the rotation period of the radar, approximately 12 seconds. Figure 15 shows a magnified view of the first radar signal seen in Figure 14 illustrating the "peak detected time signature" of the radar. Each data point represents the peak received power over an interval of

$$\frac{Sweep\ Time\ (\text{sec})}{Number\ Data\ Points - 1} = \frac{25\ sec}{8191} \cong 3.05\ msec.$$

The period of the individual pulses of the CARSR is

$$\frac{1}{prr} = \frac{1}{319pps} \cong 3.13\ msec.$$

The period of the individual pulses for the CARSR is slightly longer than the time interval used to determine each data point. This means that for some data points, an individual pulse will not have been present during the interval used to determine the peak received power. While this does not affect capturing the overall peak received power of the radar signal at all, it does make the appearance of the sweep less aesthetically appealing by causing dips to appear in the sweep that disturb the otherwise relatively smooth, monotonically increasing and decreasing waveform (see Figure 15). As in Figure 13 for the ASR-9, Figure 15 shows the roughly 60-millisecond wide main beam of the CARSR.

Since the area under the peak detected time signature of the radar signal is used to automatically detect the radar signals in the data processing (as discussed in Section 6), the dips would affect

the data processing. Since we are only interested in the peak received power over an interval for each data point, we can simply take the peak received power over every two adjacent data points in the sweep to form a new, resampled sweep. This is the same as if the number of data points taken during the measurements had been selected to be 4096 instead of 8192. For these resampled sweeps, each data point represents the peak received power over an interval of

$$\frac{Sweep\ Time\ (\text{sec})}{Number\ Data\ Points - 1} = \frac{25\ sec}{4095} \cong 6.11\ msec.$$

Figure 16 shows the new resampled sweep for the sweep shown in Figure 15. For the CARSR data processing, all measured data will be resampled as described here.

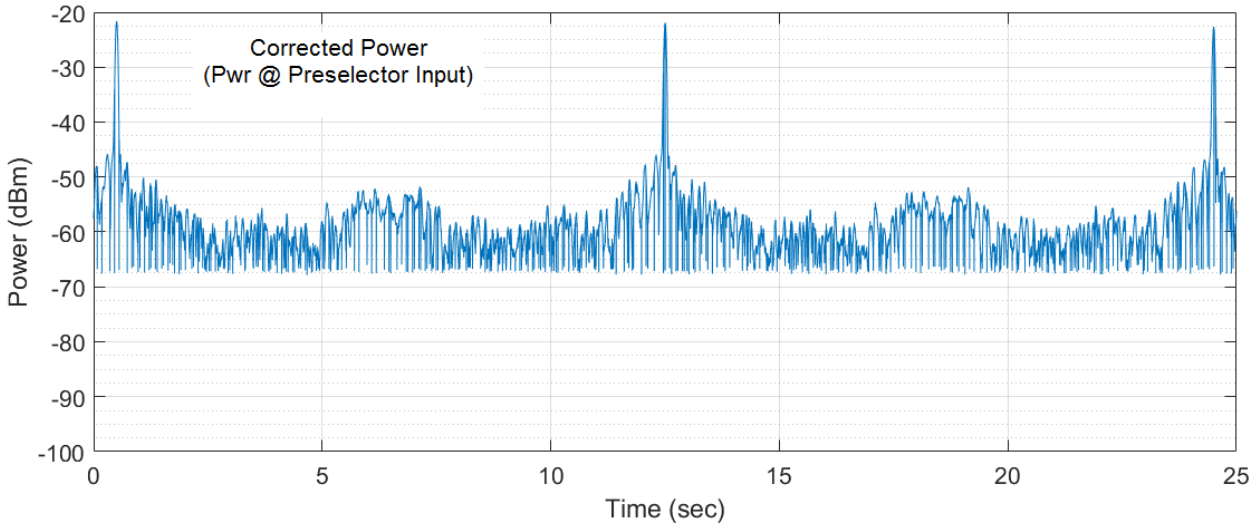

Figure 14. Example of a strong signal received at Location 4 along the 127° Radial for the CARSR.

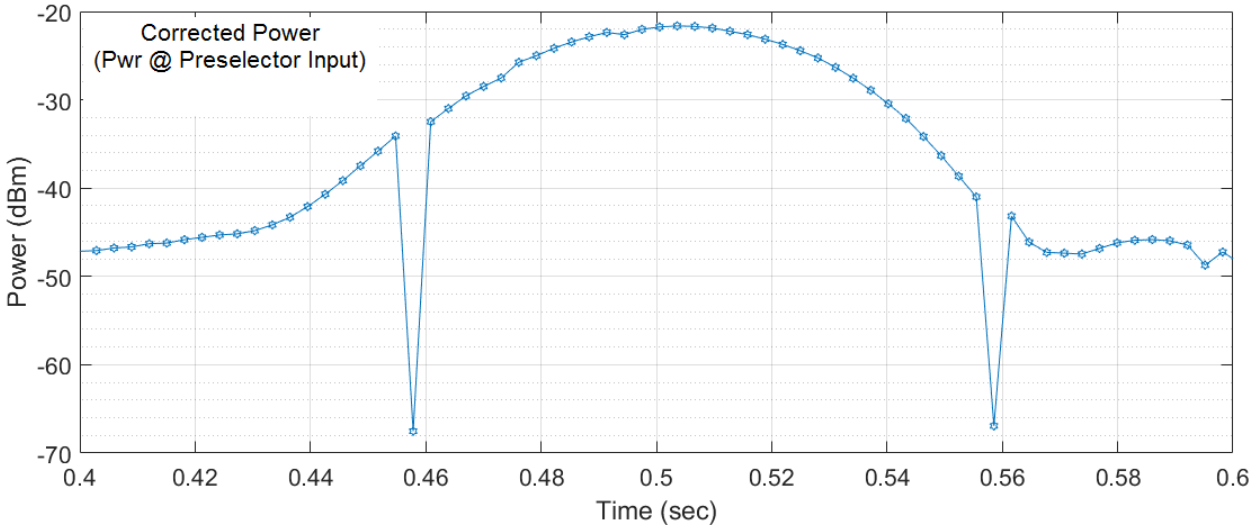

Figure 15. Magnified view of signal received at Location 4 along the 127° Radial for the CARSR.

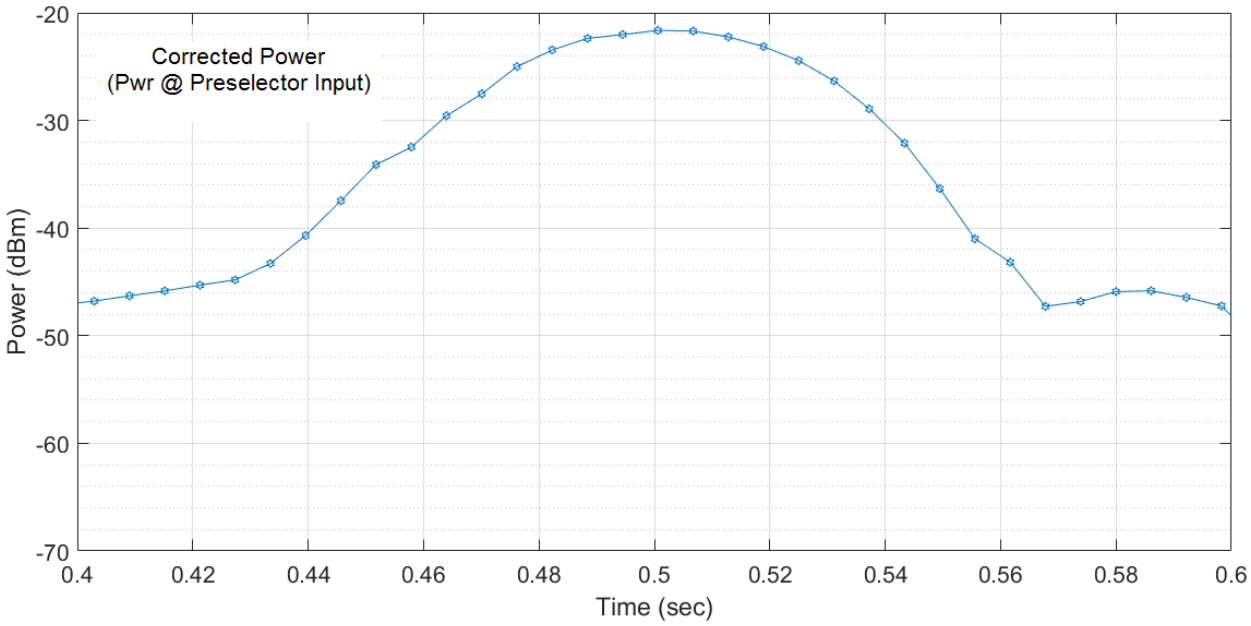

Figure 16. Magnified view of resampled signal received at Location 4 along the 127° Radial for the CARSR.

Figures 12–16 show strong received radar transmissions where radar sidelobe emissions, any multipath, or other propagation effects on the radar signal are not prominent. Received radar signals at many measurement locations, especially further away from the radar, were significantly lower in power and showed these propagation effects more prominently. Figures 17 and 18 show examples of sweeps taken for the ASR-9 and CARSR, respectively where the radar signals were significantly weaker and some of these propagation effects are more prominent. The

four received signal clusters seen in Figure 17 are due to multipath, i.e., signals generated by the radar transmitter including those from reflections off objects in the environment as the radar transmit antenna rotates.

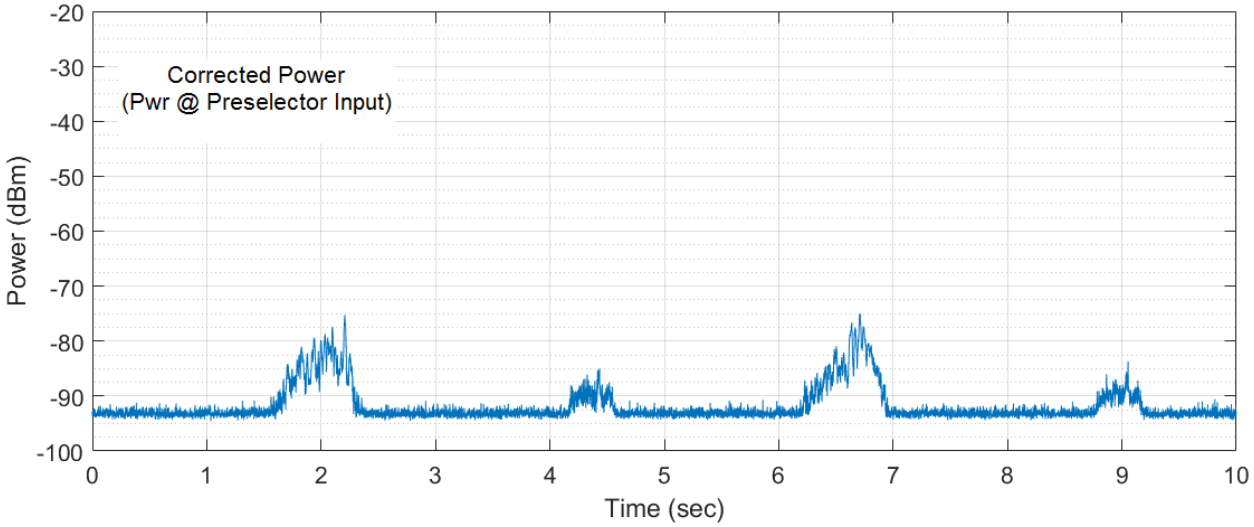

Figure 17. Example of a relatively weak signal received at Location 2 along the 1° Radial for the ASR-9.

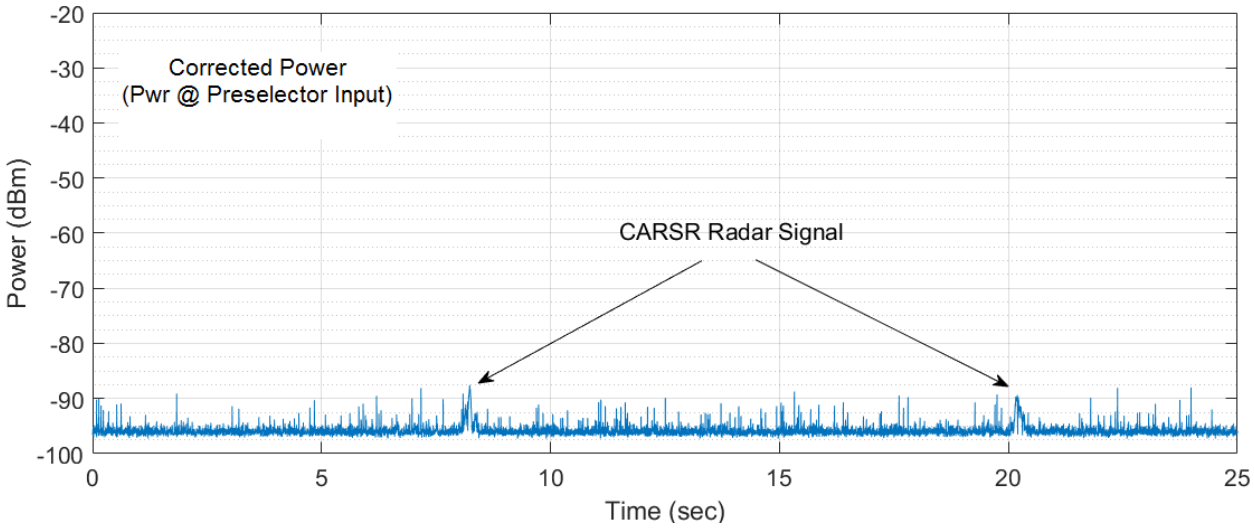

Figure 18. Example of a relatively weak signal received at Location 1b along the 98° Radial for the CARSR.

6. DATA PROCESSING AND ANALYSIS

Accurate peak power measurements of the ASR-9 and CARSR radars at the various measurement locations are required. To accomplish this, the radar signals in each sweep of the raw measured data must be accurately identified and then the peak power in those signals must be determined. An automated data processing algorithm was developed that processes the raw measured data taken at each measurement location. The algorithm identifies the radar signals in each sweep, determines the peak power of these signals, and generates received signal power statistics for all sweeps taken at that measurement location.

The data processing is performed over all fifty sweeps taken at each measurement location. For each of the fifty sweeps taken at each measurement location, the first step in the data processing is to accurately detect the presence of any radar signals. Initially auto- and cross-correlation techniques were investigated to detect the radar signals. The performance of these techniques proved to be inadequate, however. A radar detection technique was developed based on exploitation of the peak detected time signature of the radar. Looking at the peak detected time signatures of the ASR-9 and the CARSR (Figures 13 and 16, respectively) it is seen that these signatures exhibit a significantly larger area under the curve than noise emissions. Therefore a technique was implemented to look for the largest sum of *n* contiguous data points of each sweep which is proportional to an approximation of the area under the curve. This identifies a potential radar signal.

The number of data points to sum, *n*, is chosen to be 10 for the ASR-9 and 8 for the CARSR (resampled sweep). This represents the number of data points in the peak detected time signature that fall roughly within 1 to 2 dB of the peak of the radar signal. Once the largest sum of *n* contiguous data points is found for a sweep, indicating a potential radar signal, the processing algorithm exploits the known rotation period of the radar and looks for other possible radar signals in the sweep.

Recall from Section 5 that data collection is an asynchronous process and, therefore, the initially identified potential radar signal can occur at any time in the sweep. Based on when in time this first identified potential radar signal occurs, a search is performed for other potential radar signals in the sweep. The search is performed in small regions around plus and minus one or two radar rotation periods away from the originally identified potential radar signal. Here, the technique of looking for the largest sum of *n* contiguous data points within a specific region of the sweep is employed again to identify any other potential radar signals in the sweep. Once all potential radar signals in a sweep have been identified (there can be up to three), an additional test is performed on the potential radar signals to determine if they are valid radar signals.

To be considered a valid radar signal, all *n* data points of a potential radar signal must be above a threshold. The threshold is set to a certain amount (6 dB) above the median peak over-the-air system noise power level. The median peak over-the-air system noise power levels are determined by taking the median of the dB values and are shown in Table 1 in Section 2.2. This represents a conservative approach; radar signals can certainly be identified using a lower threshold. However, the power levels determined using a lower threshold may not be accurate.

Once valid radar signals are identified, the received power level of each valid received radar signal is determined. First the *n* data points for each valid radar signal are examined. Any potential noise spikes that appear on these *n* data points (noise spikes were observed at some locations where very weak radar signals were detected) are eliminated from the identification of the maximum received power of the radar. A noise spike is defined here as a data point whose power is more than 3 dB greater than both the previous and the next data points. After any noise spikes are removed from the *n* data points for each radar signal, the maximum power of the remaining data points is used as a measurement of the peak received power of the radar signal.

Recall that the raw measured data provides the peak received power at the RF input to the preselector. These power values are further corrected to provide the peak received power at the RF output of the antenna. The antenna cable loss was measured from the RF output of the antenna to the RF input of the preselector. The antenna cable loss was measured as 1.1 dB for the ASR-9 and 0.9 dB for the CARSR. The peak received power at the RF output of the antenna is found by adding the antenna cable loss to the peak received power at the RF input to the preselector.

For each measurement location, statistics are computed of the peak received power values (referenced to the RF output of the antenna) for all of the valid radar signals over all fifty sweeps. These statistics include a histogram and maximum, minimum, median, 75% quartile, and 25% quartile values. Seventy-five percent of the power values in the data set fall below the 75% quartile. Similarly, 25% of the power values in the data set fall below the 25% quartile. The histograms for each measurement location for both the ASR-9 and CARSR are shown in Appendices A and B. Tables 2 and 3 provide a statistical summary of the peak received power measured at each measurement location for the ASR-9 and the CARSR, respectively.

For each location in Tables 2 and 3, the number of valid radar signals that were determined over all fifty sweeps is provided along with the received power statistics. The latitude and longitude of the location are given as well as the distance from the radar transmitter. The columns for the propagation mode and peak predicted ITM power are provided for future use to provide a convenient way to compare the measured results with ITM predictions. To further facilitate this comparison, Tables 4 and 5 provide radar transmitter and receiver parameters that would be required to perform the ITM predictions for both the ASR-9 and CARSR, respectively.

Looking more closely at the ASR-9 data in Table 2, the median peak received power generally decreases as the distance from the transmitter increases along a radial as would be expected. Locations along the 326° Radial illustrate a significant exception to this general trend. Analysis of the terrain data may help explain deviations from this general trend but was not performed as it was out of scope for this measurement effort. Note that there was only one measurement location (Location 2 along the 326° Radial) where no valid radar signals were found. Location 1 along the 35° Radial and Location 1 along the 326° Radial had only 1 and 3 valid radar signals, respectively. While power measurements were obtained for these locations, sufficient statistics could not be obtained with that few valid radar signals. Although the power measurements out to the predicted spectrum usage contour for the ASR-9 (shown in Figure 10) were obtained, some of the locations had too few valid radar signals to provide statistically significant results. Looking at the minimum peak received power values in Table 2 shows that the lowest power

values that can be accurately measured for the ASR-9 with this measurement system are around -85 dBm (referenced to the antenna RF output terminal).

The CARSR data in Table 3 reveals that the median peak received power decreases as the distance from the transmitter increases along a radial except for some very minor aberrations. Note that there were five measurement locations where no valid radar signals were found. All of these measurement locations were at or near the predicted spectrum usage contour edge. In addition, Location ContEnd along the 1° Radial had only 1 valid radar signal. For the CARSR, power measurements were only able to be made out to the predicted spectrum usage contour along the 1° and 178° Radials as shown in Figure 11. Additionally, the power measurement at Location ContEnd along the 1° Radial, having only 1 data point, is not statistically significant. Looking at the minimum peak received power values in Table 3, shows that the lowest power values that can be accurately measured for the CARSR with this measurement system are around -88 dBm (referenced to the antenna RF output terminal).

From the histograms in Appendix A and B (or the received power statistics in Tables 2 and 3), depending on the location, the variation in power levels at a given location over all fifty sweeps can be small or large. Locations that exhibit only a small variation in power levels typically exhibited a single, smooth, monotonically increasing and then decreasing peak detected time signature for each rotation of the radar with very little detected sidelobe emissions. Examples of these types of data captures are seen in Figures 13 and 16 from Section 5. Although not unequivocally, locations that exhibit only a small variation in power levels tended to be those with fairly high received signal power.

Table 2. Measured received power statistics at measurement locations for the ASR-9 radar in Platteville, Colorado.

Radial (deg)	Location	Lat (deg)	Lon (deg)	Num Valid Signals	Measured Peak Power					Distance from Tx (km)	Prop_Mode	ITM_PeakPwr (dBm)
					Max (dBm)	75% Quart (dBm)	Median (dBm)	25% Quart (dBm)	Min (dBm)			
1	Loc4	40.64099	-104.70846	108	-29.3	-29.9	-30	-30.1	-30.6	45.64552		
1	Loc3	40.90687	-104.71471	107	-42.3	-46.3	-46.5	-46.7	-47.1	75.16377		
1	Loc2	41.17651	-104.70194	108	-68.4	-71.9	-73	-74.1	-76.1	105.11766		
1	Loc1	41.72558	-104.67225	67	-75	-80	-81.9	-83.3	-84.7	166.135		
35	Loc4	40.27942	-104.67788	107	0.3	-0.2	-0.4	-0.5	-0.9	6.49032		
35	Loc3	40.65443	-104.27661	106	-29.5	-30.1	-30.3	-30.5	-30.8	60.2284		
35	Loc2	41.03841	-103.97213	108	-54.7	-59.9	-62.3	-65.1	-71.4	109.75813		
35	Loc1	41.30767	-103.70253	1	-82.4	N/A	-82.4	N/A	-82.4	147.24294		
127	Loc4	40.12233	-104.52809	106	-27.9	-28.7	-28.9	-29.2	-29.7	20.15551		
127	Loc3	39.95651	-104.24559	105	-32.3	-32.6	-32.8	-32.9	-33.3	50.49094		
127	Loc2	39.81043	-103.99916	96	-78	-81.6	-82.4	-83.3	-85.5	77.08816		
127	Loc1	39.52028	-103.52919	19	-77.1	-79.1	-82.1	-83.4	-85.1	128.69735		
178	Loc4	40.02957	-104.71171	107	-29.5	-33.9	-34.8	-35.6	-37.9	22.26313		
178	Loc3	39.60614	-104.69253	106	-41.9	-42.3	-42.4	-42.6	-44.9	69.30533		
178	Loc2	39.02786	-104.66714	12	-75.1	-79.6	-82.7	-83.4	-84.9	133.54319		
178	Loc1	38.92815	-104.66238	108	-75.2	-76	-76.4	-76.9	-77.5	144.62082		
326	Loc4	40.6127	-105.07493	106	-57.3	-61.4	-63.1	-65	-68.2	52.15708		
326	Loc3	41.02805	-105.43359	106	-26.9	-27.8	-27.9	-28	-28.2	107.29645		
326	Loc2	41.31827	-105.65799	0	N/A	N/A	N/A	N/A	N/A	144.54661		
326	Loc1	41.36173	-105.74921	3	-83	N/A	-83.3	N/A	-84.2	152.83701		
Boulder Labs		39.9942	-105.26096	106	-37.6	-39.7	-40.8	-42.1	-44.1	53.1359		

Table 3. Measured received power statistics at measurement locations for the CARSR radar in Parker, Colorado.

Radial (deg)	Location	Lat (deg)	Lon (deg)	Num Valid Signals	Measured Peak Power					Distance from Tx (km)	Prop_Mode	ITM_Peak Pwr (dBm)
					Max (dBm)	75% Quart (dBm)	Median (dBm)	25% Quart (dBm)	Min (dBm)			
1	Loc4	39.63486	-104.72718	104	-17.7	-18.3	-18.5	-18.6	-19.9	5.35864		
1	Loc3	40.08974	-104.61359	102	-57	-58.5	-59.2	-59.8	-61.8	55.44928		
1	Loc2	40.58691	-104.66788	104	-63.5	-66.2	-67.3	-68.1	-69.9	110.25283		
1	Loc1	41.15954	-104.63634	6	-84.9	-85.2	-85.9	-86.7	-87.3	173.88986		
1	ContEnd[7]	41.75535	-104.64876	1	-84.9	N/A	-84.9	N/A	-84.9	240.02427		
35	Loc4	39.74965	-104.56848	102	-34.1	-37.8	-38.7	-39.8	-42.4	20.32905		
35	Loc3	40.14537	-104.18661	100	-68.1	-70.2	-70.7	-71	-73.5	75.01379		
35	Loc2	40.56298	-103.82164	43	-78.8	-84.1	-85	-85.9	-87.4	130.77959		
35	Loc1	40.89718	-103.45879	0	N/A	N/A	N/A	N/A	N/A	178.80594		
35	ContEnd[7]	41.58685	-102.81081	0	N/A	N/A	N/A	N/A	N/A	272.68861		
98	Loc4	39.56553	-104.58811	103	-12.5	-13	-13.1	-13.3	-13.7	9.60576		
98	Loc3	39.57013	-104.4562	101	-47.8	-49.7	-49.8	-49.8	-50	20.57049		
98	Loc2	39.50583	-103.97103	16	-79.9	-83.6	-84.5	-85.5	-86.3	62.87675		
98	Loc1b	39.43258	-103.11754	78	-78.8	-82.5	-83.9	-85.5	-87.4	136.71793		
98	Loc1	39.43351	-103.25454	9	-85.5	-86.1	-86.7	-87	-87	125.03256		
98	ContEnd[7]	39.30864	-102.29719	0	N/A	N/A	N/A	N/A	N/A	208.68272		
127	Loc4	39.53636	-104.56937	104	-19.9	-20.7	-21	-21.3	-21.9	12.45679		
127	Loc3	39.49154	-104.51561	101	-37.8	-38.6	-38.8	-39.1	-39.7	19.07716		
127	Loc2	39.13699	-103.92039	100	-72.1	-83.3	-83.6	-83.8	-84.9	83.76435		
127	Loc1	39.04054	-103.75806	33	-77.8	-83.4	-85.1	-86	-87.9	101.42465		
127	NewContEnd[7]	38.73512	-102.77660	0	N/A	N/A	N/A	N/A	N/A	191.16031		
178	Loc4	39.46281	-104.68978	101	-16.2	-17	-17.2	-17.4	-18.2	14.58823		

[7] ContEnd, NewContEnd, and NearContEnd refer to supplementary measurement locations along the various radials near the CARSR spectrum usage contour as seen in Figure 11.

Radial (deg)	Location	Lat (deg)	Lon (deg)	Num Valid Signals	Measured Peak Power					Distance from Tx (km)	Prop_Mode	ITM_Peak Pwr (dBm)
					Max (dBm)	75% Quart (dBm)	Median (dBm)	25% Quart (dBm)	Min (dBm)			
178	Loc3	39.37527	-104.68648	101	-35.2	-35.6	-35.8	-36.1	-36.8	24.31032		
178	Loc2	38.99905	-104.66913	103	-78.5	-79.5	-79.8	-80.2	-81.1	66.10464		
178	Loc1	38.19791	-104.63139	102	-79	-80.1	-80.6	-81.1	-84.5	155.0973		
178	NearContEnd[7]	37.73496	-104.65983	102	-81.6	-82.2	-82.4	-82.6	-83.6	206.41		
178	ContEnd[7]	37.80238	-104.64069	0	N/A	N/A	N/A	N/A	N/A	198.95927		

Table 4. ASR-9 radar transmitter and receiver parameters for ITM predicted power.

Tx Pwr	1000000 W
Tx Freq	2715.00 MHz
Tx Ant Gain	33.0 dBi
Rx Ant Gain	-0.3 dBi
Tx Lat	40.23°
Tx Lon	-104.71861110°
Tx Height	9.0 m
Rx Height	3.0 m

Table 5. CARSR radar transmitter and receiver parameters for ITM predicted power.

Tx Pwr	75000 W
Tx Freq	1320.59 MHz
Tx Ant Gain	33.0 dBi
Rx Ant Gain	-4.1 dBi
Tx Lat	39.59416667°
Tx Lon	-104.69361110°
Tx Height	14.0 m
Rx Height	3.0 m

7. SUMMARY

The objective of this work was to conduct received signal power measurements on select air traffic control radars and provide measured data results that can be used (in a separate effort) to validate spectrum usage contours and the Quantitative Assessments of Spectrum Usage methodology used to generate them, as developed by OSM. To achieve the objective, ITS performed received signal power measurements on two radars: the CARSR operating in the 1300–1370 MHz band in Parker, Colorado and the ASR-9 operating in the 2700–2900 MHz band in Platteville, Colorado. Measurements were taken at a received antenna height roughly 3 m AGL, using the ITS modified Chevrolet Express 3500 Extended Cargo Van. A set of fixed-location measurements were taken along radials extending from each radar transmitter. Multiple measurements at each fixed location were made to provide statistically significant results.

The measurement system consisted of an antenna, an ITS custom-built preselector, a spectrum analyzer, a GPS antenna and receiver, and an ITS custom-built measurement controller. Automated control of the preselector and spectrum analyzer is provided by the measurement controller. The spectrum analyzer, GPS antenna and receiver, and measurement controller combination collects the received signal RF peak power measurement data tagged with location information, formats the data, and saves the data to a local hard drive on the measurement controller.

Measurement sites were chosen roughly along radials emanating from the transmitter locations. Five radials for each radar transmitter were chosen. An attempt was made to select four or five measurement locations along each radial for each transmitter where the predicted received signal power (determined from ITM) varied from a relatively strong to weak (but still detectable) level. An attempt was also made to select locations along the radials where as many different propagation modes as possible could be represented.

The radar measurements were made using the swept-measurement mode of the RSMS-5G software. The spectrum analyzer was set up in the zero-span mode (providing time-domain measurements) using peak detection, a 3 MHz RBW, and with a sweep time set slightly longer than two times the rotation period of the radar to be measured. Fifty spectrum analyzer sweeps were taken at each location. The number of sweeps was chosen to be as large as practicable to provide statistically significant results of peak received signal power.

An automated data processing algorithm was developed that processes the raw measured data taken at each measurement location. The algorithm identifies the radar signals in each sweep, determines the peak power of these signals (referenced to the RF output of the antenna), and generates peak received signal power statistics for all fifty sweeps taken at that measurement location.

For the ASR-9, the median peak received power generally decreased as the distance from the transmitter increased along a radial as would be expected. Locations along the 326° Radial illustrate a significant exception to this general trend. Analysis of the terrain data may help explain deviations from this general trend but was not performed as it was out of scope for this measurement effort. For the CARSR, the median peak received power also decreased as the distance from the transmitter increased along a radial except for some very minor aberrations.

Although the power measurements out to the predicted spectrum usage contour for the ASR-9 were obtained, some of the locations had too few valid radar signals to provide statistically significant results. For the CARSR, power measurements were only able to be made out to the predicted spectrum usage contour along the 1° and 178° Radials. Additionally, the power measurement at Location ContEnd along the 1° Radial, having only one data point, was not statistically significant.

A considerable amount of insightful, statistically significant data were collected during the measurement campaign. However, as noted above, statistically significant results were unobtainable for some locations far from the transmitter. Ideas for improving the measurements periodically surfaced during the measurement campaign. While it was not feasible to implement these during this set of measurements, they will be considered for future efforts. These potential improvements are described in the recommendations below.

1) Select locations based on roads. Instead of running ITM on radials from the transmitter, consider running ITM along available roads if possible. Locations should be selected as close as possible to major roads. A lot of time was spent driving on small, rural dirt roads to access locations. Measurement time could be saved if driving long distances on rural, dirt roads could be eliminated or minimized.

2) Radio noise from the measurement van gasoline generator was noticeable at 1300 MHz but not at 2740 MHz. Using a diesel generator would most likely reduce radio noise emissions, but this would need to be tested to know for sure. Using a diesel generator would require towing the generator, which would make maneuverability significantly more difficult and therefore may not be a viable option. Radio noise from the measurement van engine itself was not measured as all fixed location measurements were performed with the vehicle engine turned off. If the vehicle engine needed to be running for future fixed-location measurements (e.g., to run the air conditioner) or for mobile measurements, radio noise measurements using the measurement van engine itself should be taken.

3) Captures of the radar were made to ensure that the peak power in the radar was recorded. Recordings were made using the E4440A spectrum analyzer with the peak detector in zero-span mode. The sweep time was set to capture at least two radar rotations with a RBW of 3 MHz. The number of points per sweep was set to the maximum (8192) to give the finest time resolution. While the peak power of the radar is captured and the peak of every pulse of the radar that the receiver can detect is captured, for the CARSR sometimes the spectrum analyzer display points show the peak of the radar emission between pulses. While this does not affect the ability to capture the peak power of the radar it makes the displayed data less aesthetically pleasing and makes the data processing slightly more difficult. A recommendation for any future testing is to decrease the number of points per sweep to ensure that every display point could capture at least one peak of each radar pulse (if it can be detected/received). This would mean that the number of points per sweep should be chosen such that (Sweep Time / (# Points – 1)) is slightly greater than the maximum expected time between radar pulses.

4) Practical limitations of the measurement system sensitivity made measurements at or near the contours difficult or impossible due to the very low signal levels. The measurement system

and methodology used for these measurements were based on conventional, well-tested, and proven methods. These methods, while providing solid measurement results, suffered from the limitation of modest system sensitivity. Alternative methods of measurement may be considered for future work to try to alleviate this limitation; however, it may not be practicable to use alternative methods.

8. ACKNOWLEDGEMENTS

The authors would like to thank the following individuals for their efforts in helping to complete this project: Frank Sanders, drawing on his experience and expertise on radar systems, provided the basis for developing the measurement methodology used. Stephen McCormick of First RF Corporation was instrumental in teaching us the use of the antenna turntable for performing the antenna gain and pattern measurements at Table Mountain. Additional thanks go to Erik Hill and Christopher Anderson for their assistance in performing the antenna measurements at Table Mountain. William Kozma helped perform field measurements, providing a much-needed respite for the primary measurement team. Finally, special thanks go to Michael Cotton for his assistance and guidance during all phases of this project, especially in performing field measurements to assist the primary measurement team. Without the assistance of these individuals, this work would not have been possible.

9. REFERENCES

[1] National Telecommunications and Information Administration, *Quantitative Assessments of Spectrum Usage* (Nov. 17, 2016), available at https://www.ntia.doc.gov/report/2016/quantitative-assessments-spectrum-usage.

[2] Anita G. Longley; Philip L. Rice, "Prediction of Tropospheric Radio Transmission Loss Over Irregular Terrain: A Computer Method - 1968," NTIA Technical Report ERL 79-ITS 67, July 1968

APPENDIX A: RECEIVED POWER HISTOGRAMS FOR ASR-9 MEASUREMENTS

This appendix contains the received radar signal power histograms and maximum, median, minimum, 75% quartile, and 25% quartile statistics for each measurement location for the ASR-9 measurements. The received signal power was too low to accurately measure (i.e., no valid radar signals could be determined) at one measurement location as listed in Table A-1; accordingly, no histograms or statistics for this location are shown.

Table A-1. ASR-9 measurement locations with received signal power too low to accurately measure

Radial (deg)	Location	Lat (deg)	Lon (deg)	Distance from Tx (km)
326	Loc2	41.31827	-105.65799	144.54661

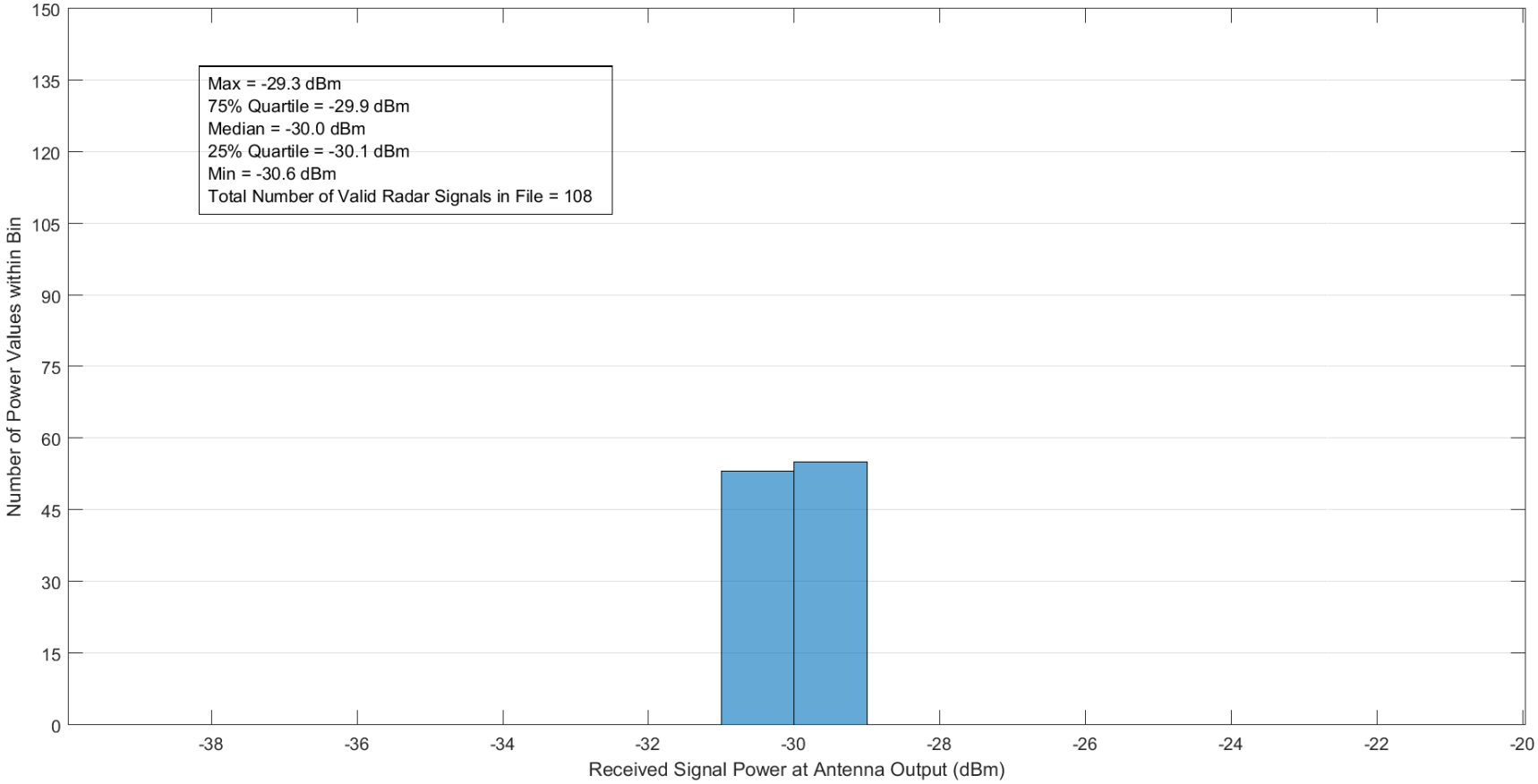

Figure A-1. Received radar signal power statistics at Location 4 along the 1° Radial for the ASR-9.

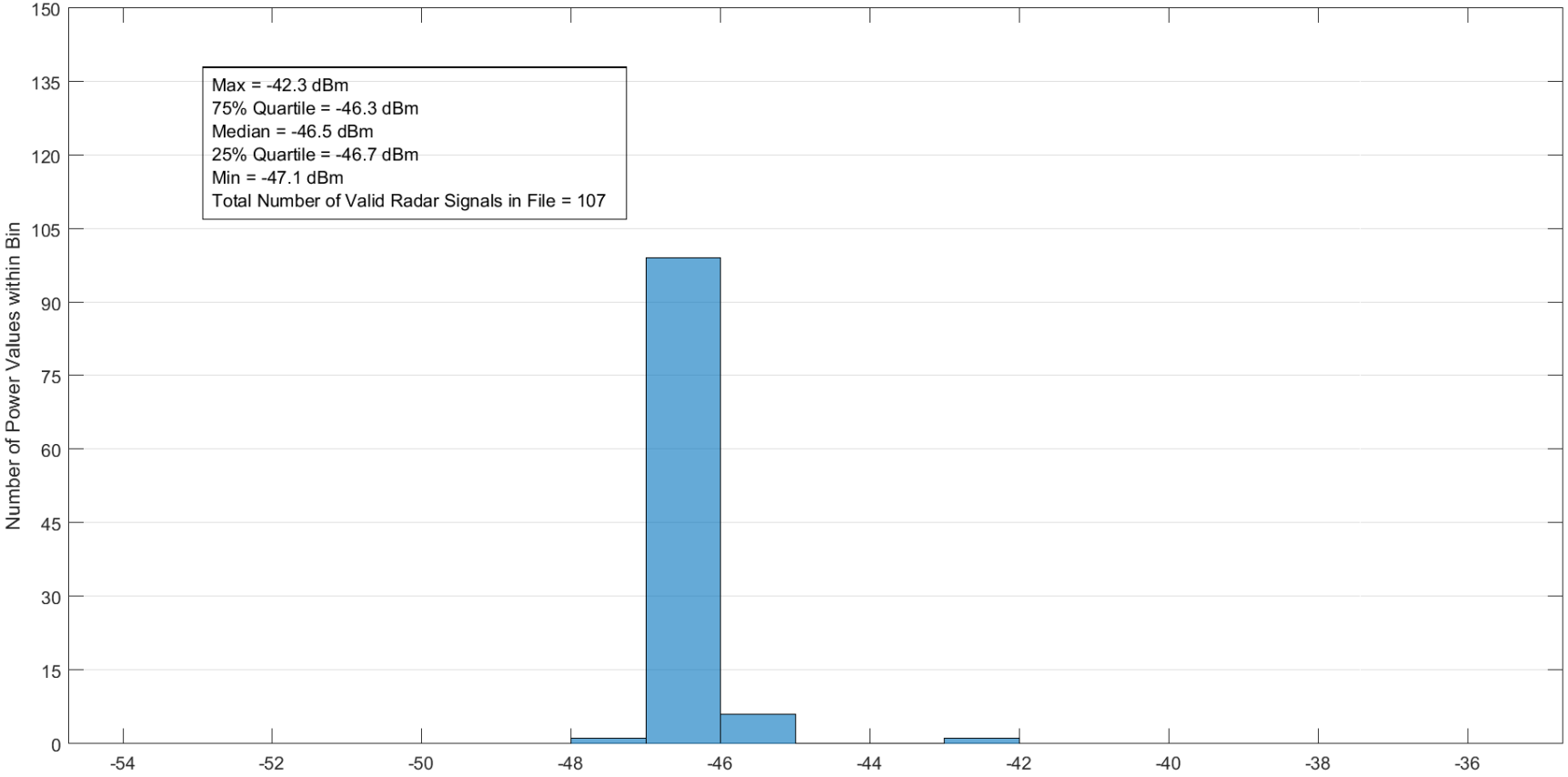

Figure A-2. Received radar signal power statistics at Location 3 along the 1° Radial for the ASR-9.

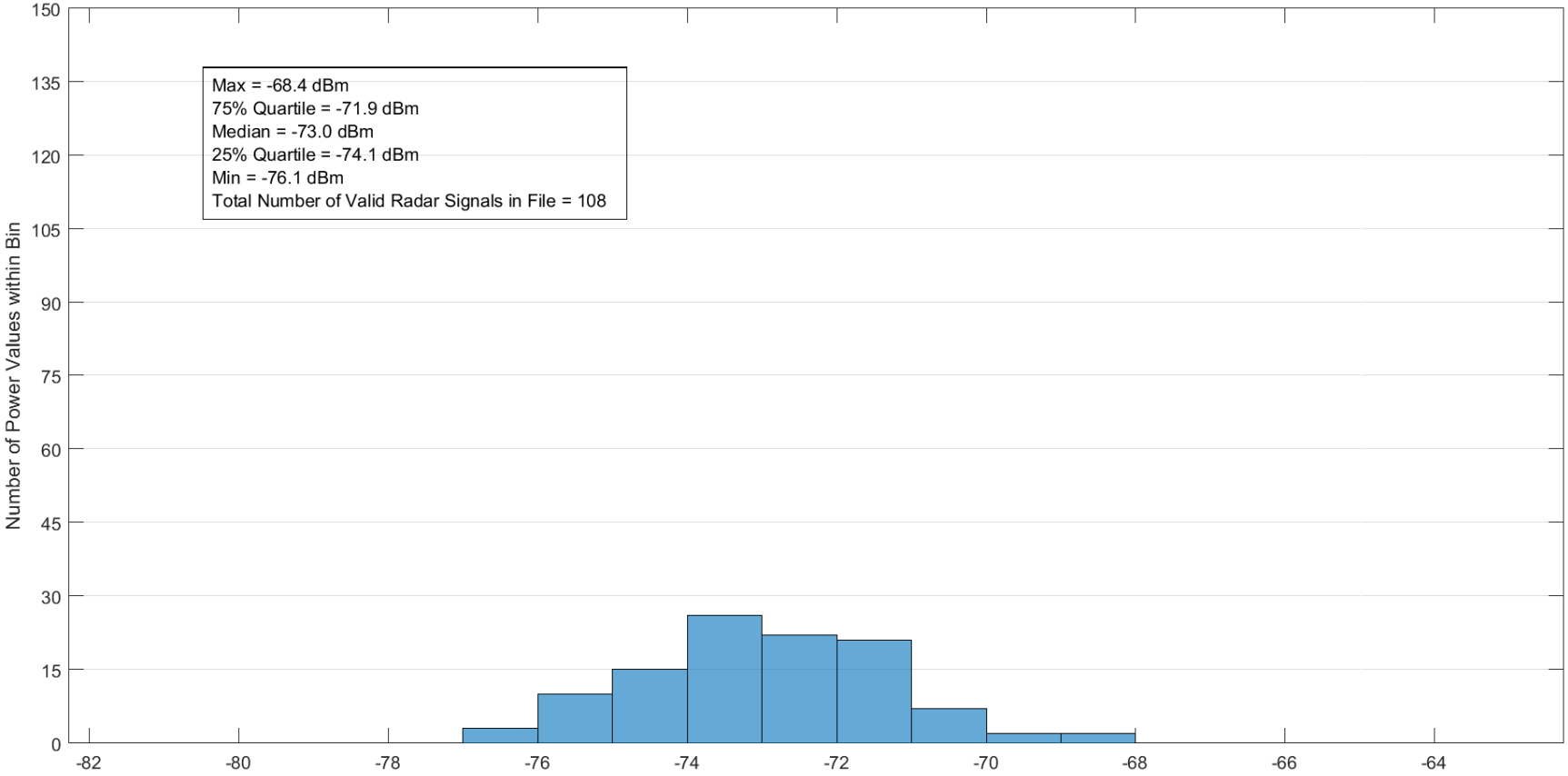

Figure A-3. Received radar signal power statistics at Location 2 along the 1° Radial for the ASR-9.

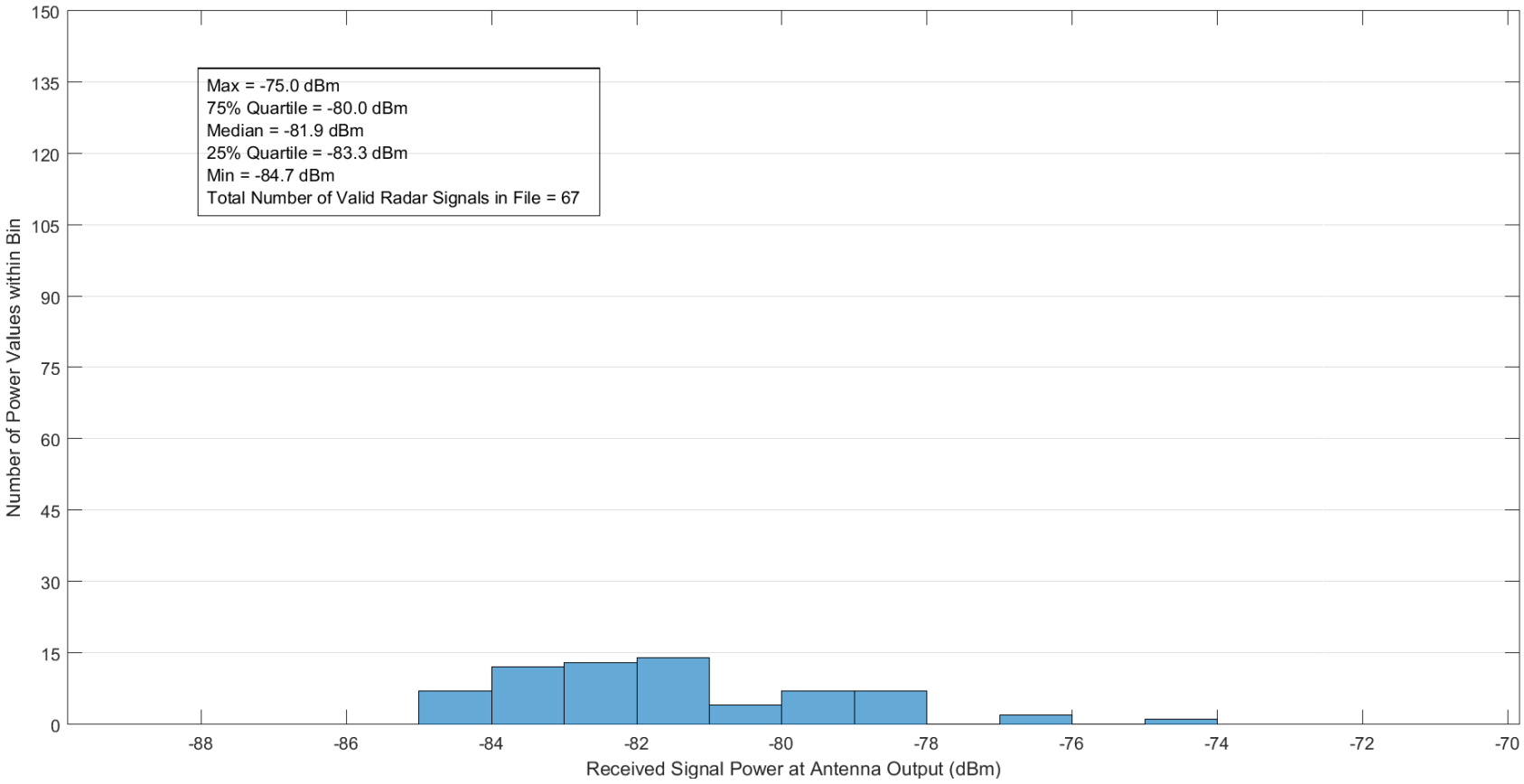

Figure A-4. Received radar signal power statistics at Location 1 along the 1° Radial for the ASR-9.

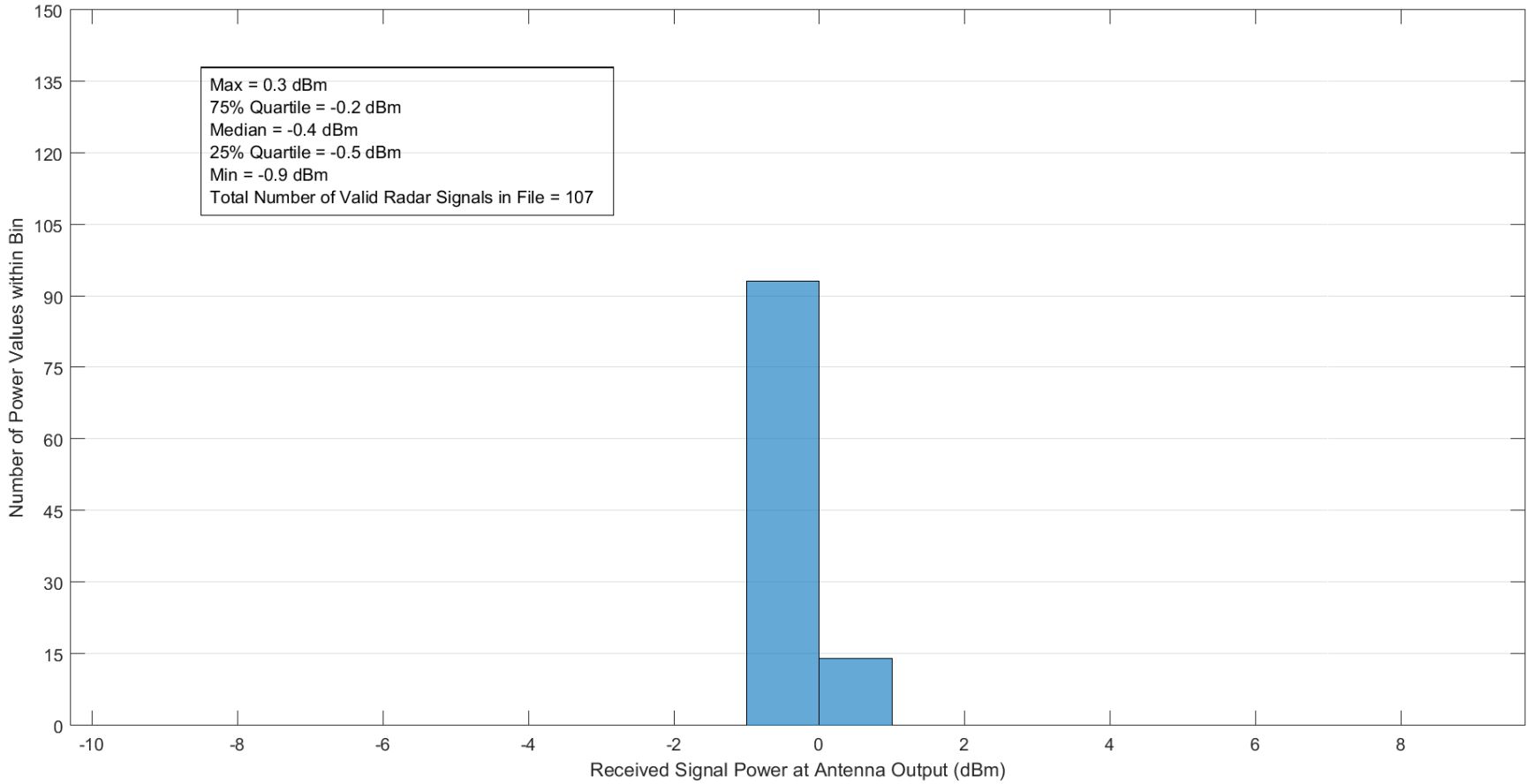

Figure A-5. Received radar signal power statistics at Location 4 along the 35° Radial for the ASR-9.

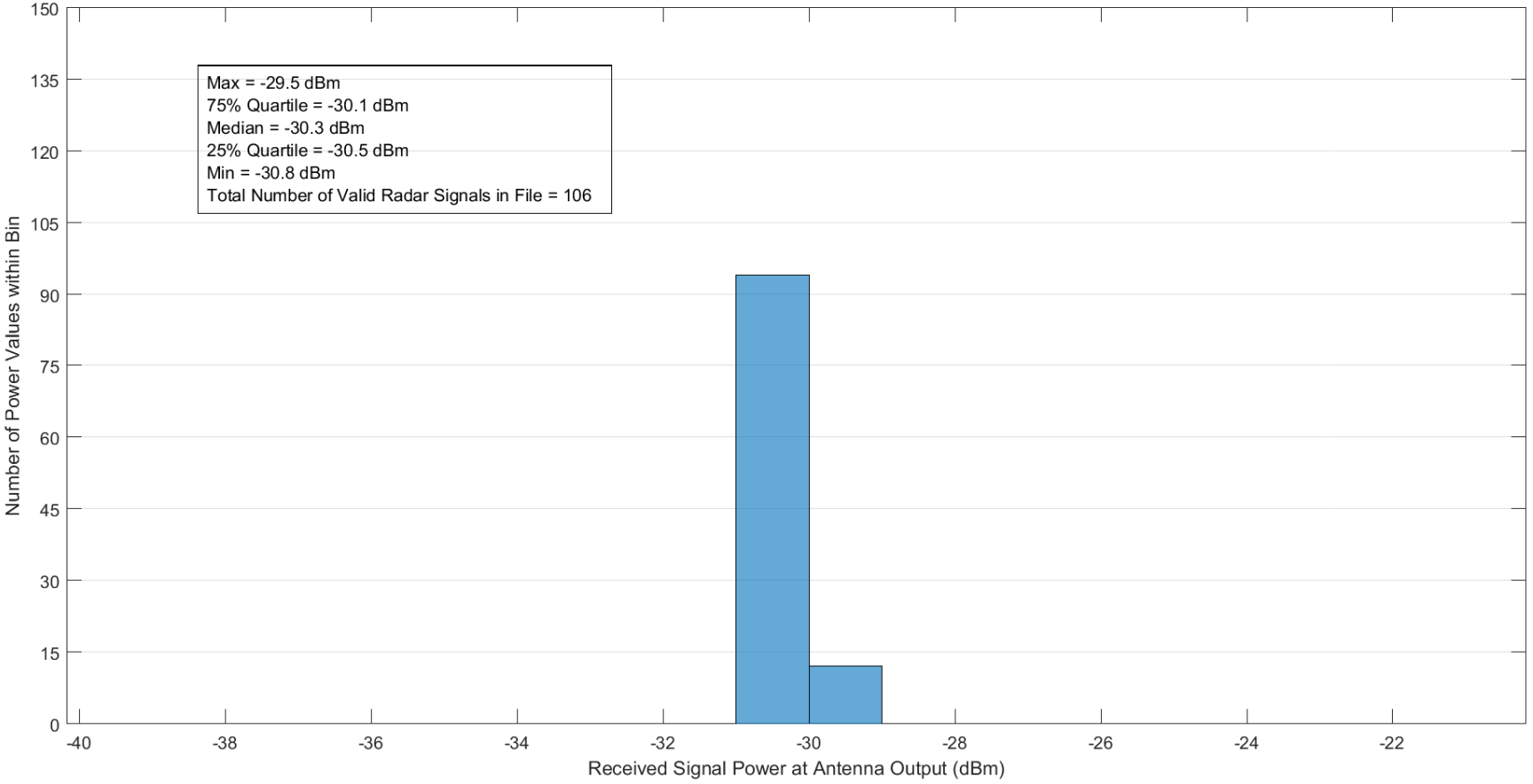

Figure A-6. Received radar signal power statistics at Location 3 along the 35° Radial for the ASR-9.

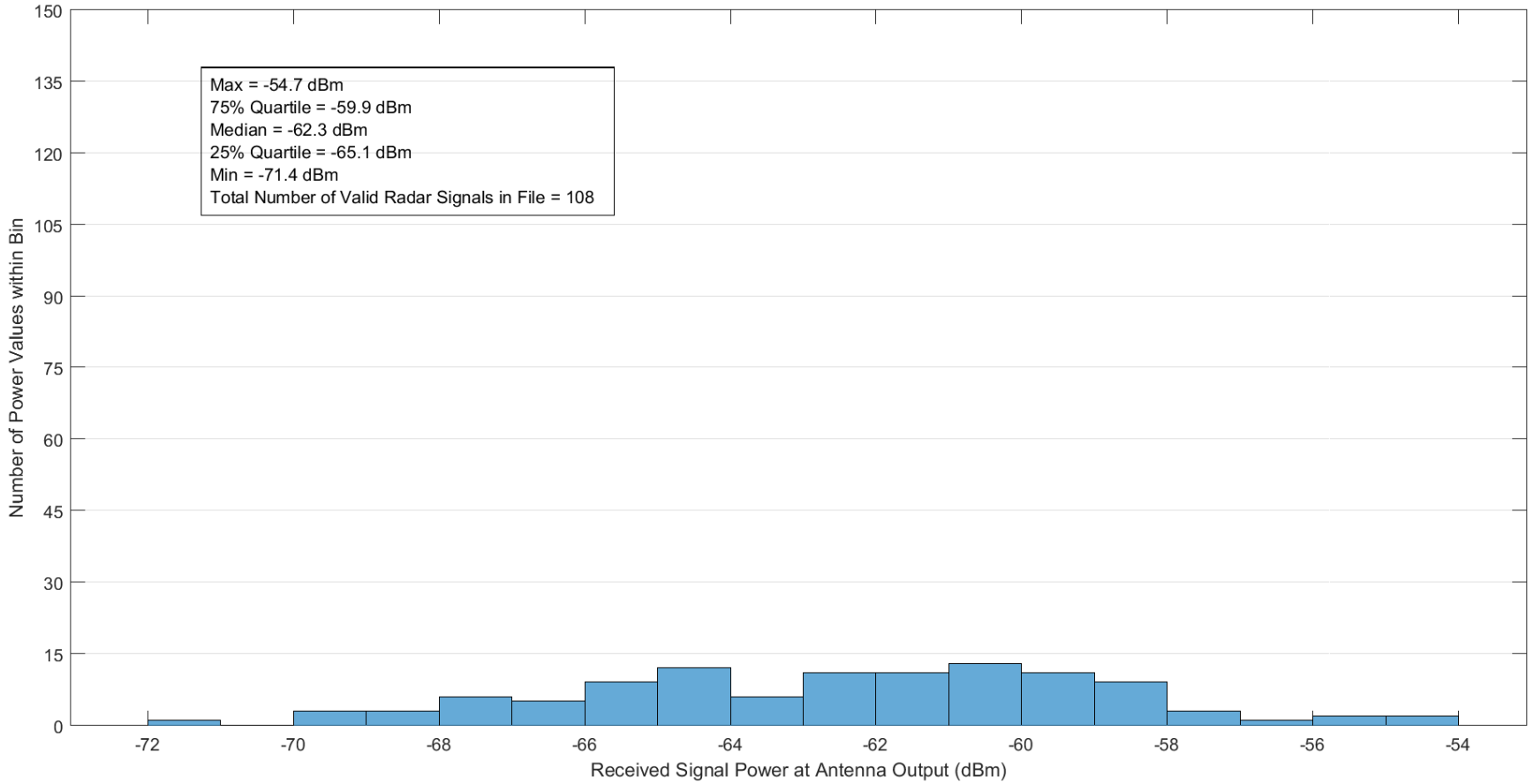

Figure A-7. Received radar signal power statistics at Location 2 along the 35° Radial for the ASR-9.

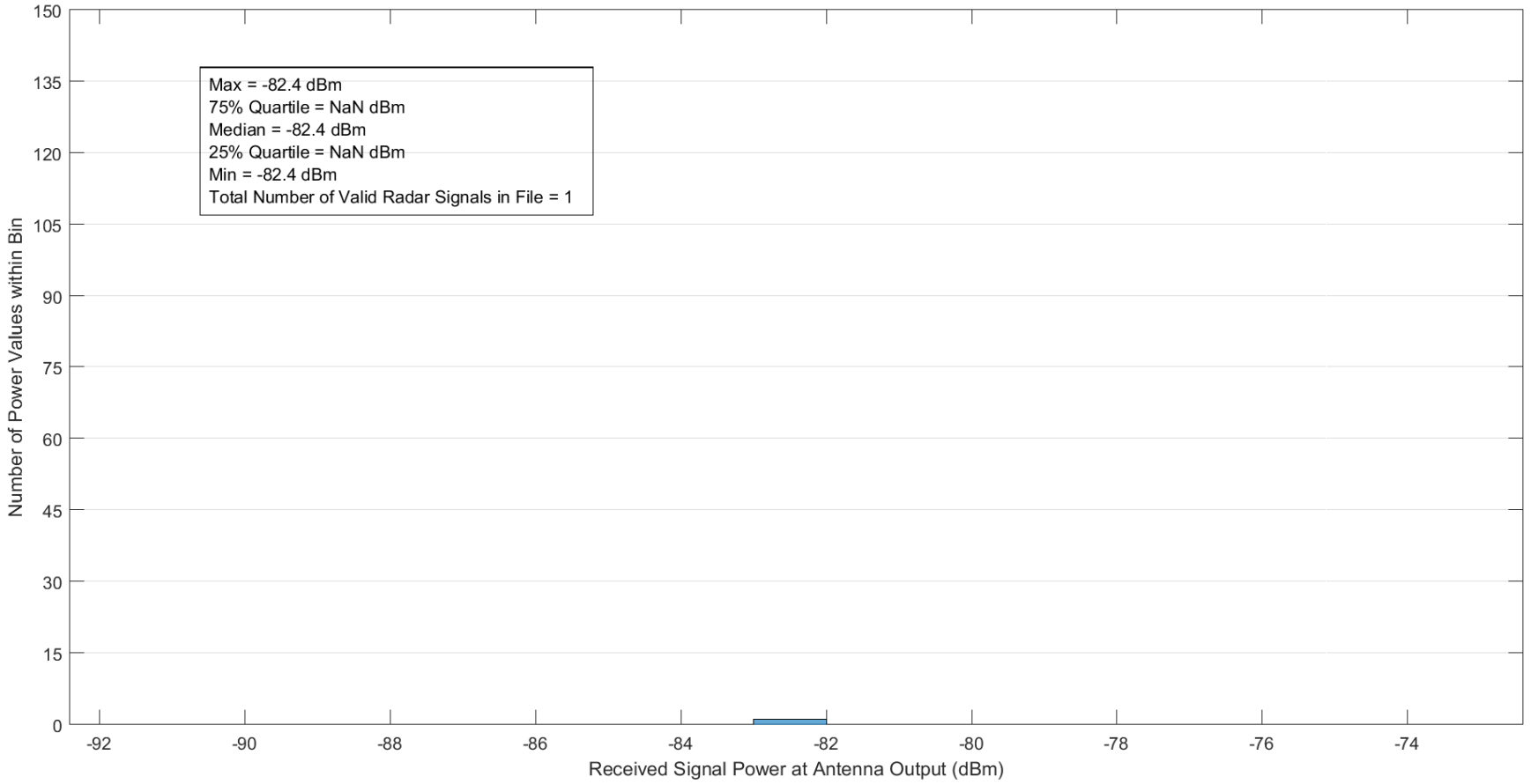

Figure A-8. Received radar signal power statistics at Location 1 along the 35° Radial for the ASR-9.

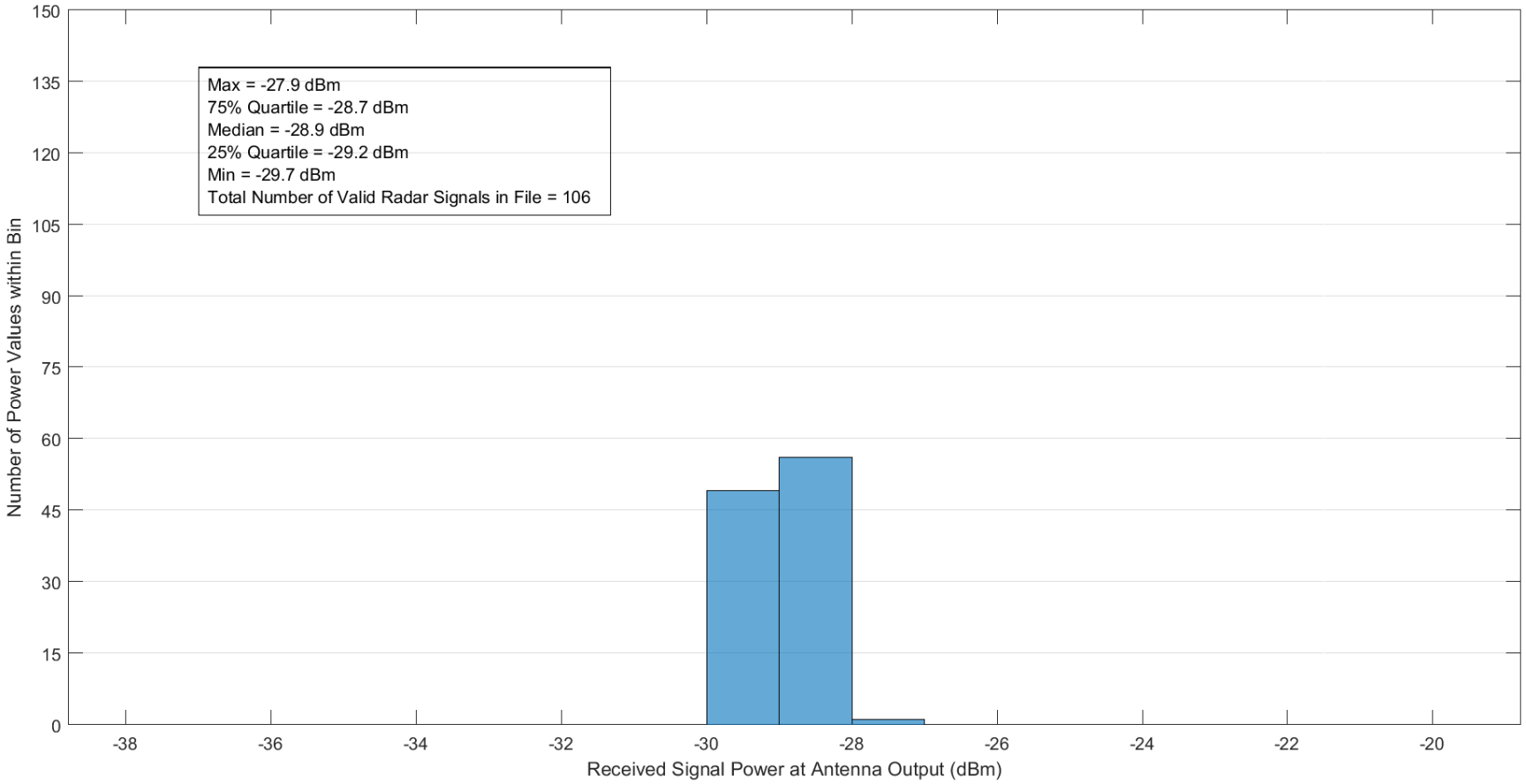

Figure A-9. Received radar signal power statistics at Location 4 along the 127° Radial for the ASR-9.

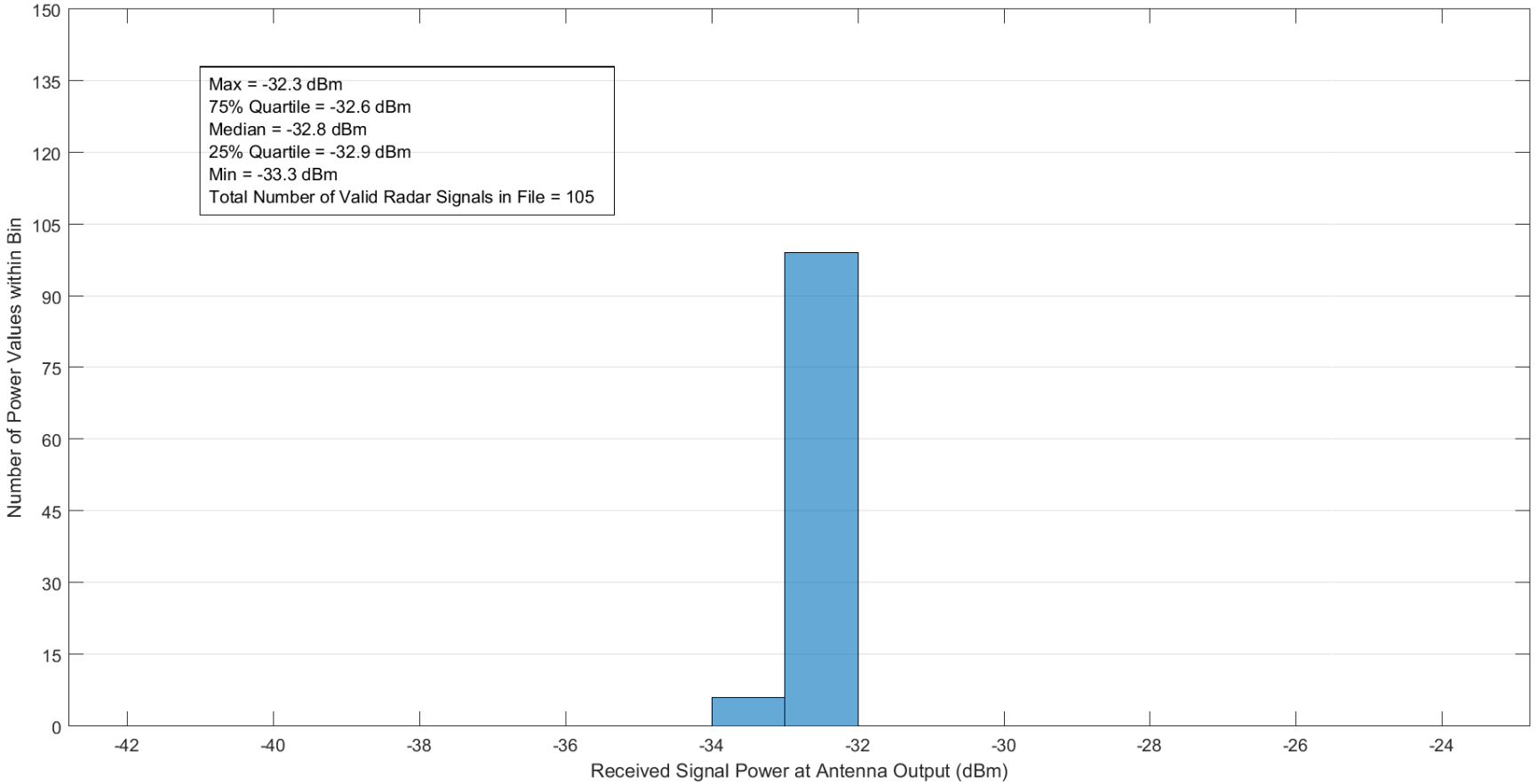

Figure A-10. Received radar signal power statistics at Location 3 along the 127° Radial for the ASR-9.

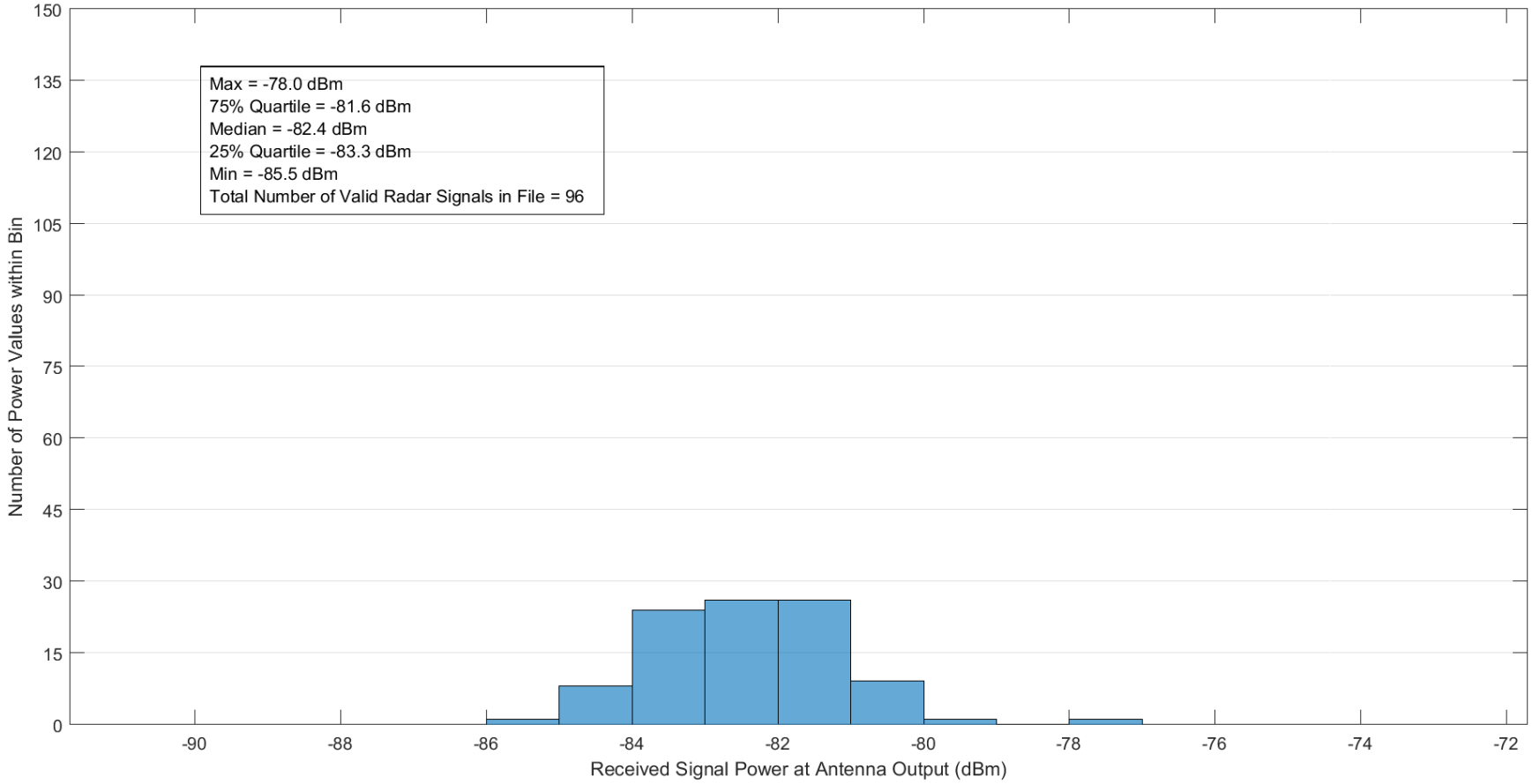

Figure A-11. Received radar signal power statistics at Location 2 along the 127° Radial for the ASR-9.

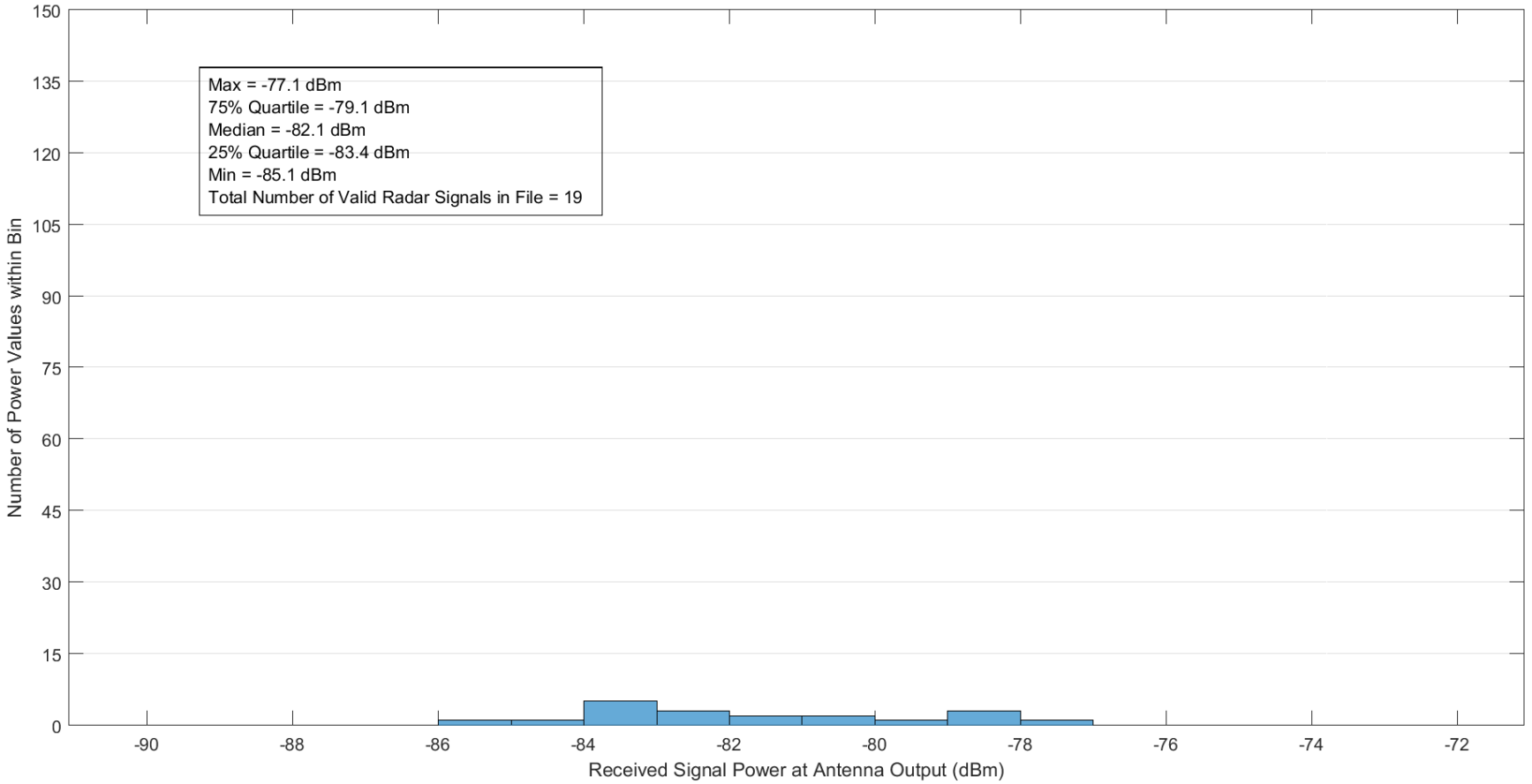

Figure A-12. Received radar signal power statistics at Location 1 along the 127° Radial for the ASR-9.

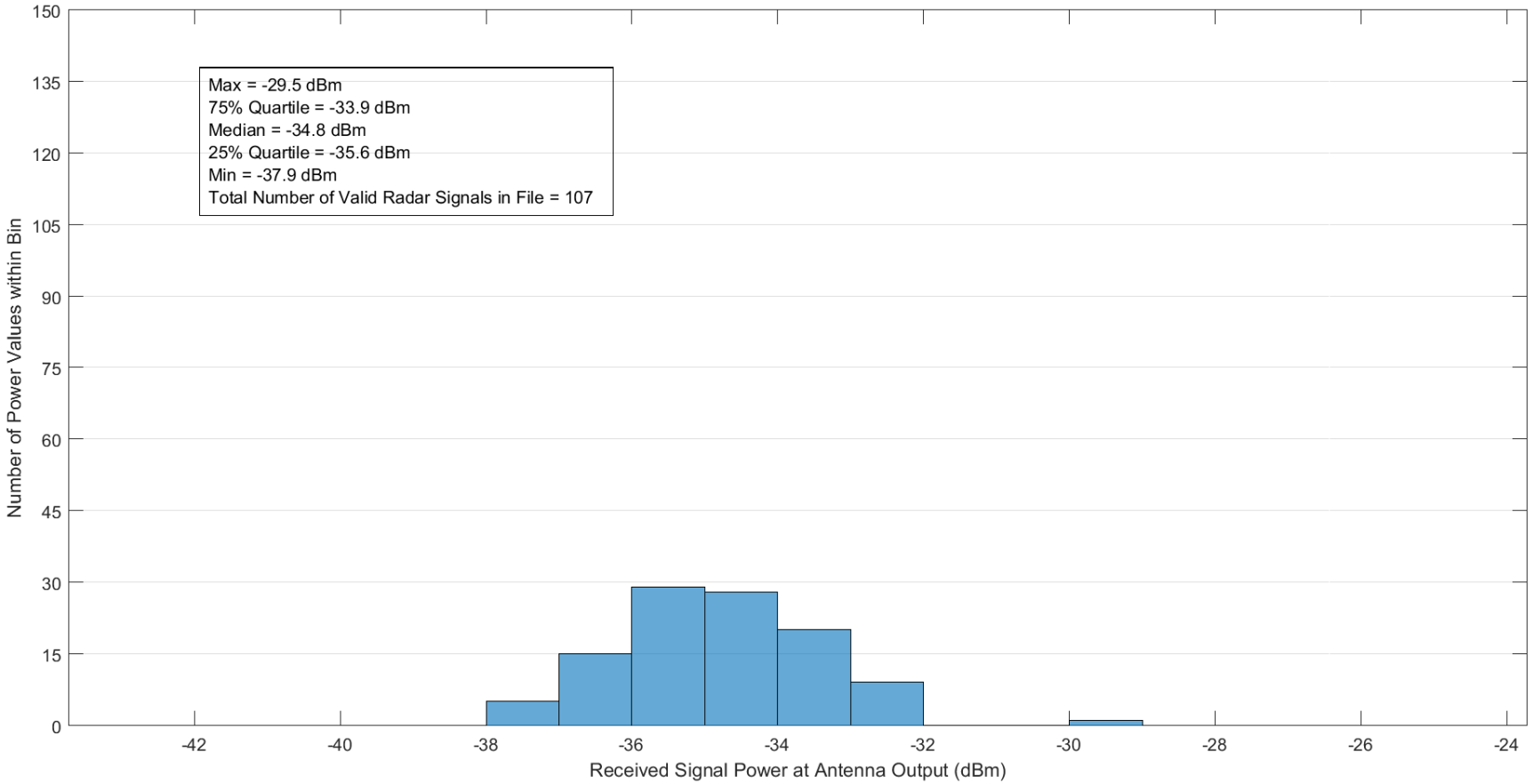

Figure A-13. Received radar signal power statistics at Location 4 along the 178° Radial for the ASR-9.

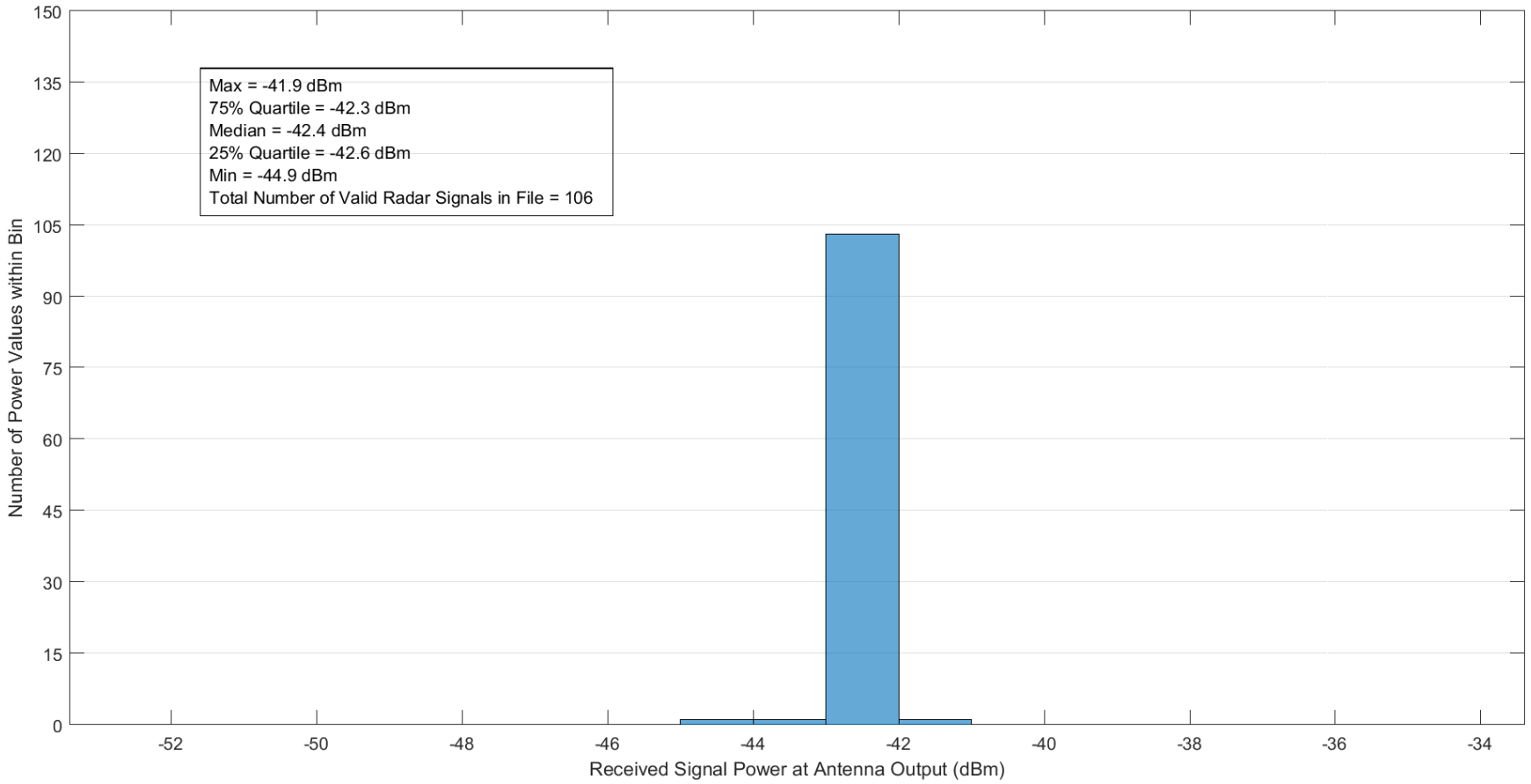

Figure A-14. Received radar signal power statistics at Location 3 along the 178° Radial for the ASR-9.

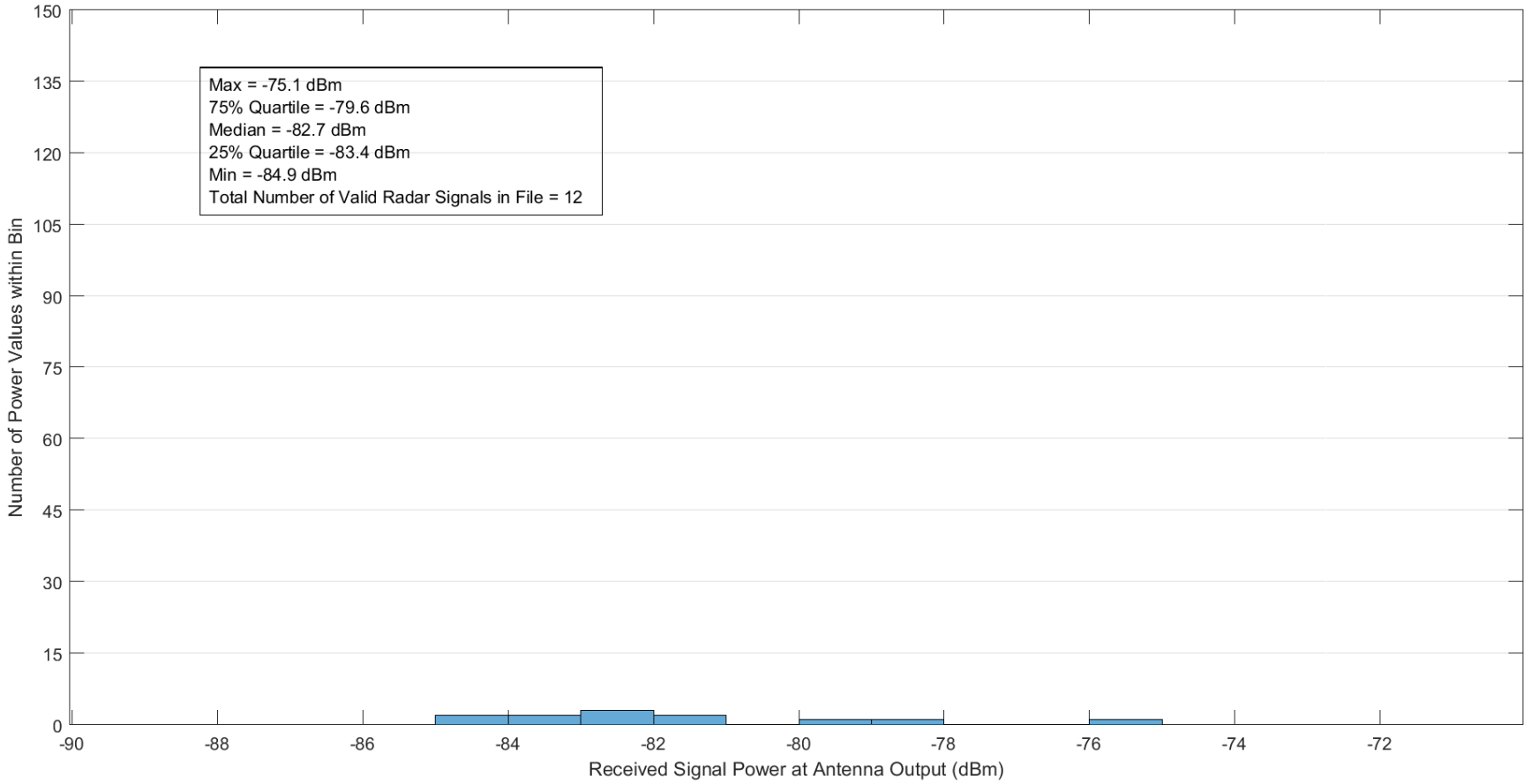

Figure A-15. Received radar signal power statistics at Location 2 along the 178° Radial for the ASR-9.

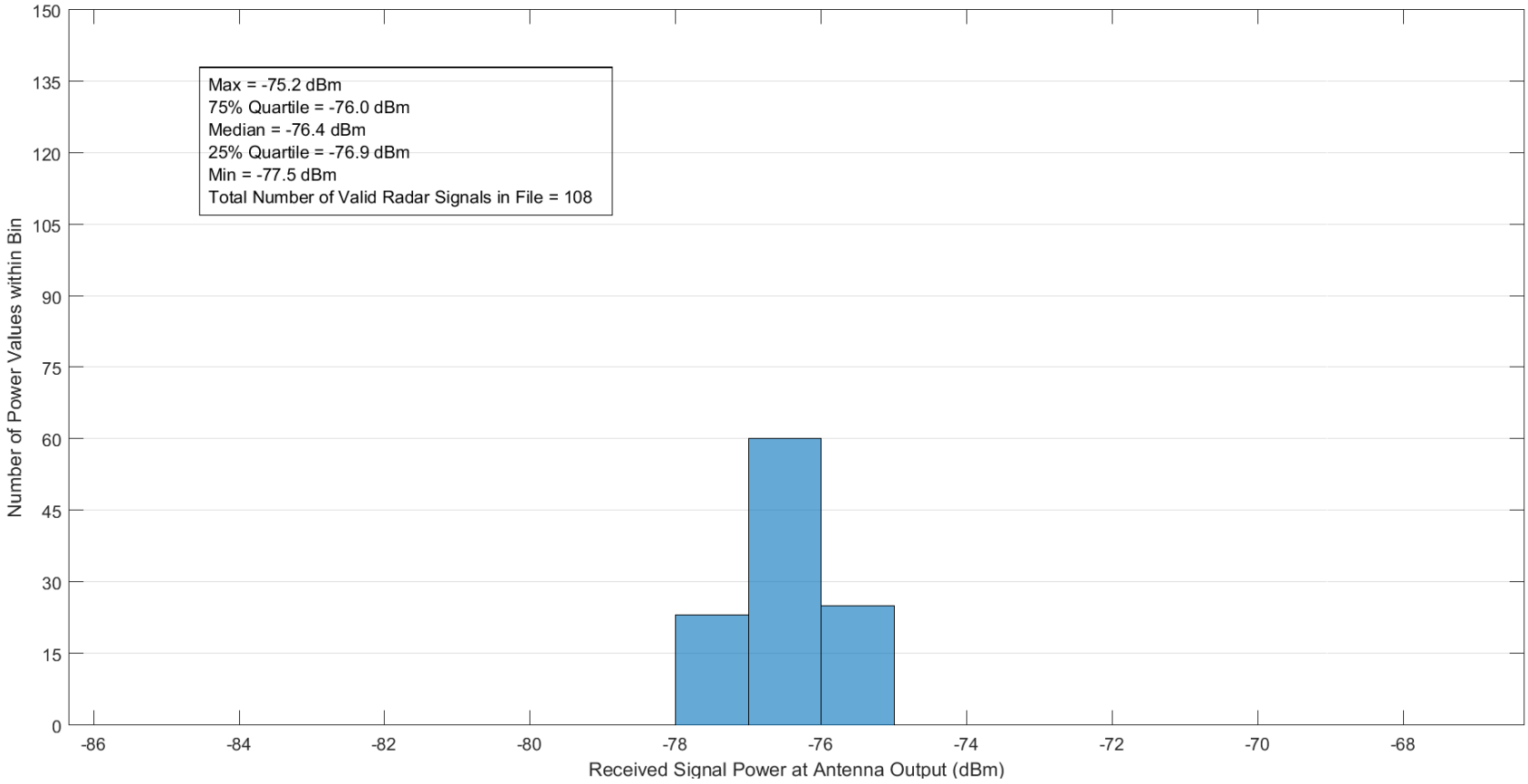

Figure A-16. Received radar signal power statistics at Location 1 along the 178° Radial for the ASR-9.

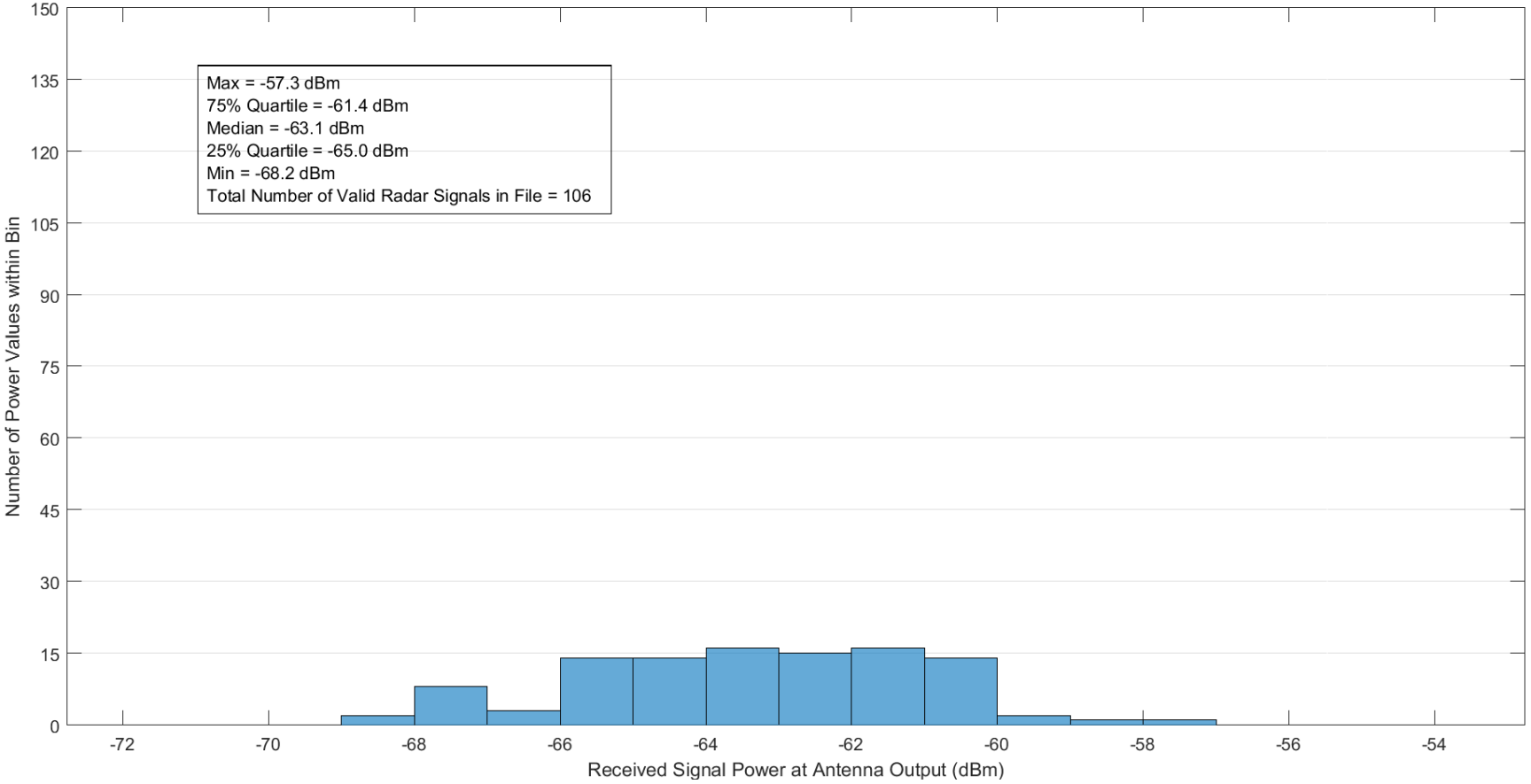

Figure A-17. Received radar signal power statistics at Location 4 along the 326° Radial for the ASR-9.

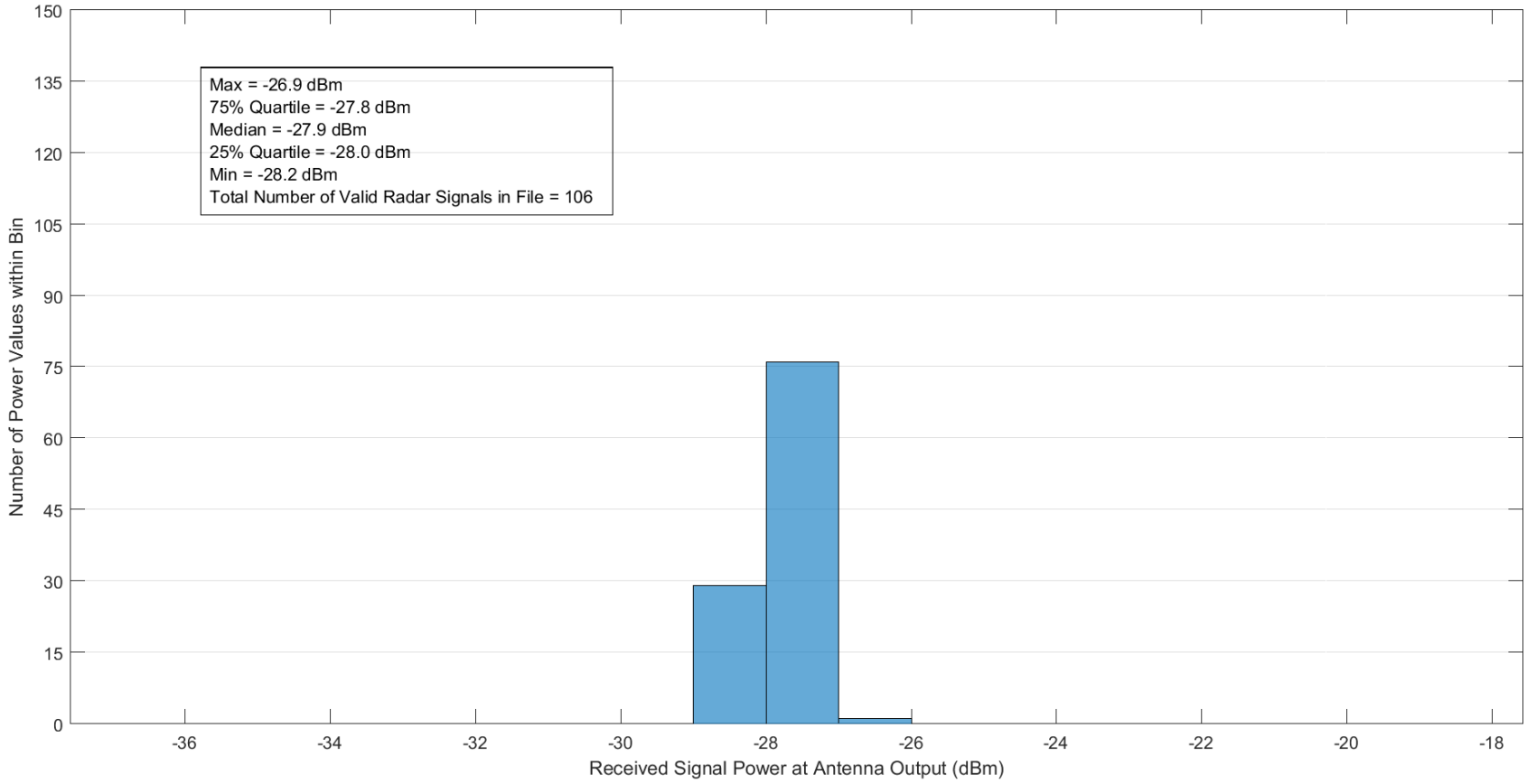

Figure A-18. Received radar signal power statistics at Location 3 along the 326° Radial for the ASR-9.

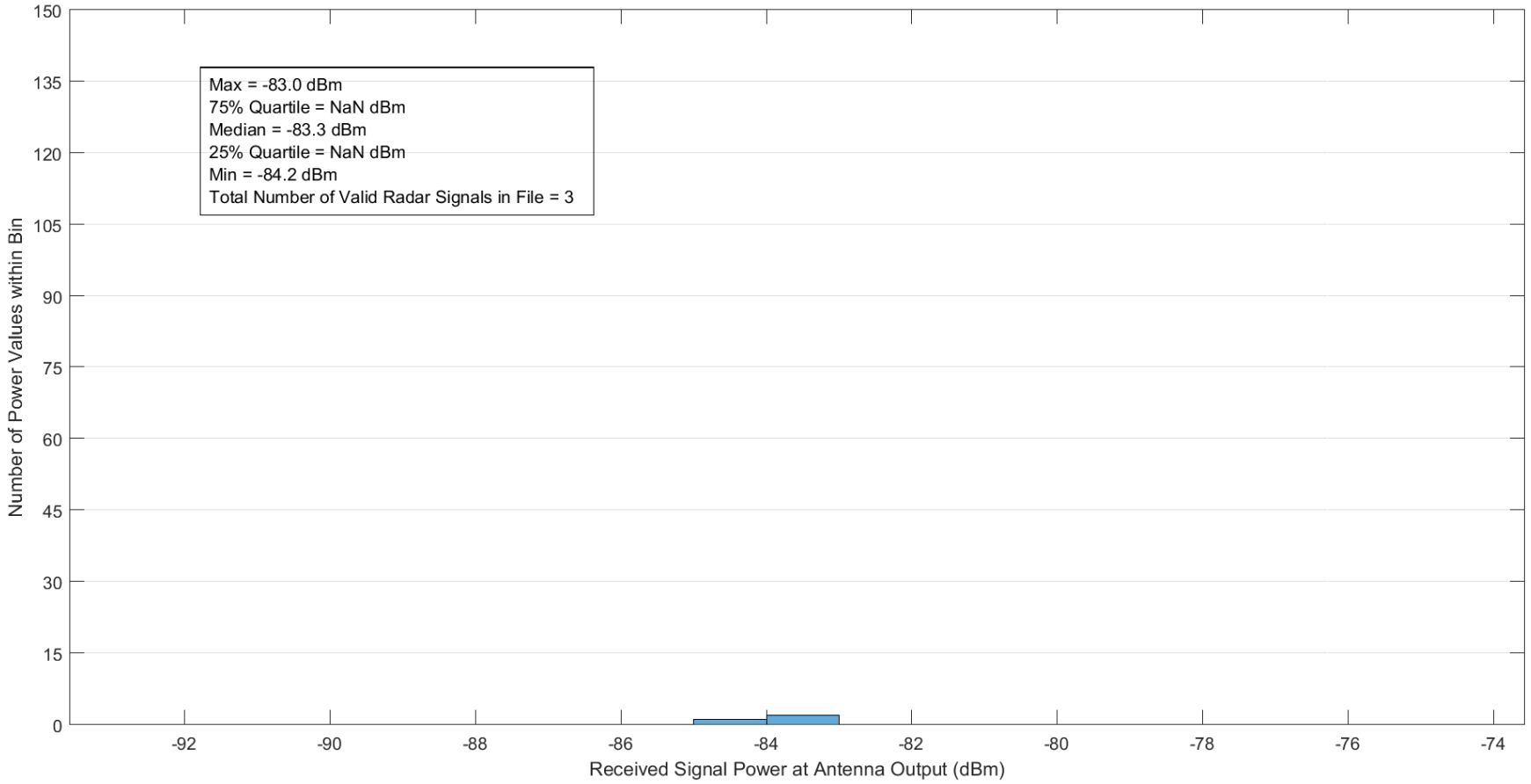

Figure A-19. Received radar signal power statistics at Location 1 along the 326° Radial for the ASR-9.

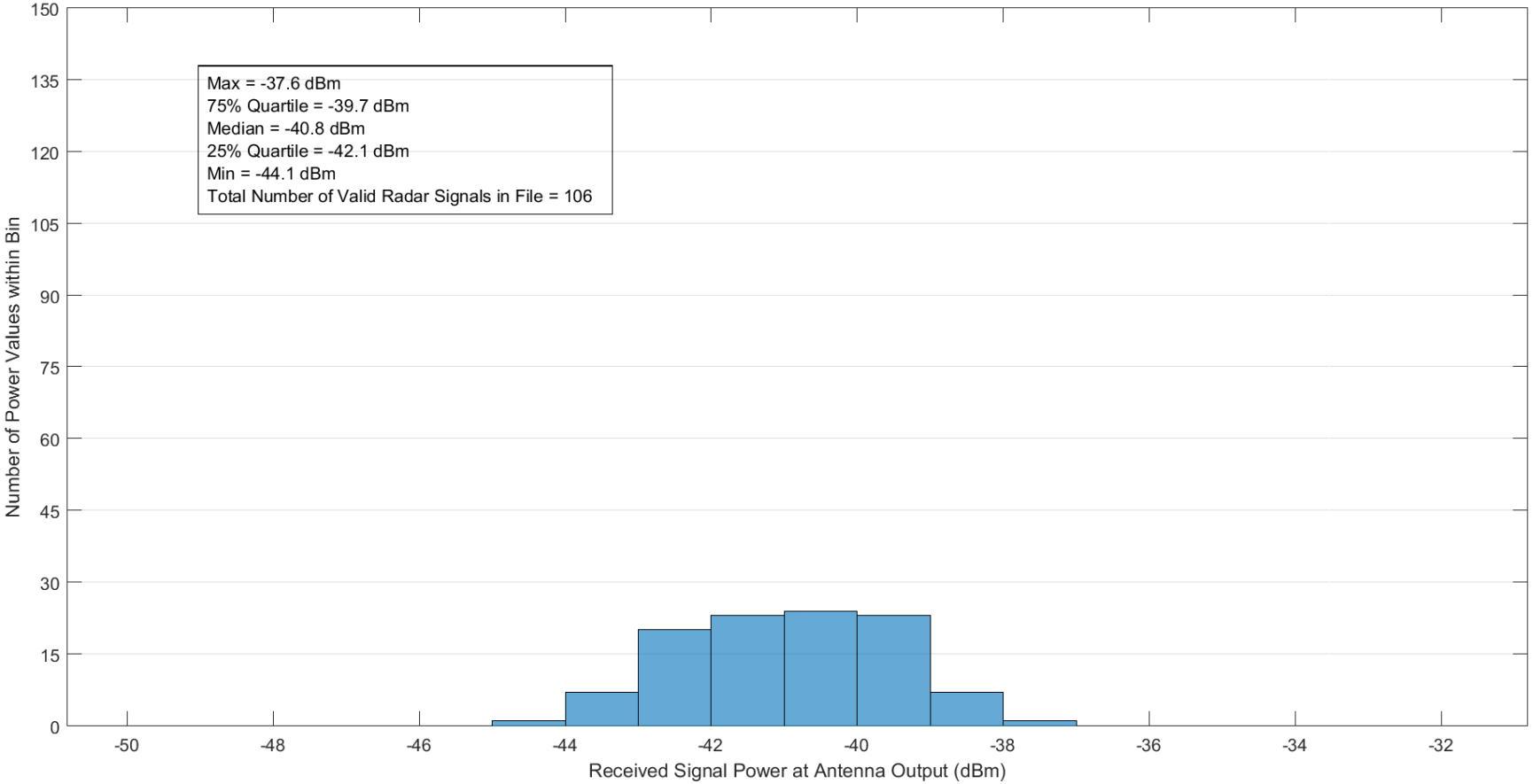

Figure A-20. Received radar signal power statistics at the Boulder Labs Location for the ASR-9.

APPENDIX B: RECEIVED POWER HISTOGRAMS FOR CARSR MEASUREMENTS

This appendix lists the received radar signal power histograms and maximum, median, minimum, 75% quartile, and 25% quartile statistics for each measurement location for the CARSR measurements. The received signal power was too low to accurately measure (i.e., no valid radar signals could be determined) at several measurement locations as listed in Table B-1; accordingly, no histograms or statistics for these measurement locations are shown. Note that at some of these locations, the radar signal was not even observed during the measurements and the data collection was terminated early.

Table B-1. CARSR measurement locations with received signal power too low to accurately measure.

Radial (deg)	Location	Lat (deg)	Lon (deg)	Distance from Tx (km)	Notes
35	Loc1	40.89718	-103.45879	178.80594	
35	ContEnd	41.58685	-102.81081	272.68861	Data collection terminated early
98	ContEnd	39.30864	-102.29719	208.68272	
127	NewContEnd	38.73512	-102.77660	191.16031	Data collection terminated early
178	ContEnd	37.80238	-104.64069	198.95927	Data collection terminated early

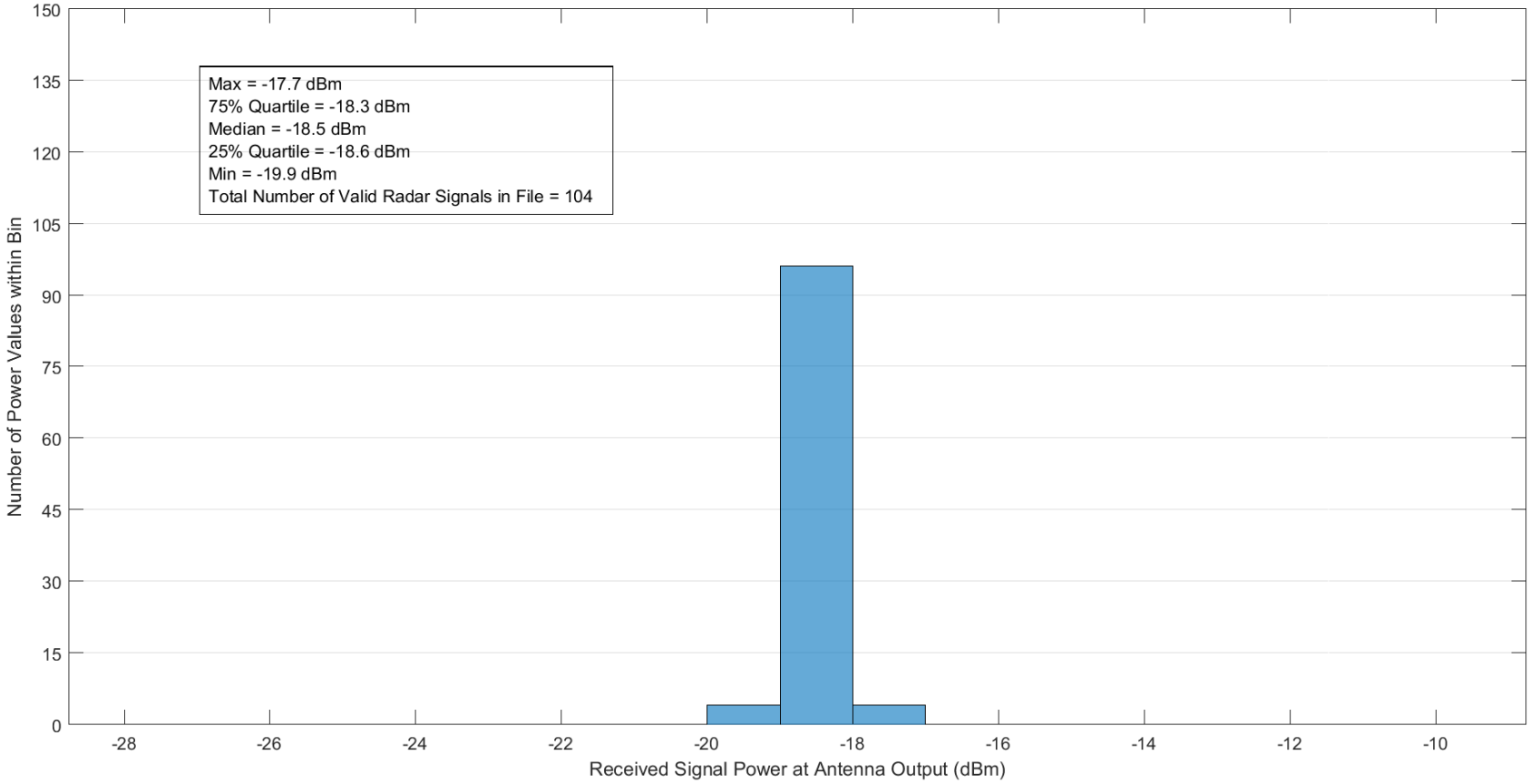

Figure B-1. Received radar signal power statistics at Location 4 along the 1° Radial for the CARSR.

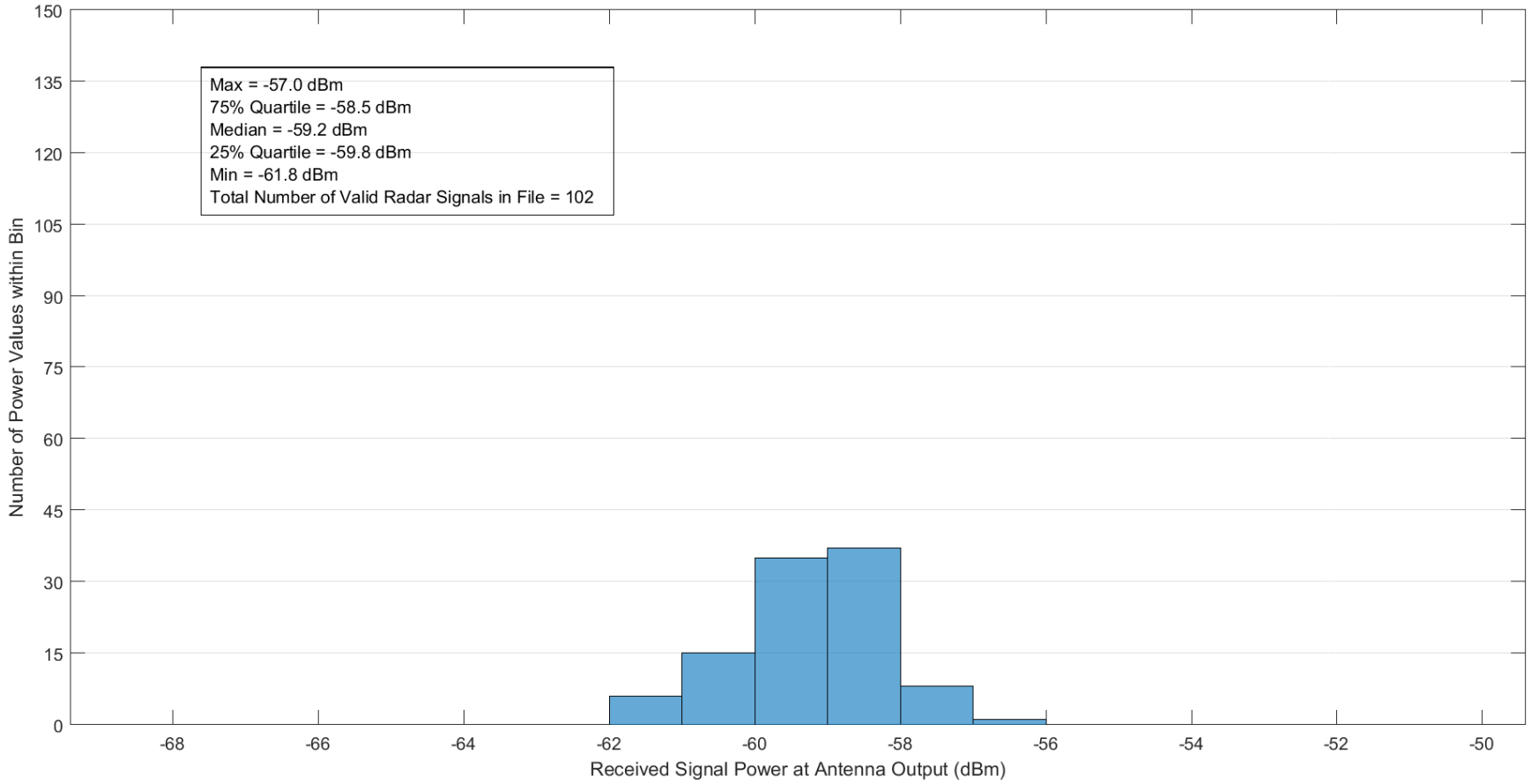

Figure B-2. Received radar signal power statistics at Location 3 along the 1° Radial for the CARSR.

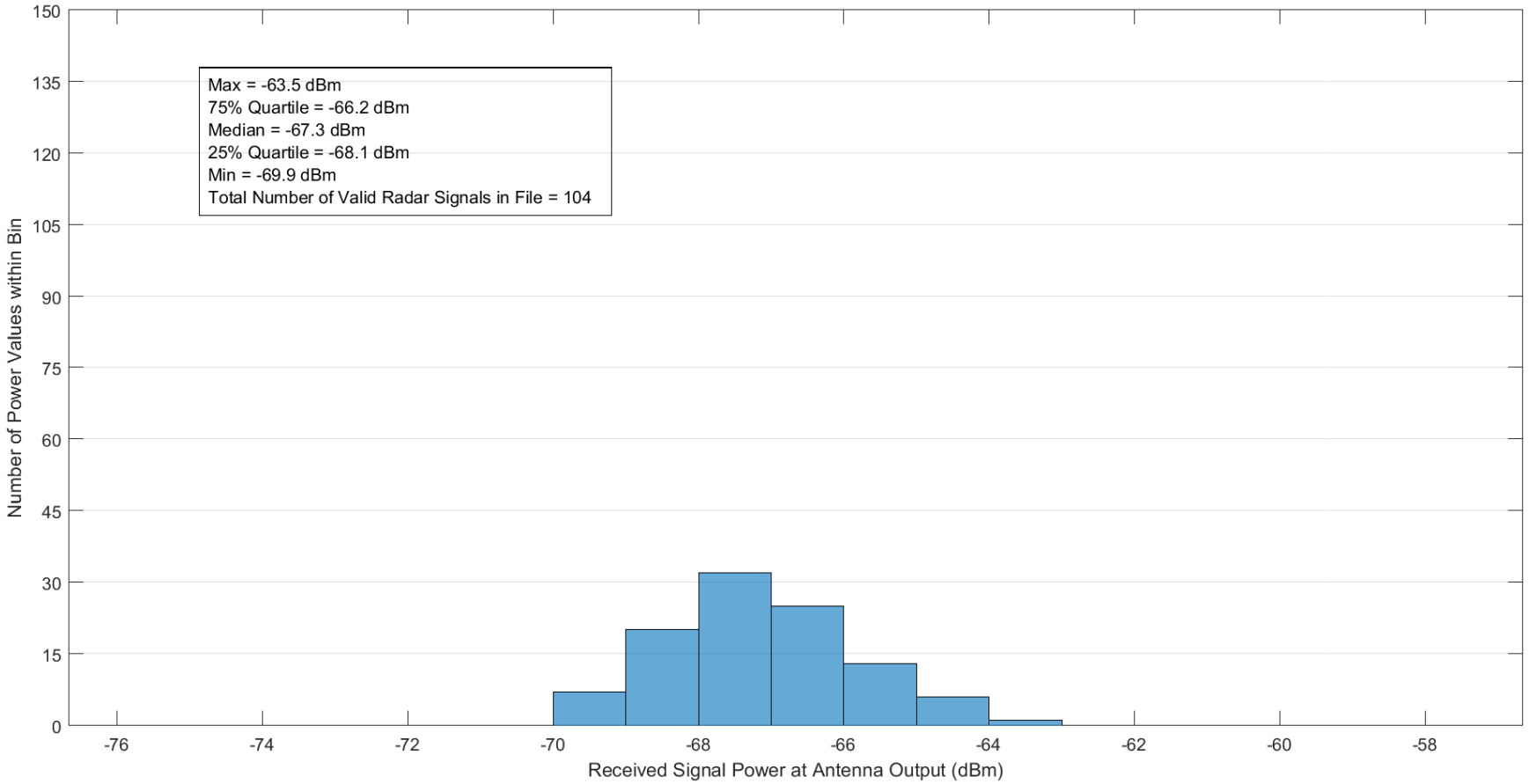

Figure B-3. Received radar signal power statistics at Location 2 along the 1° Radial for the CARSR.

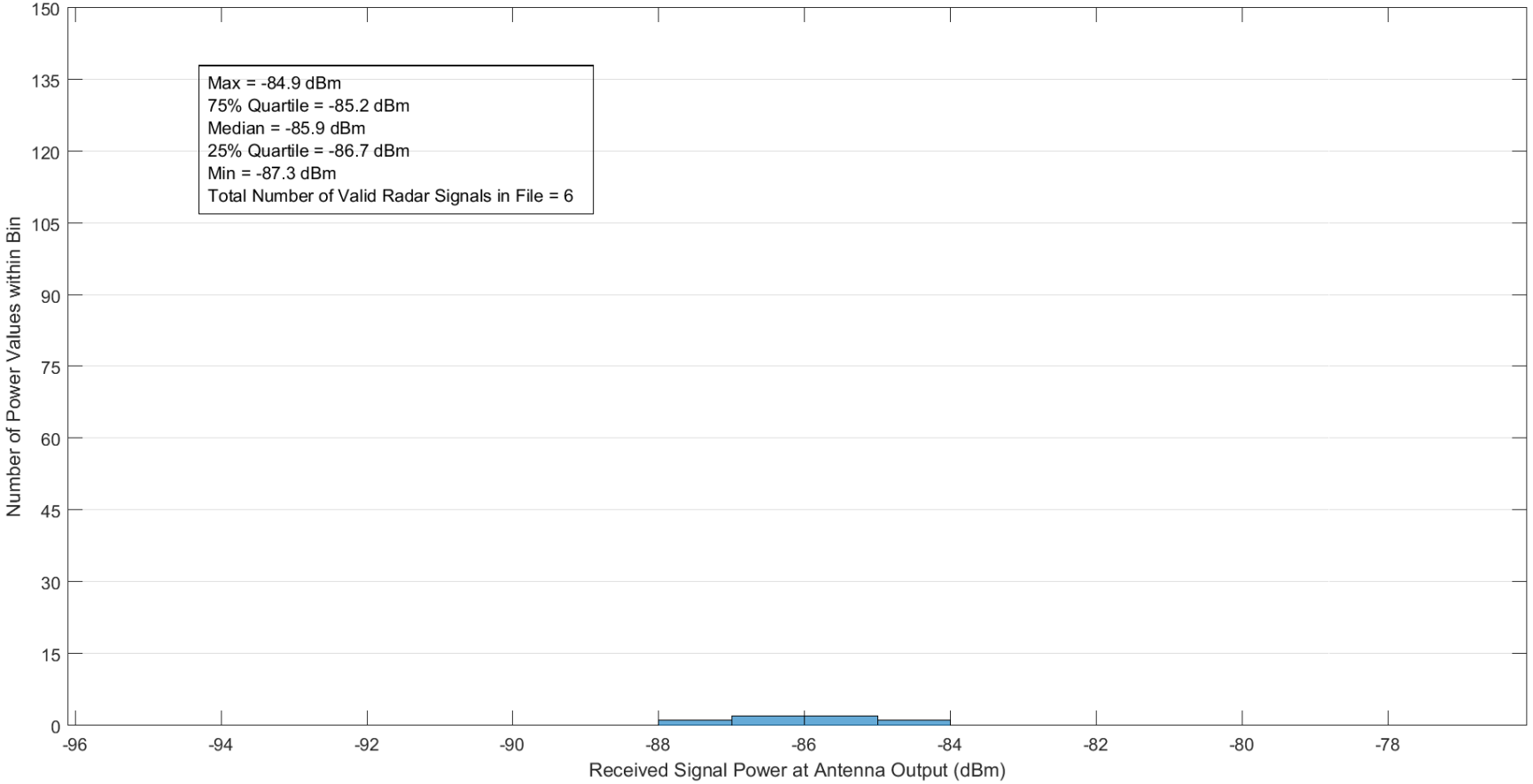

Figure B-4. Received radar signal power statistics at Location 1 along the 1° Radial for the CARSR.

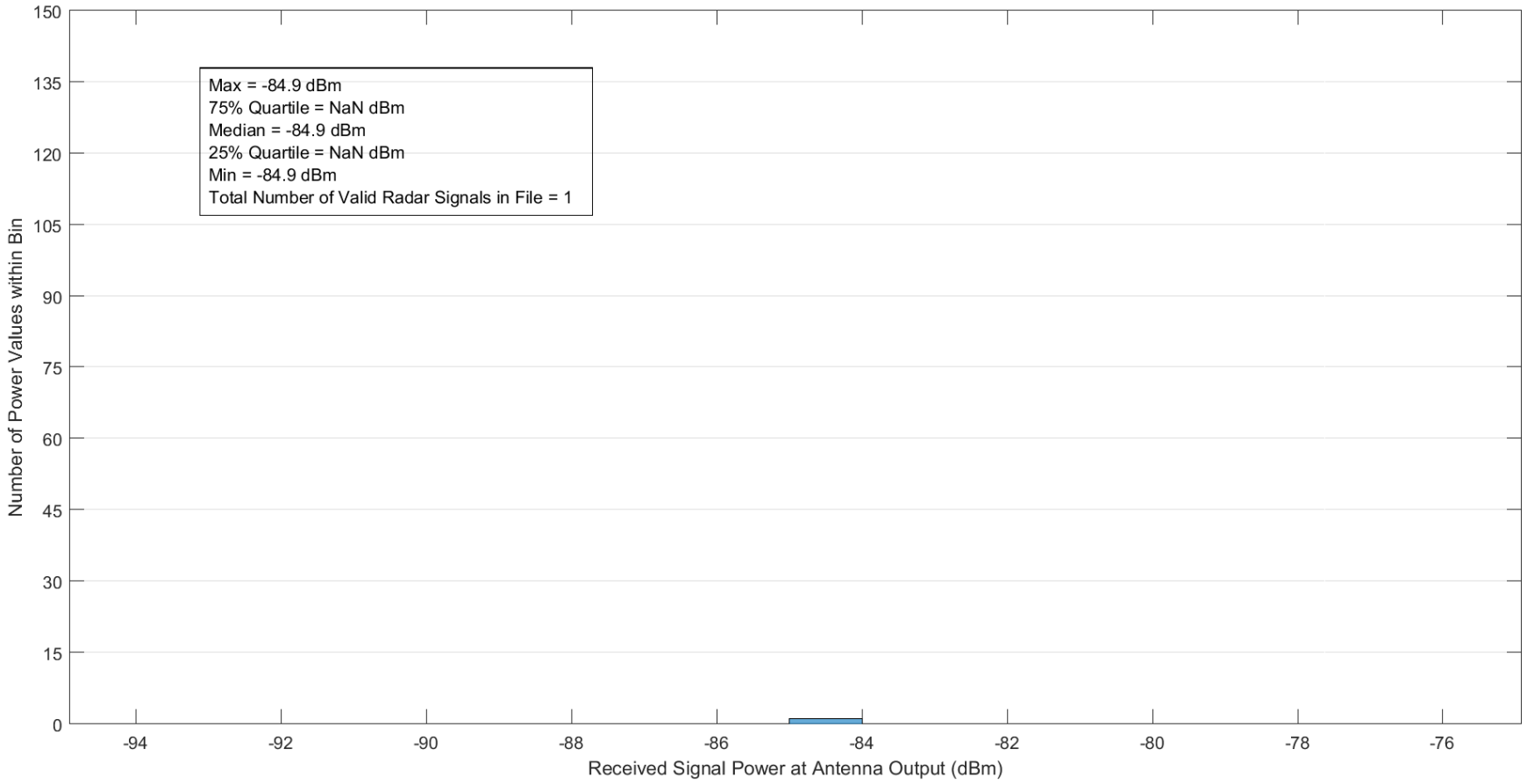

Figure B-5. Received radar signal power statistics at Location ContEnd along the 1° Radial for the CARSR.

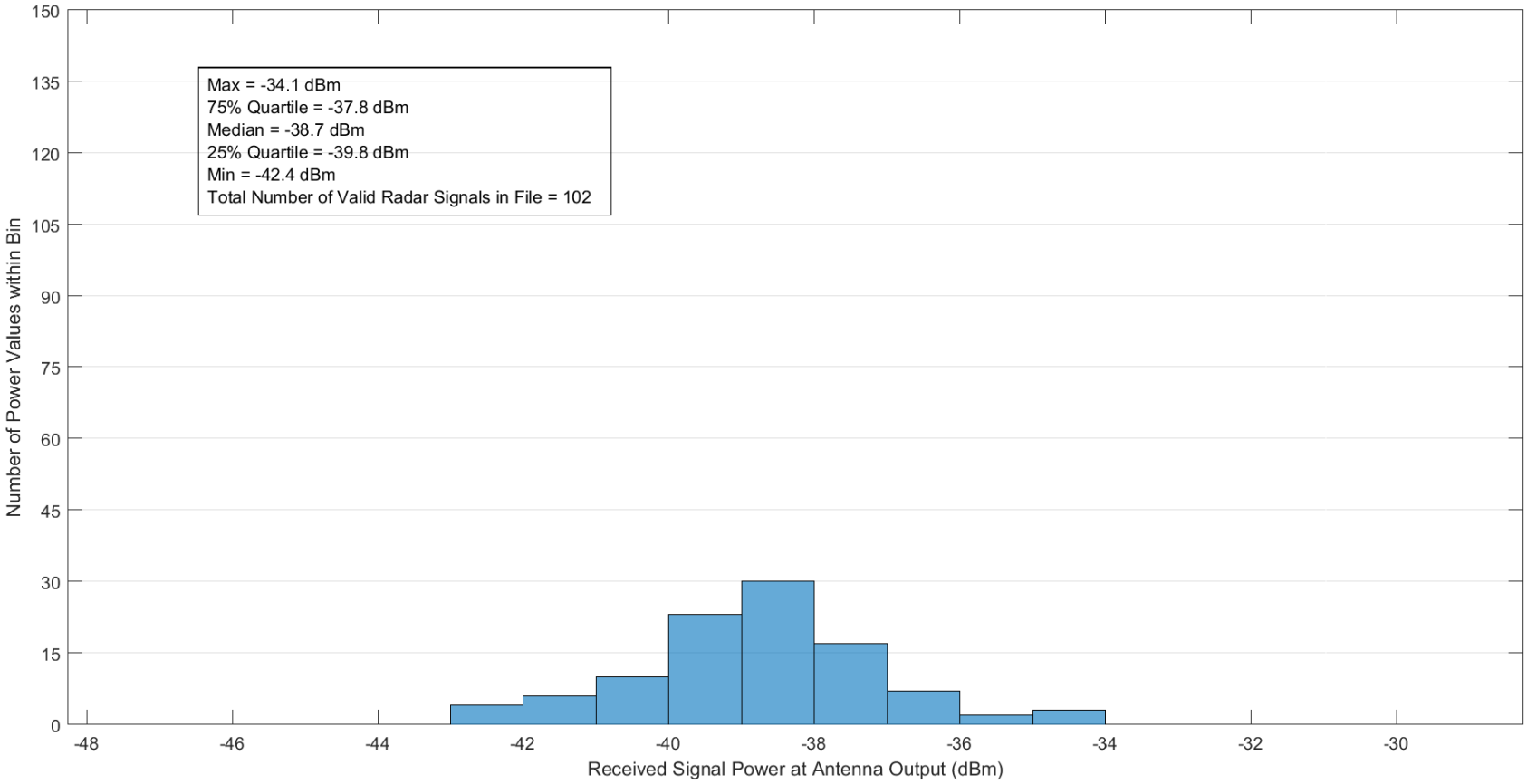

Figure B-6. Received radar signal power statistics at Location 4 along the 35° Radial for the CARSR.

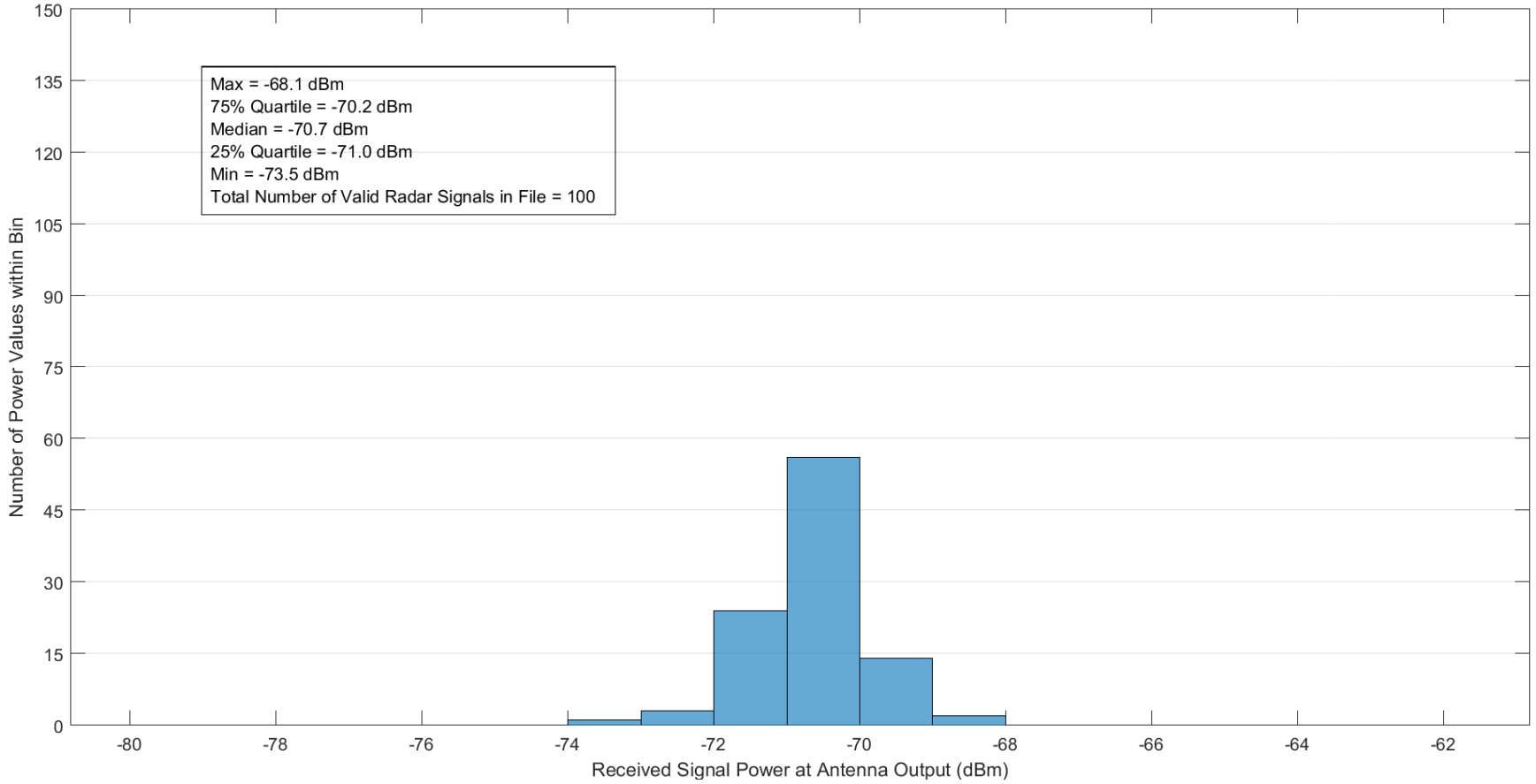

Figure B-7. Received radar signal power statistics at Location 3 along the 35° Radial for the CARSR.

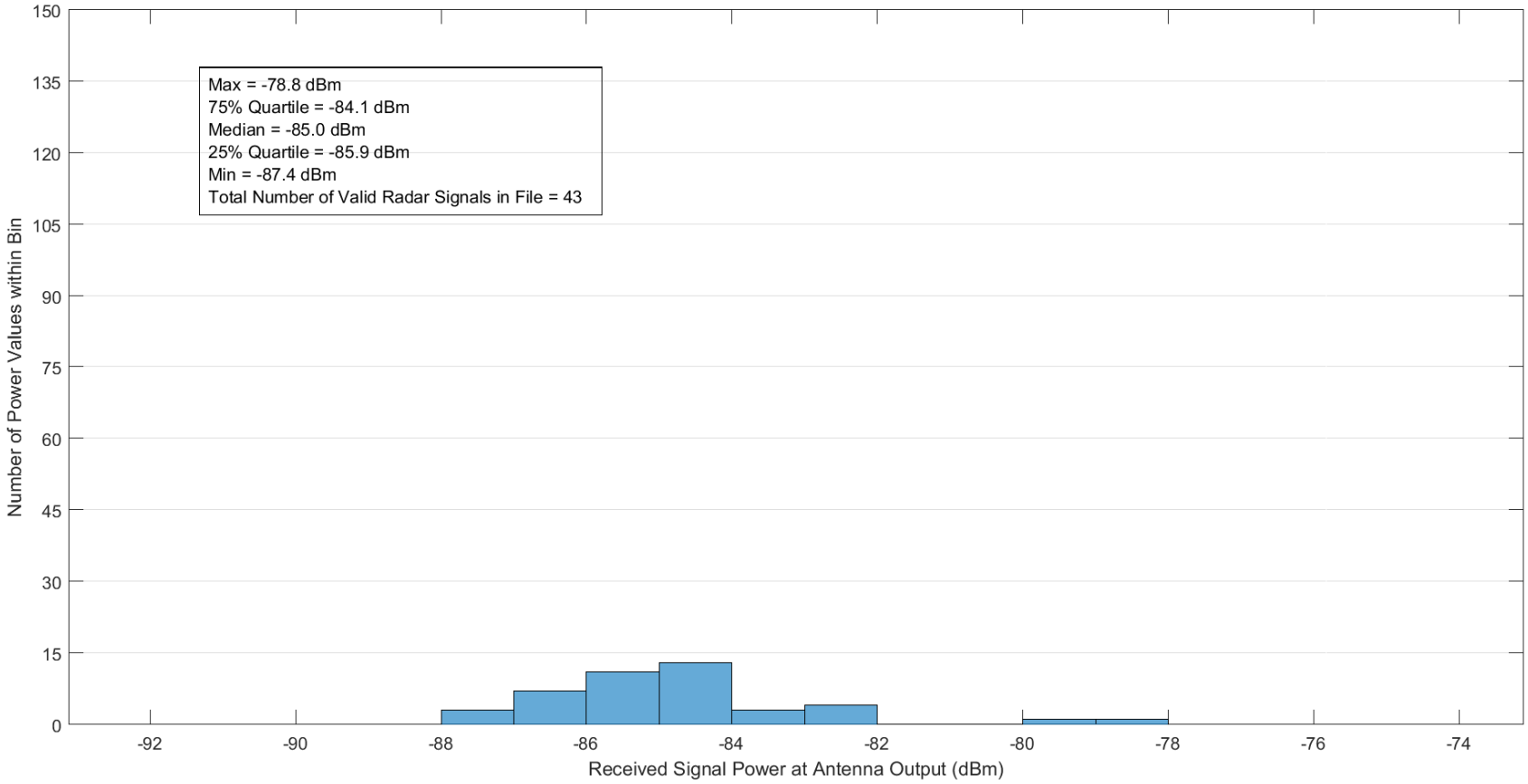

Figure B-8. Received radar signal power statistics at Location 2 along the 35° Radial for the CARSR.

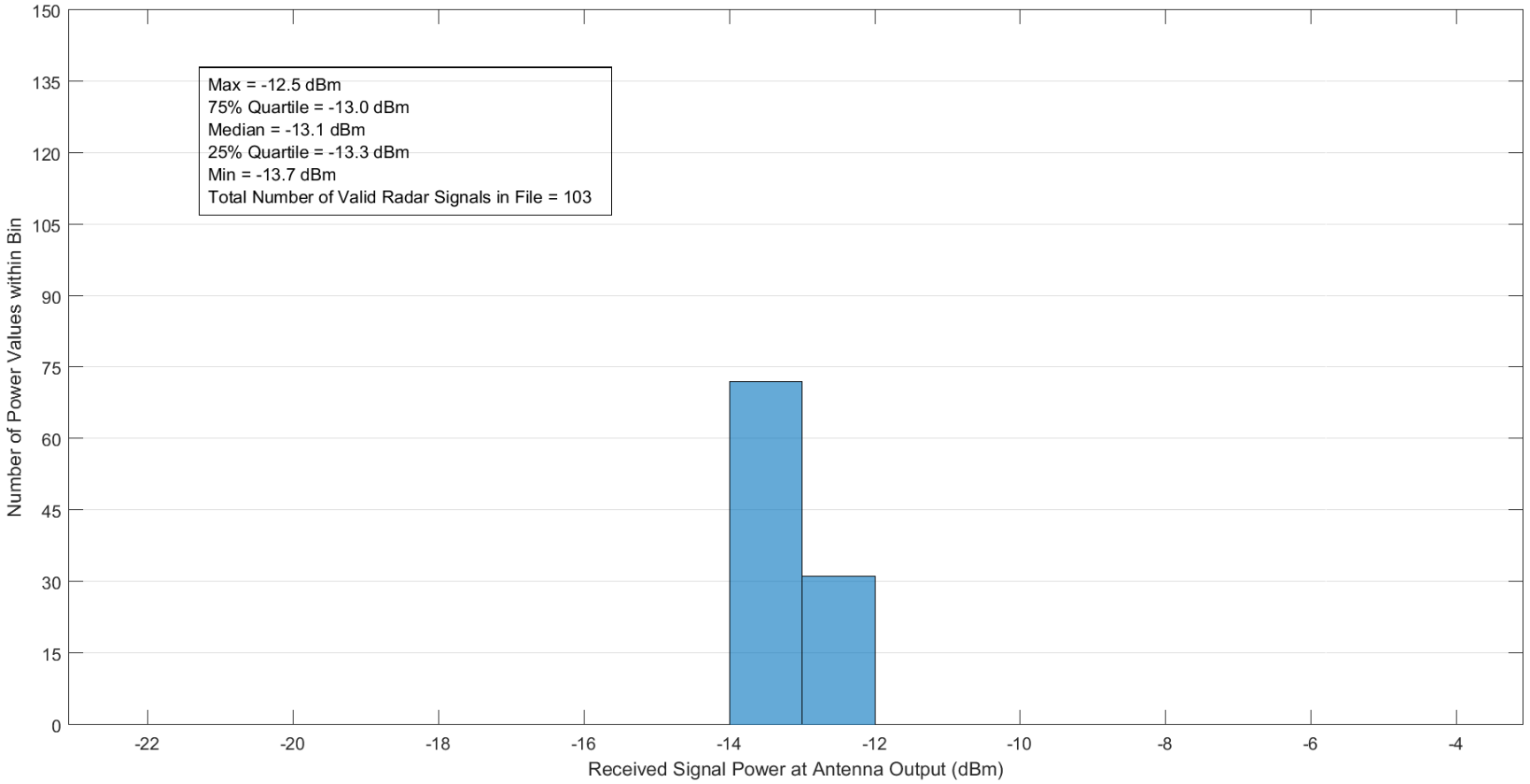

Figure B-9. Received radar signal power statistics at Location 4 along the 98° Radial for the CARSR.

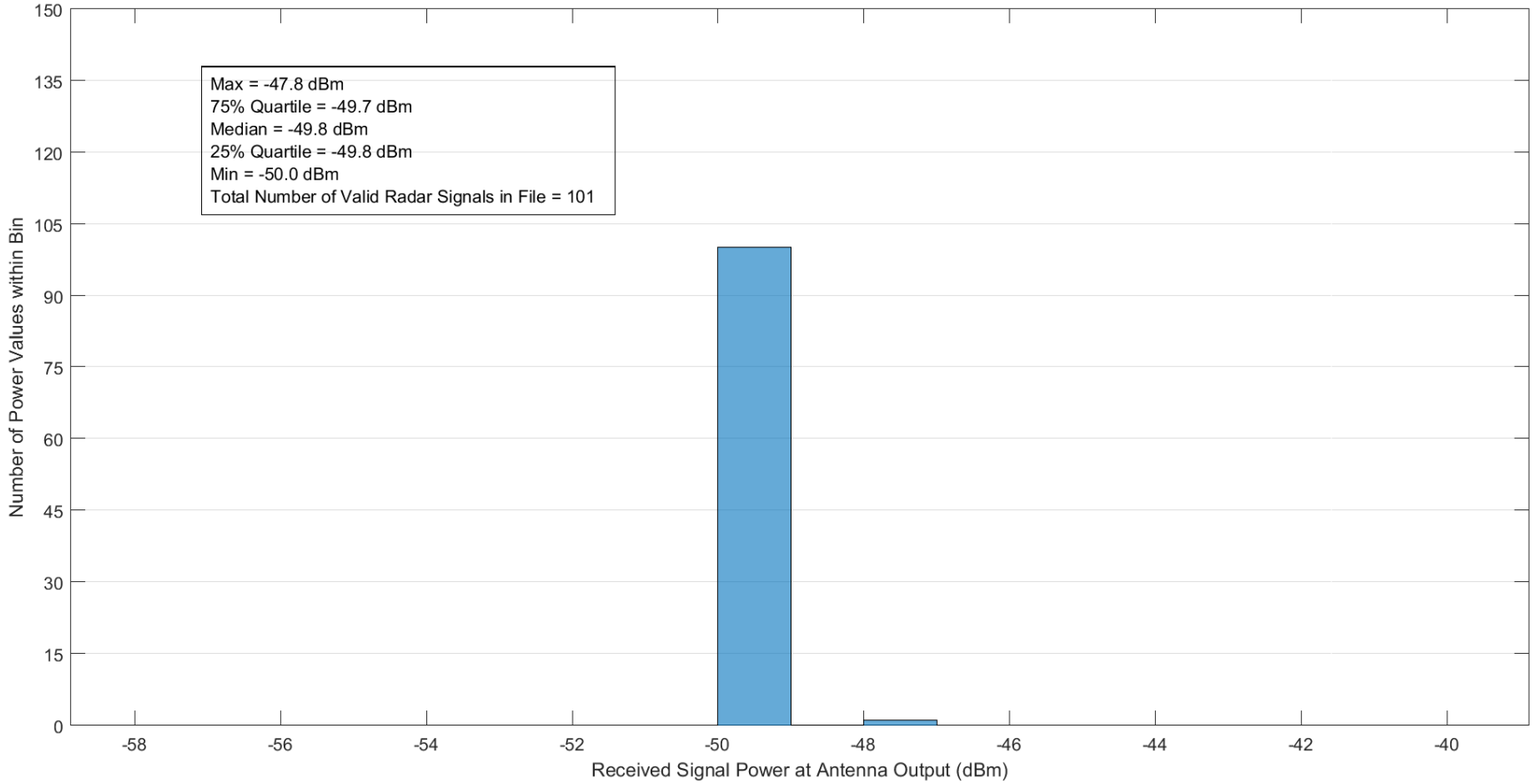

Figure B-10. Received radar signal power statistics at Location 3 along the 98° Radial for the CARSR.

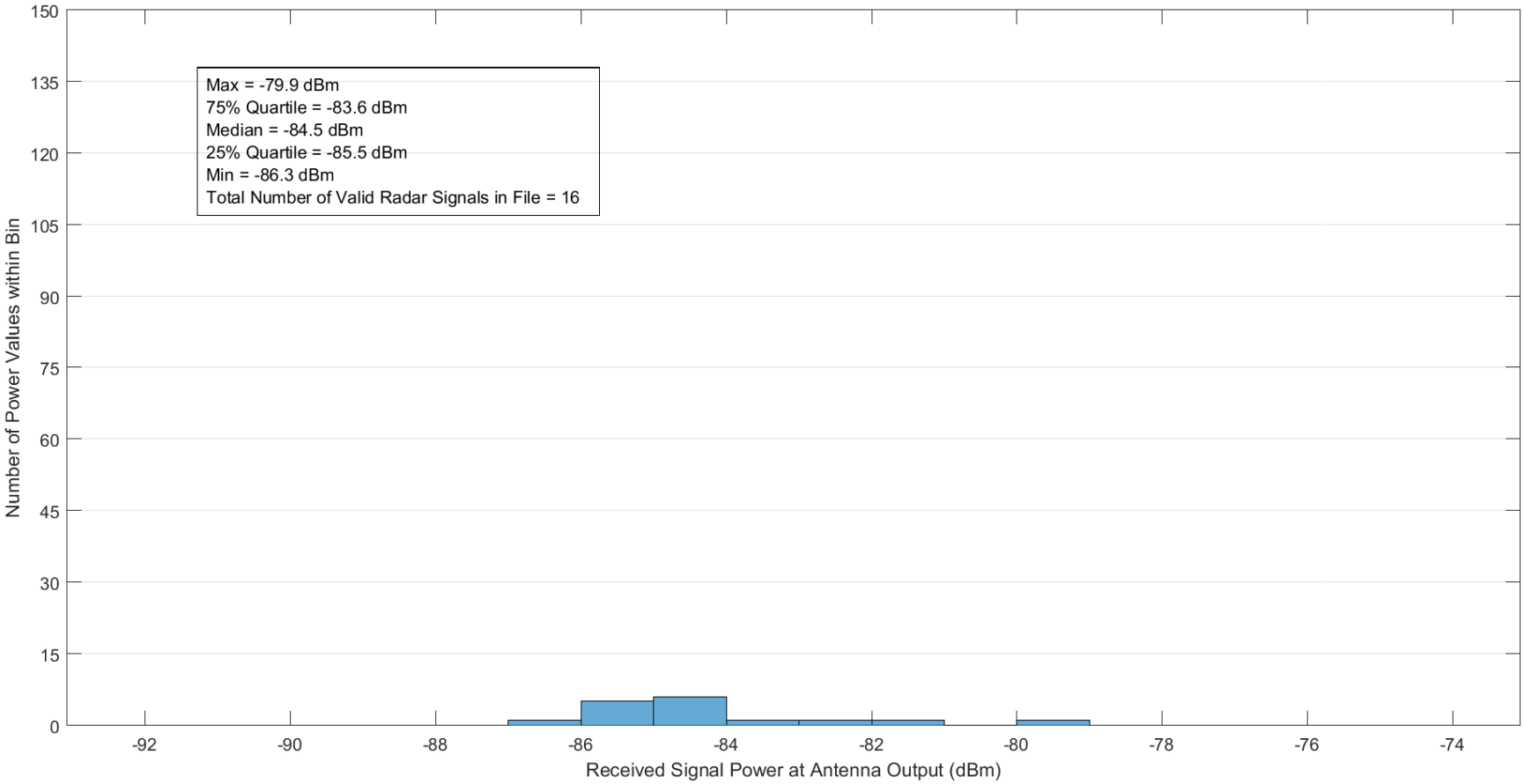

Figure B-11. Received radar signal power statistics at Location 2 along the 98° Radial for the CARSR.

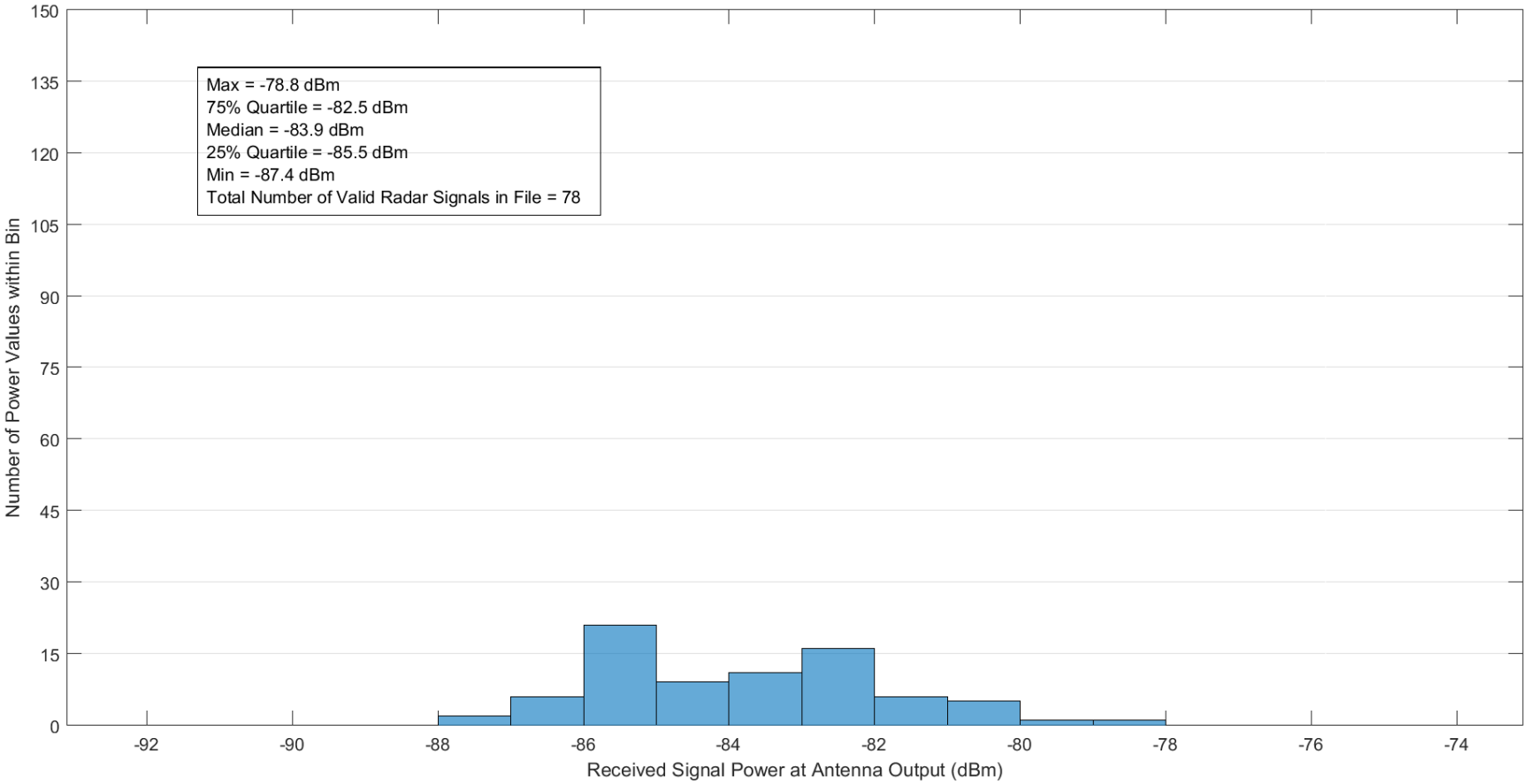

Figure B-12. Received radar signal power statistics at Location 1b along the 98° Radial for the CARSR.

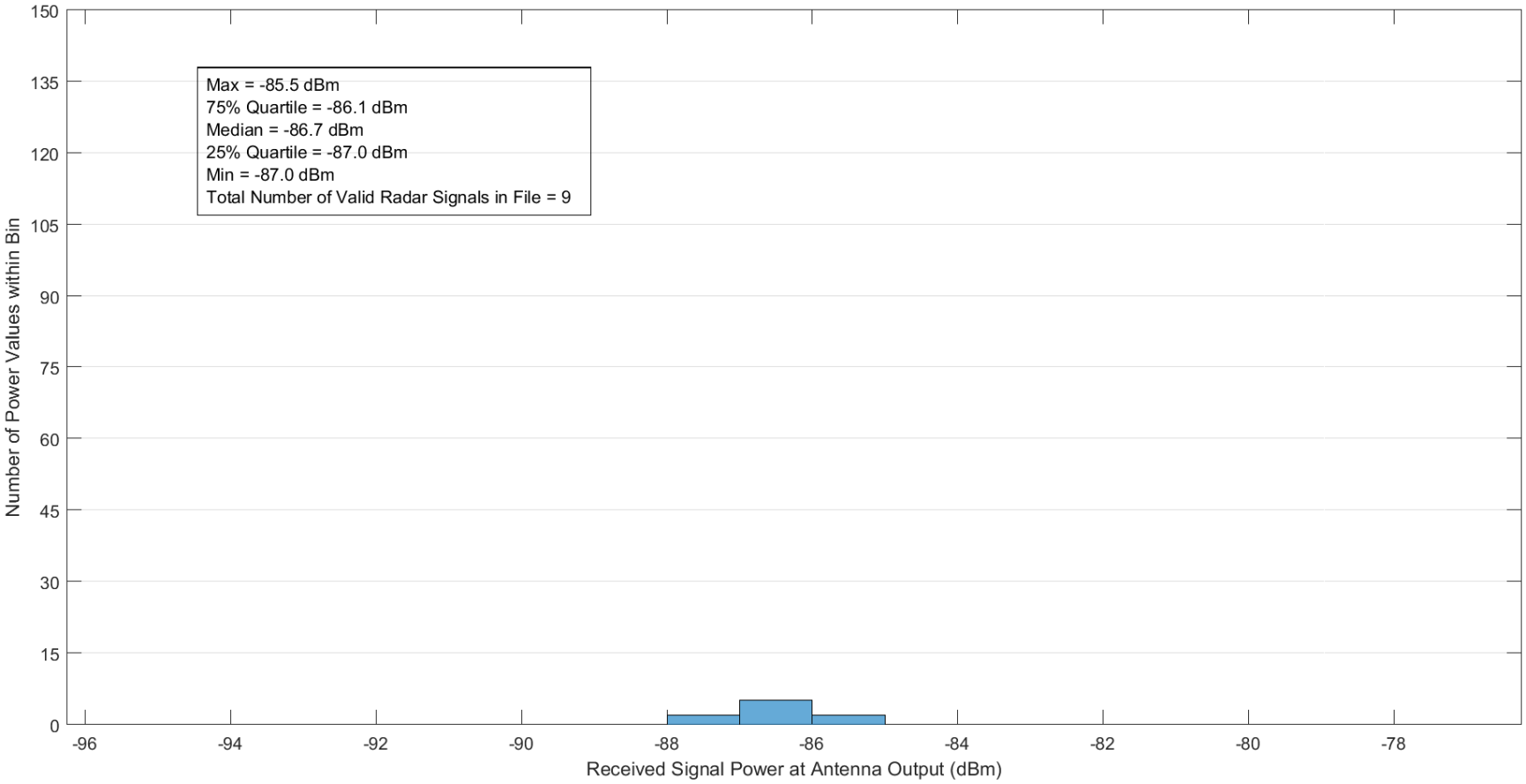

Figure B-13. Received radar signal power statistics at Location 1 along the 98° Radial for the CARSR.

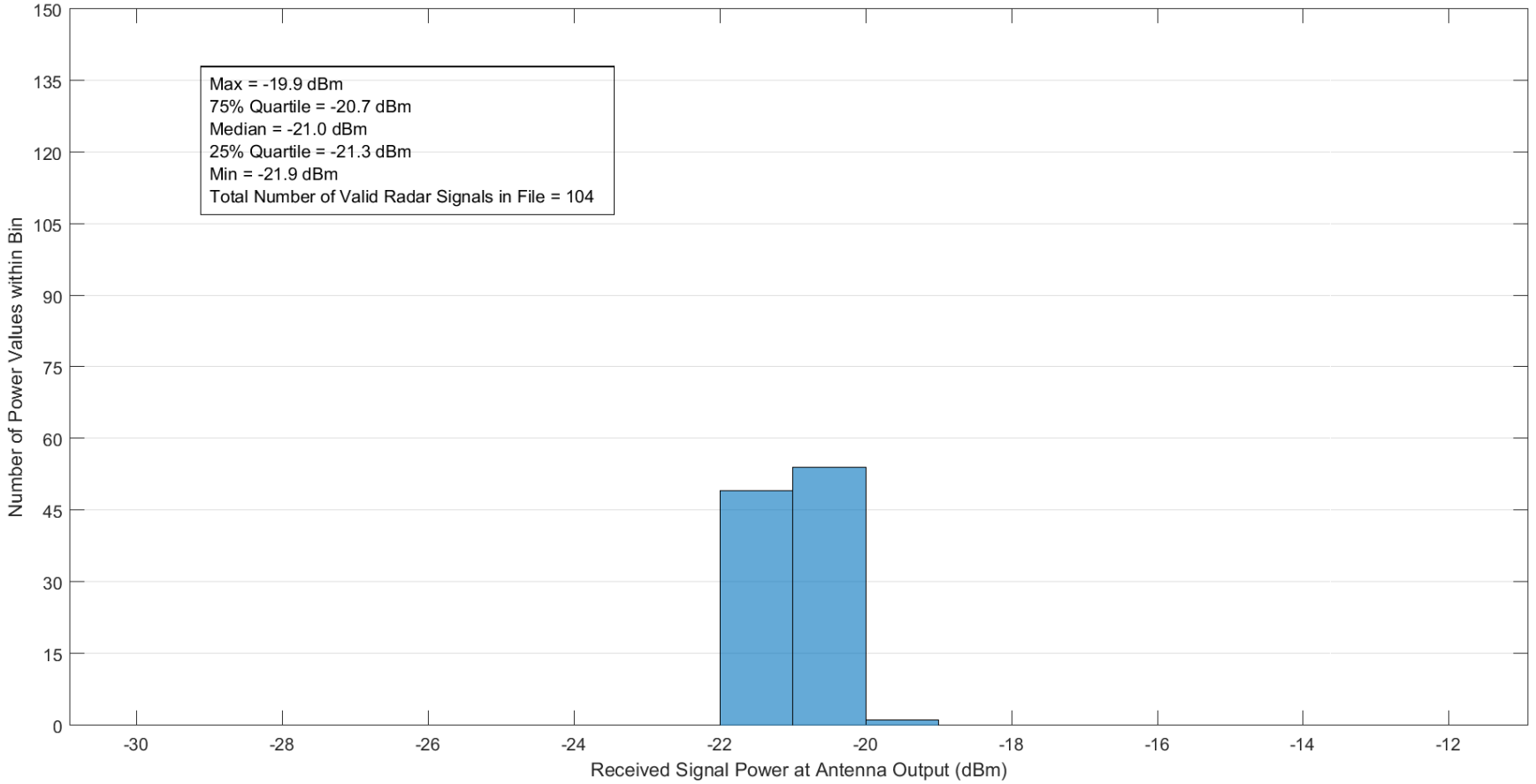

Figure B-14. Received radar signal power statistics at Location 4 along the 127° Radial for the CARSR.

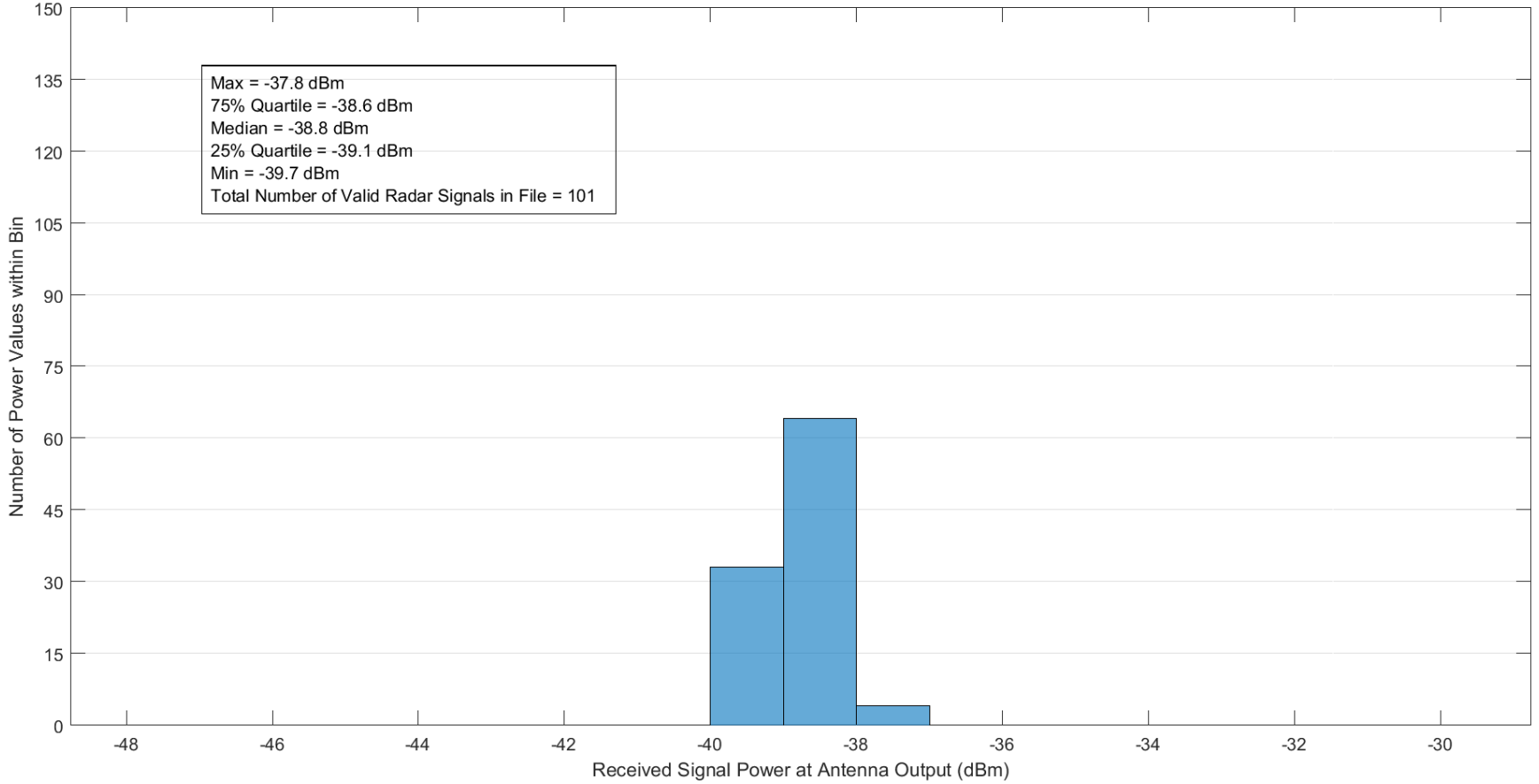

Figure B-15. Received radar signal power statistics at Location 3 along the 127° Radial for the CARSR.

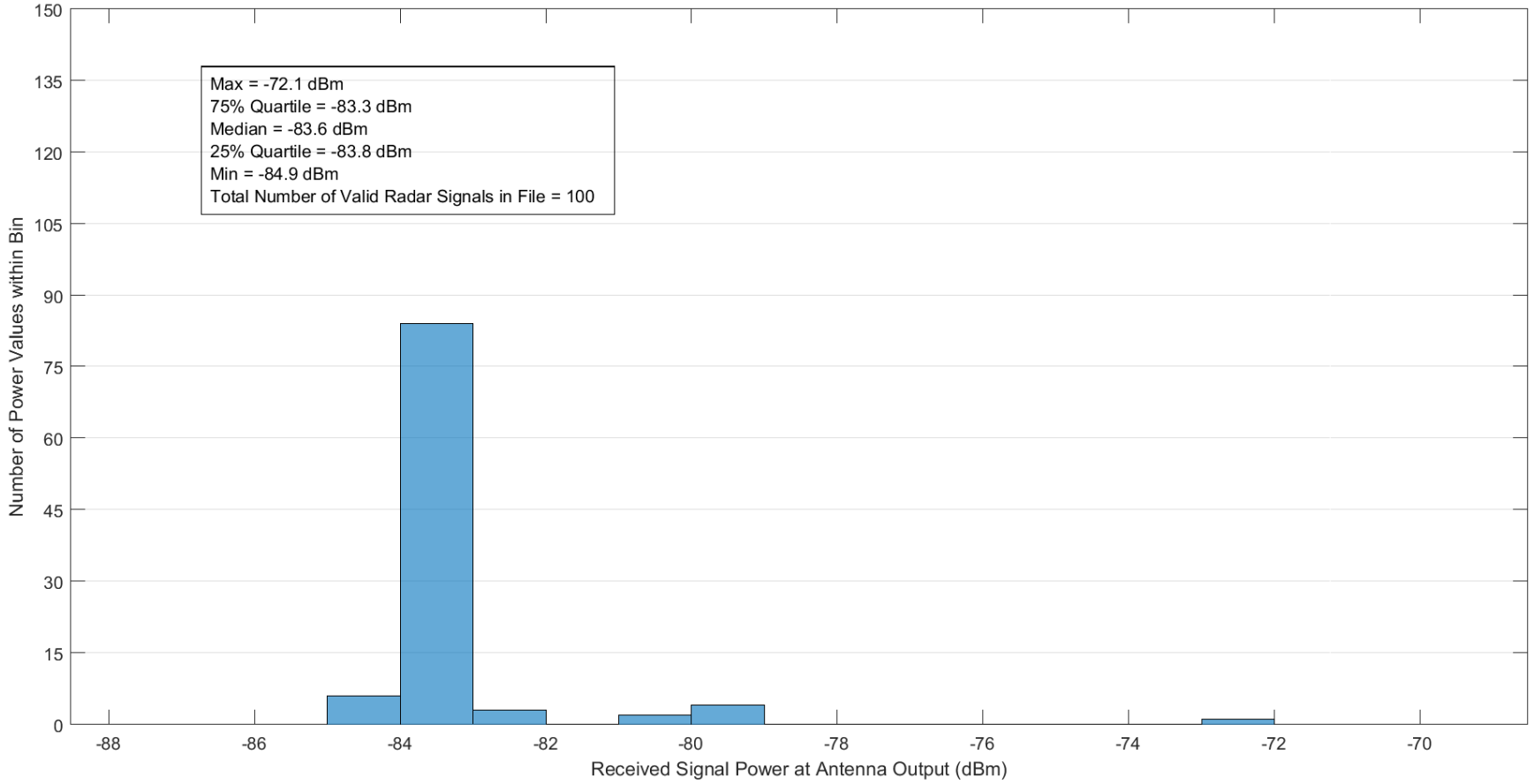

Figure B-16. Received radar signal power statistics at Location 2 along the 127° Radial for the CARSR.

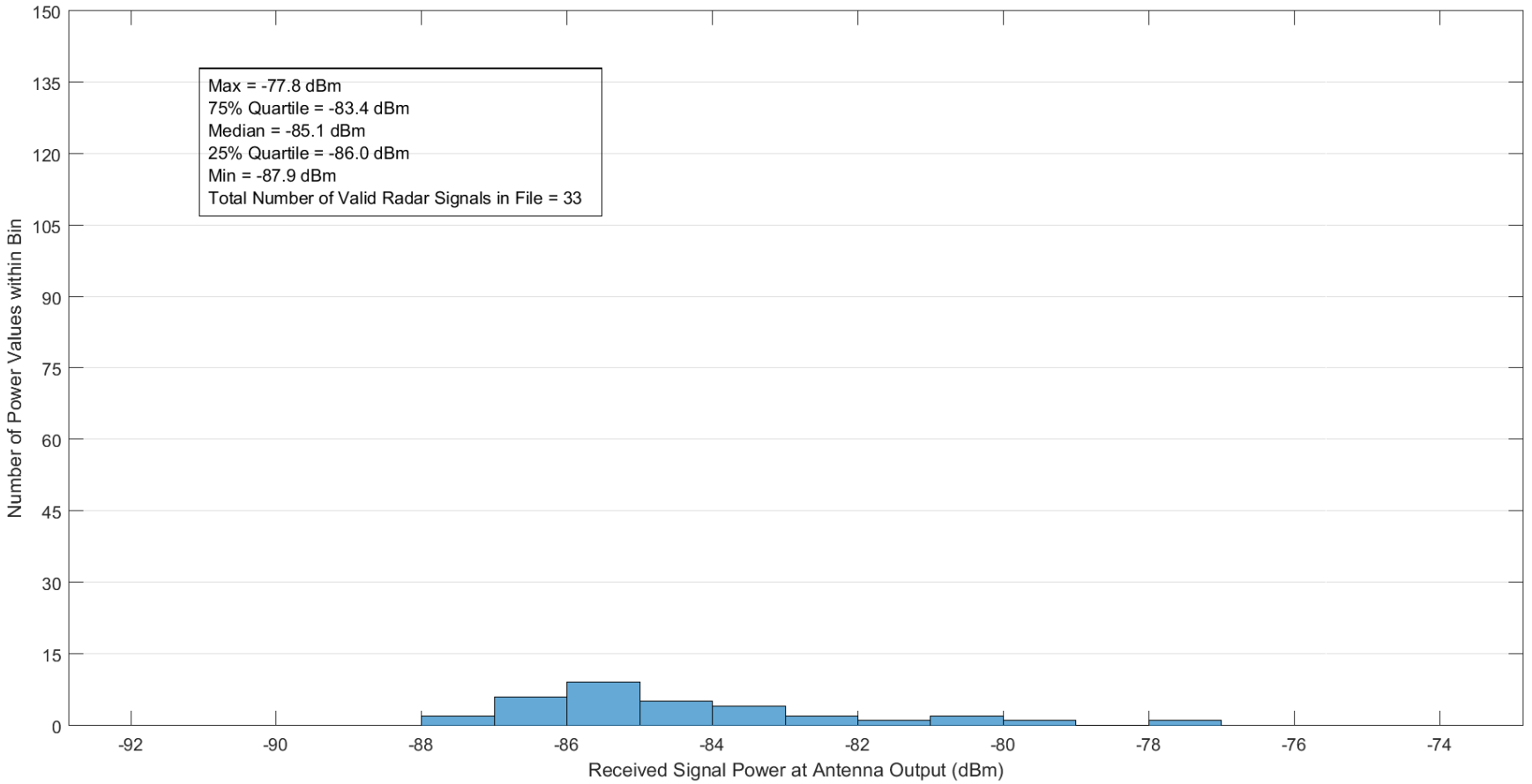

Figure B-17. Received radar signal power statistics at Location 1 along the 127° Radial for the CARSR.

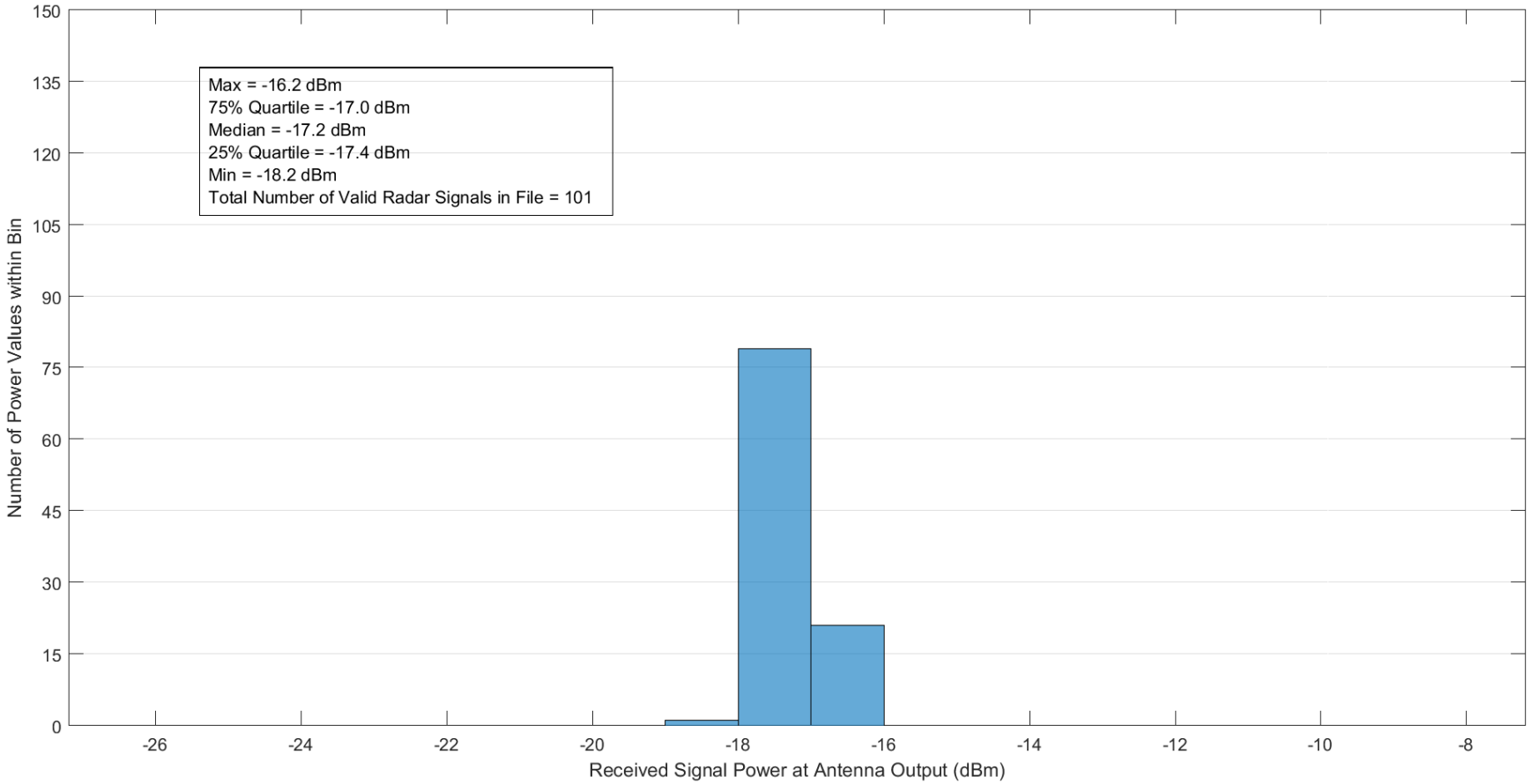

Figure B-18. Received radar signal power statistics at Location 4 along the 178° Radial for the CARSR.

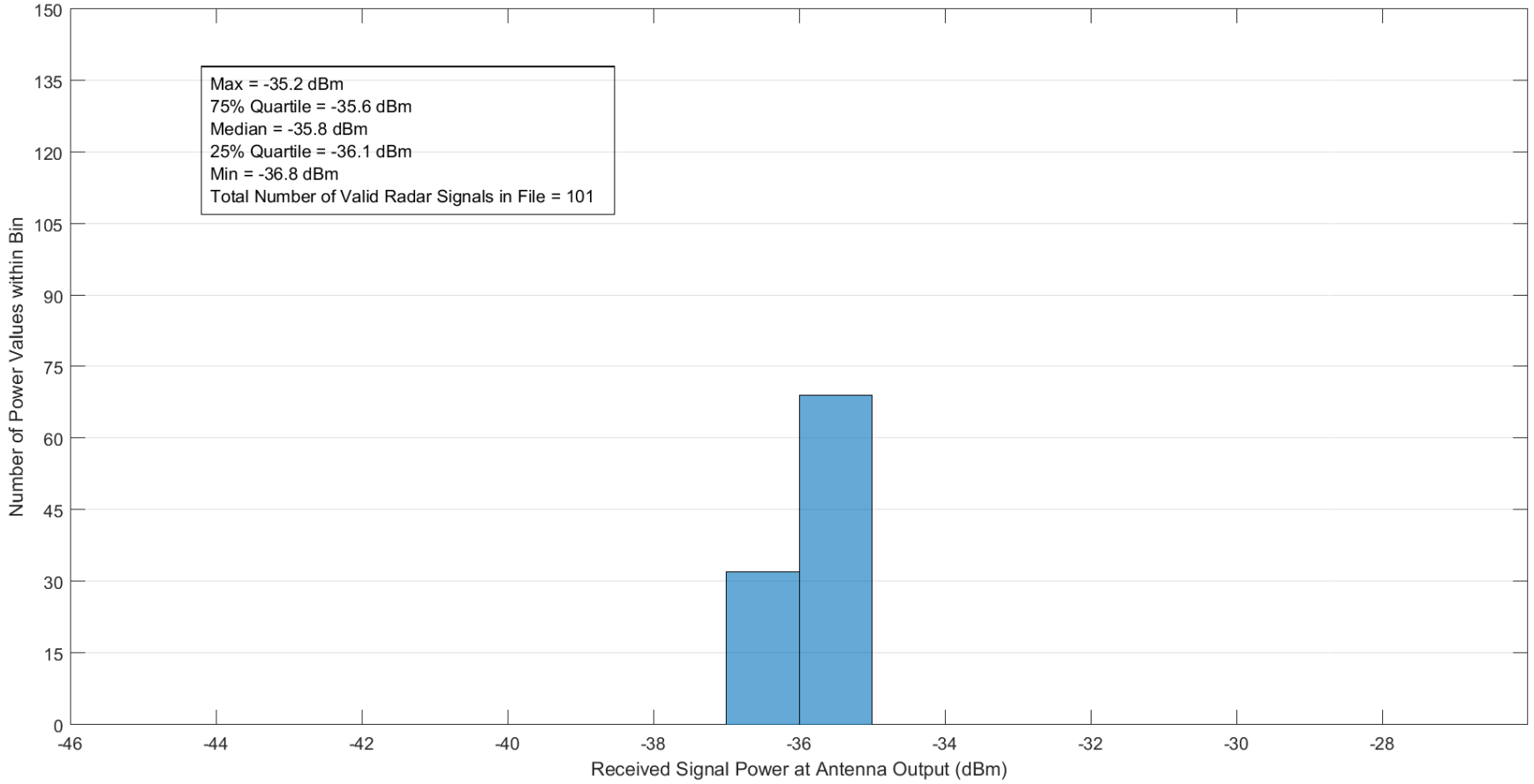

Figure B-19. Received radar signal power statistics at Location 3 along the 178° Radial for the CARSR.

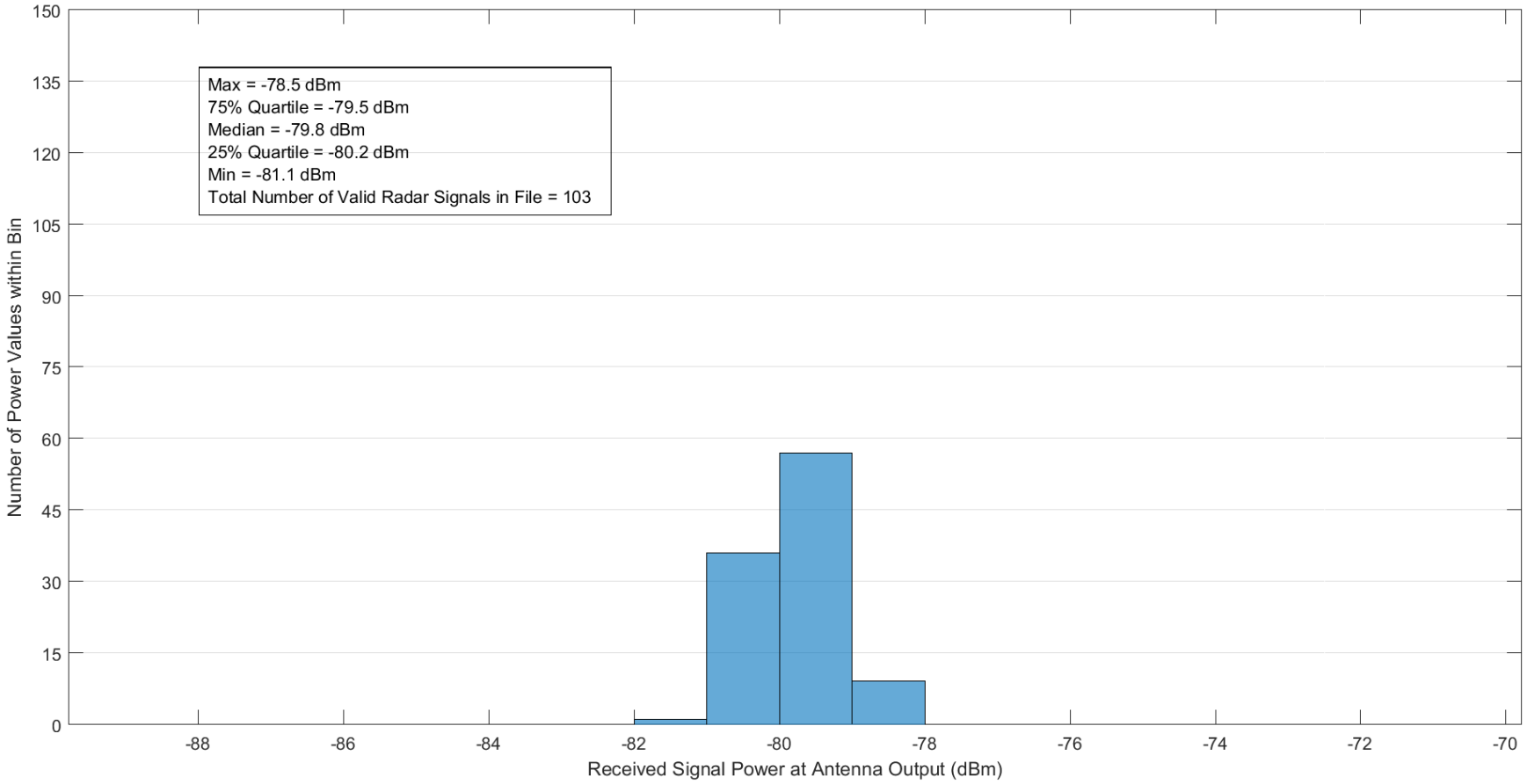

Figure B-20. Received radar signal power statistics at Location 2 along the 178° Radial for the CARSR.

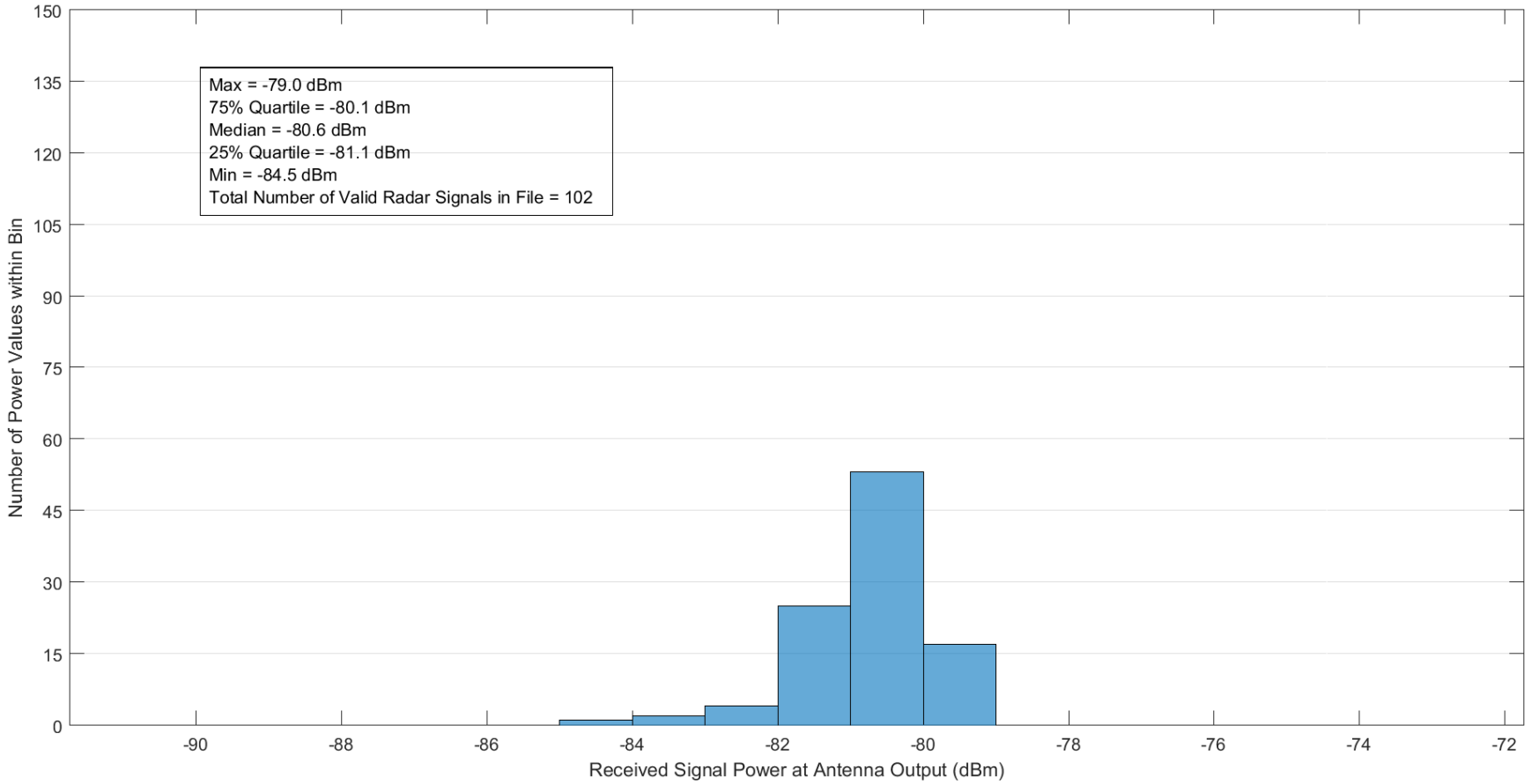

Figure B-21. Received radar signal power statistics at Location 1 along the 178° Radial for the CARSR.

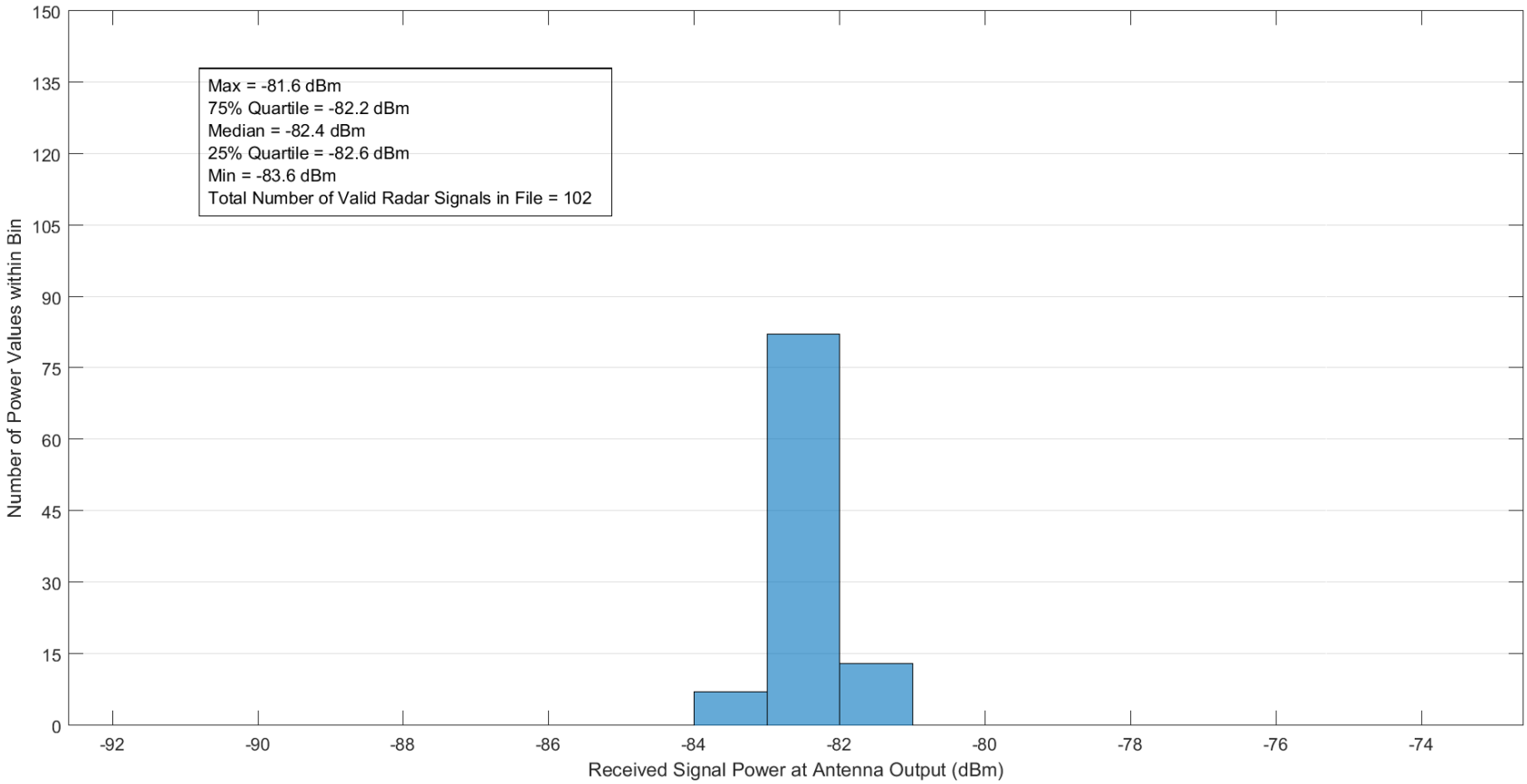

Figure B-22. Received radar signal power statistics at Location NearContEnd along the 178° Radial for the CARSR.

NTIA FORM 29 (4-80)

U.S. DEPARTMENT OF COMMERCE
NATIONAL TELECOMMUNICATIONS AND INFORMATION ADMINISTRATION

BIBLIOGRAPHIC DATA SHEET

1. PUBLICATION NO.	2. Government Accession No.	3. Recipient's Accession No.
TR-19-542		

4. TITLE AND SUBTITLE	5. Publication Date
Received Signal Power Measurements On Select Air Traffic Control Radars In Colorado	August 2019
	6. Performing Organization Code NTIA/ITS.T

7. AUTHOR(S)	9. Project/Task/Work Unit No.
Jeffery A. Wepman, Edward F. Drocella, April Lundy, Paul M. McKenna, Heather E. Ottke, and Yeh Lo	6504000-208
8. PERFORMING ORGANIZATION NAME AND ADDRESS Institute for Telecommunication Sciences National Telecommunications & Information Administration U.S. Department of Commerce 325 Broadway Boulder, CO 80305	10. Contract/Grant Number.
11. Sponsoring Organization Name and Address National Telecommunications & Information Administration Herbert C. Hoover Building 14th & Constitution Ave., NW Washington, DC 20230	12. Type of Report and Period Covered

14. SUPPLEMENTARY NOTES

15. ABSTRACT (A 200-word or less factual summary of most significant information. If document includes a significant bibliography or literature survey, mention it here.)

Received signal power measurements were performed on the Common Air Route Surveillance Radar (CARSR) operating in the 1300–1370 MHz band in Parker, Colorado and on the Airport Surveillance Radar (ASR-9) operating in the 2700-2900 MHz band in Platteville, Colorado. The measurements were taken along five radials extending from each radar transmitter. Four or five fixed locations were chosen along each radial where predicted received signal power varied from relatively strong to weak levels. Multiple peak received power measurements were made at each location to provide statistically significant results. In another effort, these measurements will be used to validate spectrum usage contours and the methodology used to generate them as developed by the Office of Spectrum Management (OSM) of the National Telecommunications and Information Administration (NTIA).

16. Key Words (Alphabetical order, separated by semicolons)

Received signal power measurements, peak received signal power, ASR-9, CARSR, radar measurements, spectrum usage contours

17. AVAILABILITY STATEMENT	18. Security Class. (This report)	20. Number of pages
☒ UNLIMITED.	Unclassified	97
☐ FOR OFFICIAL DISTRIBUTION.	19. Security Class. (This page) Unclassified	21. Price:

NTIA FORMAL PUBLICATION SERIES

NTIA MONOGRAPH (MG)

A scholarly, professionally oriented publication dealing with state-of-the-art research or an authoritative treatment of a broad area. Expected to have long-lasting value.

NTIA SPECIAL PUBLICATION (SP)

Conference proceedings, bibliographies, selected speeches, course and instructional materials, directories, and major studies mandated by Congress.

NTIA REPORT (TR)

Important contributions to existing knowledge of less breadth than a monograph, such as results of completed projects and major activities.

JOINT NTIA/OTHER-AGENCY REPORT (JR)

This report receives both local NTIA and other agency review. Both agencies' logos and report series numbering appear on the cover.

NTIA SOFTWARE & DATA PRODUCTS (SD)

Software such as programs, test data, and sound/video files. This series can be used to transfer technology to U.S. industry.

NTIA HANDBOOK (HB)

Information pertaining to technical procedures, reference and data guides, and formal user's manuals that are expected to be pertinent for a long time.

NTIA TECHNICAL MEMORANDUM (TM)

Technical information typically of less breadth than an NTIA Report. The series includes data, preliminary project results, and information for a specific, limited audience.

For information about NTIA publications, contact the NTIA/ITS Technical Publications Office at 325 Broadway, Boulder, CO, 80305 Tel. (303) 497-3572 or e-mail ITSinfo@ntia.gov.